

**The role of the novel endosomal protein Rush
hour (CG14782) in endosomal trafficking in
*Drosophila melanogaster***

PhD Thesis

in partial fulfilment of the requirements
for the degree “Doctor of Philosophy (PhD)”
in the Molecular Biology Program
at the Georg August University Göttingen,
Faculty of Biology

submitted by

IEVA GAILITE

born in

Riga, Latvia

2010

Affidavit

I hereby declare that I prepared the PhD thesis “The role of the novel endosomal protein Rush hour (CG14782) in endosomal trafficking in *Drosophila melanogaster*” on my own and with no other sources and aids than quoted.

Ieva Gailite

Göttingen, March 31st, 2010

Contents

Contents	1
Acknowledgements	3
Abstract	4
List of figures	5
List of tables	7
1. Introduction	8
1.1. Endocytosis	8
1.1.1. Endocytic compartments	9
1.1.2. Rab GTPase cycle	11
1.2. Cell polarity	13
1.2.1. Epithelial cell polarity	13
1.2.2. Endocytosis in regulation of cell polarity	17
1.2.3. The Par/aPKC complex in regulation of endocytosis	18
1.3. Rush – a new endosomal protein	20
2. Materials and Methods	23
2.1. Materials	23
2.1.1. Chemicals and enzymes	23
2.1.2. Primers	23
2.1.3. Vectors	25
2.1.4. Bacterial strains	26
2.1.5. Antibodies	27
2.2. Molecular biology methods	28
2.2.1. Polymerase chain reaction (PCR)	28
2.2.2. Long template PCR	29
2.2.3. Agarose gel electrophoresis	30
2.2.4. Estimation of DNA concentration	30
2.2.5. Gateway cloning technology	31
2.2.6. Cloning of inserts into pGEX-4T-1 vector	32
2.2.7. Transformation of chemically competent <i>E. coli</i> cells	33
2.2.8. Purification of plasmid DNA	33
2.2.9. Site-directed mutagenesis	34
2.2.10. Sequencing of DNA	34
2.2.11. Isolation of genomic DNA from flies	35
2.2.12. Culture and transfection of Schneider 2 cells	36
2.3. Biochemical methods	36
2.3.1. Protein extraction from embryos	36
2.3.2. Protein extraction from S2 cells	37
2.3.3. Determination of protein concentration	37
2.3.4. SDS-polyacrylamide gel electrophoresis	37
2.3.5. Western blot	38
2.3.6. Coomassie staining	38
2.3.7. GST and MBP fusion protein purification	38
2.3.8. MBP fusion protein pulldown	39
2.3.9. Lipid overlay assay	39
2.3.10. Endosome fractionation assay	40
2.4. Immunohistochemistry	40
2.4.1. Fixation of embryos	40
2.4.2. Immunostaining of embryos	41
2.4.3. Fixation and immunostaining of ovaries	41

Contents

2.4.4.	Fixation and immunostaining of S2 cells	42
2.4.5.	Staining of DNA	42
2.4.6.	Staining of lysosomes with LysoTracker	42
2.4.7.	Staining of actin microfilaments	42
2.4.8.	Dextran uptake assay	43
2.4.9.	Confocal microscopy, image acquisition and statistical analysis	43
2.5.	Fly genetics	43
2.5.1.	Fly breeding	43
2.5.2.	Fly stocks	44
2.5.3.	The UAS-GAL4 system	46
2.5.4.	Generation of transgenic flies	46
2.5.5.	FLP/FRT mediated gene deletion	47
3.	Results	50
3.1.	Localization of Rush	50
3.1.1.	Colocalization of Rush with polarity markers	50
3.1.2.	Rush associates with endosomes	53
3.1.3.	Effect of Rush overexpression on endocytic compartments	56
3.2.	Rush modifies the shape of Rab5-induced early endosomes	61
3.3.	Lipid binding properties of Rush	66
3.4.	Generation of <i>rush</i> mutant allele	71
3.5.	Characterization of <i>rush</i> null allele	72
3.6.	<i>rush</i> genetically interacts with <i>cdc42</i>	77
3.7.	Rush interacts with Rab GDI and <i>Drosophila</i> homolog of GDF	83
4.	Discussion	88
4.1.	Localization of Rush	88
4.1.1.	Subcellular localization of Rush	88
4.1.2.	Role of lipid binding domains in Rush localization	89
4.2.	Function of Rush in endocytosis	90
4.2.1.	Rush regulates late endosome formation	90
4.2.2.	Rush changes the morphology of Rab5CA vesicles	92
4.3.	Possible role of Rush in signaling pathways	93
4.4.	Genetic interaction between <i>rush</i> and <i>Cdc42</i>	94
4.5.	Rush interaction with Rab GDI and GDF	96
4.6.	Model of Rush function	97
5.	Summary and conclusions	99
6.	Bibliography	101
	Abbreviations	115
	Appendix	117
	Curriculum vitae	122

Acknowledgements

First of all, I want to thank Prof. Andreas Wodarz for the supervision during these years, for the support and advice during the many turns of the project, and for giving me the possibility to develop my own ideas.

I thank Prof. Ivo Feussner and Prof. Reinhard Schuh for being a part of my thesis committee and for the helpful comments during committee meetings.

I am grateful to Dr. Steffen Burkhardt, Ivana Bacakova and Kerstin Grüninger from the Molecular Biology program for the enormous support of students and for the excellent organization of the program.

I want to thank all members of the Stem Cell Biology department for making these years highly enjoyable. Thanks to Mona, Katja and Claudia for the excellent technical support and for keeping the lab together and running, Tobi for many untranslatable German expressions, Nils for surreal conversations, Hamze and Karen for the fun times in the big lab, Gang for the optimism and delicious Chinese food, Michael for the help in the world of flies, Sasha for the best fly food and Patricia for the guidance through the kingdom of papers and documents. Thanks to Tanja for being the best supervisor and for the help in the first year, Soya for the optimism and for the collaboration, and Ankathrin for the introduction to the fly work.

Thanks to my office mates Irina, Ulli and Fred for the great atmosphere, mutual support and for keeping the spirits up.

Thanks to Konstantina, Katharina and Marija for the friendship through these years and the infrequent, but necessary escape from the lab life, Martina, Nora and Kerstin for extended Gromo breakfasts, Achim and Adema for the fights of Titans, and Ilze for keeping me from forgetting Latvian language.

Special thanks to Sabi for the immense support in my „hatching“ as a doctor, for the great time together and for making me feel at home in Germany.

My biggest thanks to my family for supporting their „lost“ daughter/sister and for their constant belief in me and my abilities.

Abstract

Endocytosis regulates multiple cellular processes, including the protein composition of the plasma membrane, intercellular signaling and cell polarity. Cell polarity is defined by asymmetric localization of membrane-associated protein complexes. Defects in endocytosis can lead to faulty distribution of polarity proteins and ultimately to the loss of cell polarity. The small GTPase Cdc42 has recently been described to regulate endocytosis of polarity proteins in *Drosophila* epithelial cells. While the role of Cdc42 in the regulation of early endocytotic steps is quite well described, it is still not known how Cdc42 influences late endosome formation. Here I describe Rush hour (Rush), a previously uncharacterized and highly conserved protein that genetically interacts with Cdc42 in regulation of late endosome formation. Rush is a lipid interacting protein and localizes to the lateral plasma membrane of epithelial cells and to late endosomes. Rush promotes late endosome formation and *rush* mutants have a decreased late endosome size. Rush interacts with Cdc42 in regulation of endocytosis of the apical polarity protein Crumbs, and loss of *rush* rescued the phenotype caused by overexpression of dominant negative Cdc42. Rush binds directly to Rab GDI and could regulate endocytosis by affecting Rab activation on the membrane of late endosomes. Lysosomal marker staining is decreased in Rush overexpressing cells, indicating that Rush might regulate the transition between late endosomes and lysosomes. In addition, Rush causes fractionation of enlarged early endosomes that are formed by overexpression of constitutively active Rab5. These results suggest that Rush might act in trafficking steps both from the early to late endosomes and from late endosomes to lysosomes.

List of figures

Figure 1-1. A simplified scheme of endocytosis	9
Figure 1-2. The Rab GTPase cycle	12
Figure 1-3. Comparison of epithelial cell membrane domains in <i>Drosophila</i> and vertebrates	14
Figure 1-4. Interactions between Par/aPKC, Crb and Scrib complexes in <i>Drosophila</i> epithelial cells	16
Figure 1-5. Possible effects of the Par/aPKC complex on endocytosis of Crb and E-cadherin	20
Figure 1-6. Protein structure of Rush	21
Figure 2-1. Gateway recombination reaction	32
Figure 2-2. FLP/FRT mediated deletion of <i>rush</i> gene	49
Figure 3-1. The localization and structure of <i>rush</i>	51
Figure 3-4. Colocalization of Rush with endosome markers	55
Figure 3-5. Rush colocalizes with endosome markers in the oocyte	55
Figure 3-6. Rush cofractionates with endosomal markers	56
Figure 3-7. Overexpression of Rush-GFP does not affect localization of polarity markers	57
Figure 3-8. Rush-GFP colocalizes with late endosome markers	58
Figure 3-9. Rush colocalizes with Hrs and endocytosed dextran in wing discs	59
Figure 3-10. LTR staining is decreased in Rush-GFP overexpressing follicle epithelium	60
Figure 3-11. Overexpression of Rush-GFP in the follicle epithelium causes germline apoptosis	61
Figure 3-12. Rush-GFP changes the shape of Rab5CA-induced endosomes	63
Figure 3-13. Rab5CA expression changes the localization of Rush-GFP	64
Figure 3-14. Rab7 localizes to Rush-GFP and YFP-Rab5CA vesicles	65
Figure 3-15. Localization of Rab11 in Rush-GFP and/or YFP-Rab5CA expressing follicle epithelium	66

List of figures

Figure 3-16. Lipid binding specificity of Rush	68
Figure 3-17. Subcellular localization in Rush lipid binding defective mutants	69
Figure 3-18. Generation of <i>rush</i> null allele	72
Figure 3-19. Loss of Rush does not affect localization of Baz	73
Figure 3-20. Egg chambers of <i>rush</i> ⁴ flies display defects in oogenesis	75
Figure 3-21. The effect of <i>rush</i> deletion on endosomal compartments	76
Figure 3-22. Formation of early endosomes is not affected in <i>rush</i> mutant cells	77
Figure 3-23. Overexpression of Rush-GFP in embryonic ectoderm leads to an increase in Crb endocytosis	79
Figure 3-24. Cdc42DN causes mislocalization of Crb and E-cadherin	79
Figure 3-25. Cdc42DN causes formation of enlarged Rab7 endosomes	81
Figure 3-26. Loss of <i>rush</i> rescues <i>arm</i> >Cdc42DN phenotype	82
Figure 3-27. Rush directly interacts with CG1418 and GDI	84
Figure 3-28. Localization of GDI and CG1418 in S2 cells	85
Figure 3-29. Localization of GFP-GDI and GFP-CG1418 in the follicle epithelium	86
Figure 3-30. GDI associates with endosomes	87
Figure 4.1. Model of Rush function in endocytosis	97

List of tables

Table 1-1. Localization of evolutionarily conserved proteins in epithelial junctions of <i>Drosophila</i> and vertebrates _____	14
Table 2-1. List of oligonucleotides _____	23
Table 2-2. List of vectors _____	25
Table 2-3. List of bacterial strains _____	26
Table 2-4. List of primary antibodies _____	27
Table 2-5. List of secondary antibodies _____	28
Table 2-6. Standard PCR program _____	29
Table 2-7. PCR mix for verification of <i>Rush</i> deletion. _____	29
Table 2-8. PCR program for long template PCR. _____	30
Table 2-9. PCR program for site-directed mutagenesis reaction _____	34
Table 2-10. PCR program for sequencing reaction _____	35
Table 2-11. List of fly stocks. _____	44
Table 2-12. Transgenic constructs used for injection in flies. _____	47

1. Introduction

Endocytosis is one of basic cell functions and acts in a multitude of cellular processes, including regulation of the plasma membrane lipid and protein content. Endocytosed molecules can then be degraded or sent back to the plasma membrane. Thus endocytosis allows fine-tuning of the amounts of different plasma membrane components. Cell polarity is established by action of conserved protein complexes that asymmetrically localize at the plasma membrane. Epithelial cells are one of best characterized polarized cell types. In addition to having distinct membrane domains, epithelial cells adhere to each other via intercellular junctions. Uptake of polarity complexes or junctional proteins by endocytosis leads to changes in cell polarity or in the rigidity of the epithelial layer. Interestingly, polarity proteins like Cdc42 are able to regulate endocytic trafficking and therefore affect cell polarity by an additional mechanism. The mode of action of these polarity complexes in regulation of endocytosis is still largely unknown. In this work I describe characterization of CG14782, a new endosome associated protein. Due to the phenotype associated with the deletion and overexpression of CG14782 we named the gene *rush hour* (*rush*). The role of Rush in epithelial cells in regard to regulation of the endosomal pathway and uptake of polarity proteins was investigated in this work.

1.1. Endocytosis

Cells are limited from the extracellular space with a plasma membrane, which is impermeable for large molecules. While small molecules like ions, sugars or amino acids can cross the membrane via specialized channels or transporters, uptake of larger molecules is mediated by endocytosis. During the process of endocytosis, vesicles that contain the cargo bud off from the internal side of the plasma membrane. Internalized molecules are then processed through several endocytic compartments and are either degraded or delivered back to the plasma membrane. Diverse functions of endocytosis include regulation of signaling pathways, nutrient uptake, neurotransmission and regulation of cell polarity. Several modes of molecule internalization have been described, including clathrin-mediated endocytosis, caveolae-mediated endocytosis, phagocytosis and pinocytosis (Doherty and McMahon, 2009). These pathways differ in the type of endocytosed cargo and in molecules that are involved in vesicle budding and separation from the plasma membrane. Nevertheless, the vesicles formed by diverse internalization

pathways converge in common compartments and are then further processed along the endocytic pathway (Gruenberg, 2001). The properties of different endocytic compartments will be described in more detail in the following chapter.

1.1.1. Endocytic compartments

The endocytic pathway is comprised of a variety of organelles – early or sorting endosomes, recycling endosomes, late endosomes or multivesicular bodies (MVBs) and lysosomes (Fig. 1-1). These organelles are highly interconnected by exchange of endocytosed material and membrane. Although dynamically connected, each of the organelles has a distinct function and molecular markers that allow to distinguish these vesicular compartments. Among the most widely used markers of the endocytic pathway are Rab proteins. Rabs are small GTPases that are specifically located to different compartments and are thought to maintain the functional identity of endosomes (Pfeffer, 2001; Zerial and McBride, 2001).

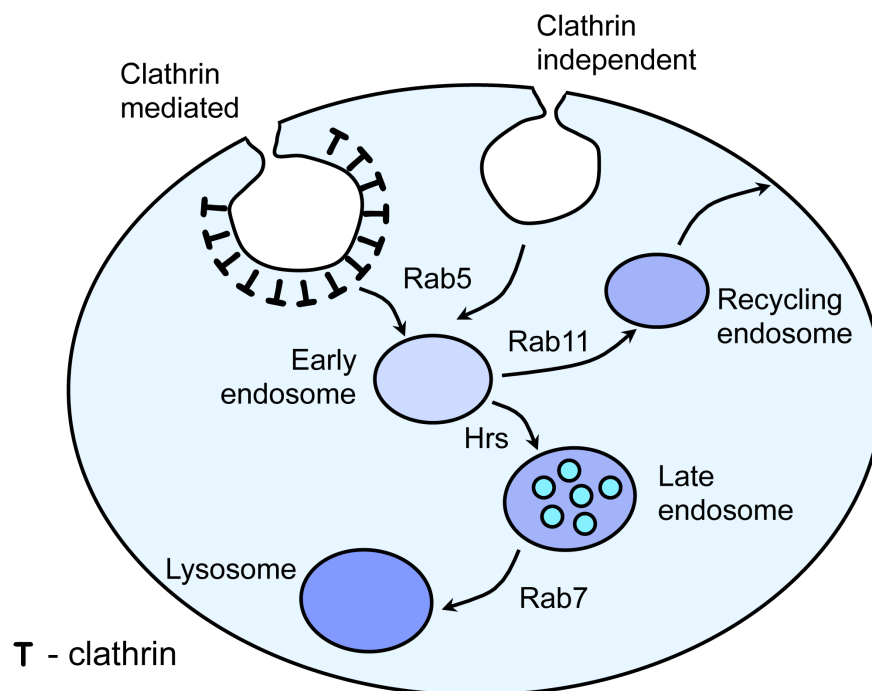


Figure 1-1. A simplified scheme of endocytosis. Cargo is taken up by either clathrin dependent or independent endocytosis and then transported to early endosomes. Molecules are then either sent back to the plasma membrane via recycling endosomes or degraded via late endosome/lysosome pathway.

Early endosomes

The early or sorting endosome is the first station at which various endocytosed vesicles converge. At this level sorting of cargo takes place. Molecules that will be delivered back to the plasma membrane are delivered either directly from the early endosome or sorted into recycling endosomes (Sheff et al., 1999). Endocytosed molecules that are destined for degradation will end up in late endosomes and finally in lysosomes. Rab5 is the main molecular marker of early endosomes. Rab5 is involved in budding of clathrin-coated vesicles from the plasma membrane (McLauchlan et al., 1998) and later promotes fusion of these vesicles with early endosomes (Bucci et al., 1992, Morrison et al., 2008). In addition, Rab5 regulates fusion of early endosomes with each other or so called homotypic fusion (Gorvel et al., 1991). Early endosomes are characterized by high phosphatidylinositol-3-phosphate (PI(3)P) content due to Rab5-mediated recruitment of the class III phosphatidylinositol-3-kinase (PI(3)K) (Christoforidis et al., 1999, Murray et al., 2002). PI(3)P is specifically found in early endosomes and on internal membranes of late endosomes (Gillooly et al., 2000; Gillooly et al., 2001). High PI(3)P concentration on early endosomes leads to recruitment of several proteins that contain FYVE domains - lipid binding domains with high specificity towards PI(3)P (Burd and Emr, 1998; Gaullier et al., 1998; Patki et al., 1998; Stenmark et al., 1996). One of such proteins is Hrs, a protein that is involved in multivesicular body formation and protein segregation of proteins that are targeted for degradation (Bache et al., 2003; Lloyd et al., 2002; Pons et al., 2008). Hrs also has been proposed to inhibit homotypic fusion of early endosomes (Sun et al., 2003).

Recycling endosomes

Recycling endosomes are compartments that mediate delivery of endocytosed molecules back to the plasma membrane. While constitutive recycling from early endosomes is mediated by a transport directly to the plasma membrane, regulated recycling of molecules takes place via recycling endosomes (Sheff et al., 1999). Recycling endosomes are thought to form by pinching of tubular structures off from early endosomes (Mellman 1996). Proteins are then delivered from the recycling endosome to the plasma membrane with small transport vesicles. Rab11 serves as a marker of recycling endosomes and regulates trafficking through recycling endosomes (Ullrich et al., 1996; Trischler et al., 1999). Rab11 has also been found on the *trans*-Golgi network (TGN) and regulates transport between TGN and recycling endosomes (Chen et al., 1998; Lock and Stow, 2005).

Late endosomes

Late endosomes or MVBs deliver molecules for degradation in lysosomes. Proteins that are destined for degradation become monoubiquitinated and are sorted by Hrs and ESCRT (endosomal complexes required for transport) proteins in microdomains on the endosome membrane (Lloyd et al., 2002; Pons et al., 2008). This leads to a sequential recruitment of three ESCRT complexes – ESCRT-I, ESCRT-II and ESCRT-III (Babst et al., 2002a; Babst et al., 2002b; Katzmann et al., 2001). These complexes are necessary for invagination and budding off of these domains inside of the late endosome. This leads to formation of small intraluminal vesicles, hence the term MVBs. Proteins and lipids that are sorted in intraluminal vesicles as well as the soluble cargo are then degraded upon fusion with lysosomes. Both lysosomes and late endosomes have acidic intraluminal pH, which promotes the activity of hydrolases (Bond and Butler, 1987). Late endosomes can be distinguished from lysosomes by the presence of Rab7 (Chavrier et al., 1990).

The mechanism of transition between early and late endosomes is still not completely clear. Two models have been proposed: first - transport of material from early to late endosomes by small endosomal carrier vesicles (Vonderheit and Helenius, 2005); second - formation of late endosomes by early endosome maturation (Rink et al., 2005). Although the debate is still ongoing, the model of endosome maturation has received substantial experimental support over the last years (Lakadamyali et al., 2006; Rink et al., 2005). According to this model, Rab7 becomes loaded on early endosomes as they undergo the maturation process to late endosomes (Del Conte-Zerial et al., 2008; Rink et al., 2005). Active Rab5 is able to bind Rab7 guanine nucleotide exchange factor (GEF) and could thus promote activation of Rab7 and transition to the late endosome (Rink et al., 2005).

The function of Rab7 in endocytosis is still under discussion, with some observations indicating its function in transition from early to late endosomes (Vonderheit and Helenius, 2005), while other results point towards a role of Rab7 in fusion of late endosomes to lysosomes (Vanlandingham and Ceresa, 2009).

1.1.2. Rab GTPase cycle

Rab proteins play a central role in endocytosis and other major vesicle trafficking pathways. 33 *Rab* genes are encoded in *Drosophila* genome, while more than 60 *Rab* genes are present in human cells (Zhang et al., 2007). Main functions of Rabs are in vesicle budding, transport and fusion (Grosshans et al., 2006; Zerial and McBride, 2001). Rabs are

small GTPases of the Ras superfamily and cycle between a GTP bound active state and a GDP bound inactive state. Conversion between these two conformations is driven by action of several Rab interacting proteins (Fig. 1-2). Rabs are converted to an active state by a guanine nucleotide exchange factor (GEF) that catalyzes GDP exchange to GTP. In the active state Rabs are bound to membranes with their geranygeranyl anchor and interact with their effector proteins, thus exerting their functions. Inactivation of Rabs by GTP hydrolysis is facilitated by a GTPase activating protein (GAP). In the GDP bound state Rabs are removed from the membrane by binding to a GDP dissociation inhibitor (GDI) and reside in the cytosol.

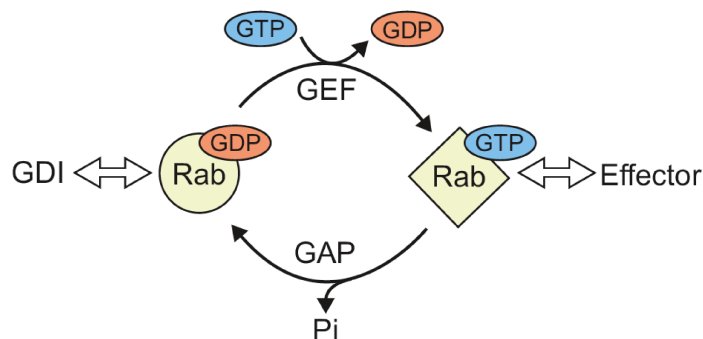


Figure 1-2. The Rab GTPase cycle. Inactive GDP bound Rab is converted to the active form by nucleotide exchange, catalyzed by GEF. Inactivation of Rab takes place by GAP-catalyzed hydrolysis of GTP. In the active form Rab is bound to a membrane and interacts with its effector proteins, while inactive Rab associates with GDI and is cytosolic. Adapted from Stenmark and Olkkonen, 2001.

Rabs have a highly specific localization to membranes of different cell compartments. To achieve this, GDI has to be able to deliver inactive Rab to the specific target membrane, where it can be activated and exert its function. It has been proposed that GDI is recruited to target membranes by a GDI displacement factor (GDF), which promotes release of otherwise tightly bound Rab from GDI (Dirac-Svejstrup et al., 1997; Hutt et al., 2000; Sivars et al., 2003). So far only two GDF factors with a distinct subcellular localization, PRA and PRA2, have been described in detail (Abdul-Ghani et al., 2001), although 16 PRA family proteins are found in humans (Pfeffer and Aivazian, 2004). As the number of putative GDF factors is smaller than that of Rab proteins, it has been proposed that GDF factor mediates delivery of Rab on a membrane close to its target site. Then Rab would diffuse freely in the membrane system until Rab encounters its GEF or effector proteins

and therefore becomes stabilized in a respective membrane microdomain (Grosshans et al., 2006; Pfeffer and Aivazian, 2004).

1.2. Cell polarity

Cell polarity is an essential feature of a variety of cell types and is necessary for diverse functions like growth, chemotaxis, directed molecule transport across the cell and tissue development in multicellular organisms. Polarization of a cell is initiated by an external or internal signal or polarity cue. This signal is recognized by receptors and propagated by signaling cascades in a polarized fashion. The signaling activated by the polarity cue results in changes in the structure of the cytoskeleton, directed transport of proteins and membrane components or changes in the localization of organelles. The polarity cue can be, for example, contact with another cell or with the extracellular matrix, which causes an epithelial cell to assemble specific junction complexes and form epithelial tissue (Drubin and Nelson, 1996).

1.2.1. Epithelial cell polarity

Epithelial cells are among the most extensively investigated types of polarized cells. Polarity in an epithelial cell is established on one hand by protein complexes that regulate formation of distinct membrane domains, and, on the other hand, by polarized endocytosis and exocytosis of these polarity complexes (Leibfried and Bellaiche, 2007). Processes that lead to polarity establishment and regulation in epithelial cells are highly conserved and have been widely studied in *Drosophila melanogaster*.

Epithelial cells function as a barrier between the tissue and the external environment and separate tissues in compartments. To be able to perform these functions epithelial cells have an elaborate junction system, which separates the plasma membrane of epithelial cells in the apical and the basolateral domain. The basolateral plasma membrane is in contact with other cells or extracellular matrix, while the apical domain faces the external environment. These plasma membrane domains differ in their protein and lipid composition. Intercellular junctions and membrane domains of epithelial cells in *Drosophila* and vertebrates are shown in Fig. 1-3.

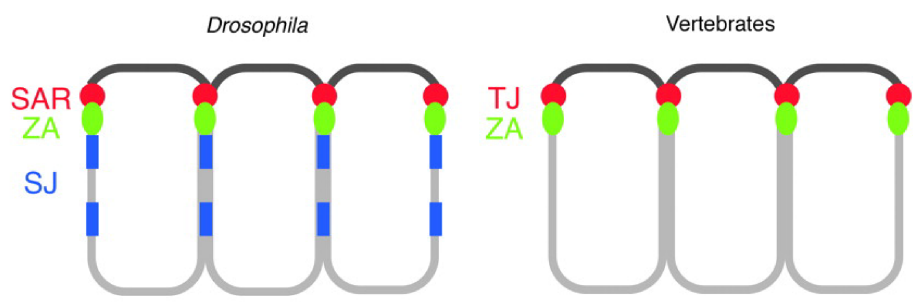


Figure 1-3. Comparison of epithelial cell membrane domains in *Drosophila* and vertebrates.

Abbreviations: SAR – subapical region, ZA – zonula adherens, SJ – septate junction, TJ – tight junction. Similar colors indicate similar protein composition in the regions (see Table 1-1). Apical membrane is indicated in black, basolateral membrane – in grey. Adapted from Knust and Bossinger, 2002.

Drosophila epithelial cells possess adherens junctions that form a belt-like structure, named zonula adherens (ZA), and septate junctions, which are located basally from the ZA along the basolateral membrane (Knust, 2000). Adherens junctions are formed by E-cadherin mediated homophilic contacts between neighboring cells. E-cadherin itself is linked to actin filaments via interaction with α -, β - and γ -catenins, thereby strengthening the tissue (Yap et al., 1997). Epithelial cells in *Drosophila* do not possess tight junctions, but the homologs of vertebrate tight junction components are found apically from adherens junctions in the subapical region (Müller, 2000; Knust and Bossinger, 2002; Johnson and Wodarz, 2003).

Table 1-1. Localization of evolutionarily conserved proteins in epithelial junctions of *Drosophila* and vertebrates (adapted from Knust and Bossinger, 2002).

<i>Drosophila</i>		Vertebrates	
<u>Subapical region:</u>	Bazooka	<u>Tight junction:</u>	Par3
	DmPar6		Par6
	DaPKC		aPKC
	Cdc42		Cdc42
	Crumbs		CRB
	Stardust		Pals1
	DPATJ		PATJ

<u>Adherens junction:</u>	Shotgun (DE-Cadherin) Armadillo (β -catenin) α -catenin	<u>Adherens junction:</u>	E-Cadherin β -catenin α -catenin
<u>Basolateral membrane, septate junction:</u>	Scribble Discs large	<u>Basolateral membrane:</u>	SCRIB hDLG

On a morphological level cell-cell junctions are one of the first landmarks of polarized epithelial cells. However, formation and proper localization of these junctions depends on a concerted action of many proteins (Table 1-1; Cox et al., 1996; Müller and Wieschaus, 1996). These proteins are evolutionarily conserved and assemble in so called polarity complexes (Margolis and Borg, 2005). Two protein complexes, the Par/aPKC complex and the Crumbs complex, are localized to the subapical region and apical plasma membrane. The Par/aPKC complex consists of Bazooka (Baz), atypical protein kinase C (aPKC), Par6 and the small GTPase Cdc42 (Suzuki and Ohno, 2006). Baz and Par6 are PDZ (PSD95, Discs large, Zona occludens-1) domain-containing scaffold proteins, while aPKC is a serine-threonine kinase. The Crumbs complex is formed by Crumbs (Crb), Stardust (Sdt) and PATJ (Bachmann et al., 2001; Hong et al., 2001). Crb is a transmembrane protein with a large extracellular part and a short cytoplasmic region, which is crucial for the function of Crb. Sdt is a MAGUK (membrane-associated guanylate kinase) protein that contains a PDZ domain, a SH3 (Src homology 3) domain and a GUK (guanylate kinase like) domain. PATJ is a PDZ domain scaffold protein. These two protein complexes confer apical characteristics to the plasma membrane (Hutterer et al., 2004; Petronczki and Knoblich, 2001; Wodarz et al., 2000; Wodarz et al., 1995).

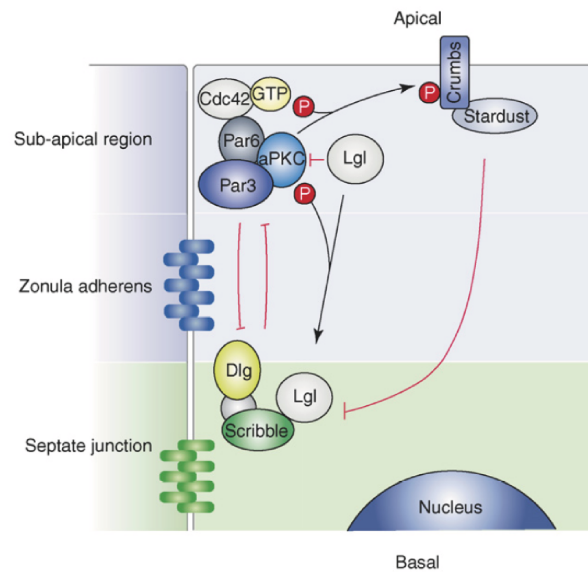


Figure 1-4. Interactions between Par/aPKC, Crb and Scrib complexes in *Drosophila* epithelial cells. Red lines indicate antagonistic interaction between complexes (Humbert et al., 2006).

Another polarity complex localizes to the basolateral plasma membrane and consists of Scribble (Scrib), Discs large (Dlg) and Lethal giant larvae (Lgl) proteins (Bilder et al., 2000). Scrib is a cytosolic protein that contains four PDZ domains and 16 leucine-rich repeats that are implicated in localization of Scrib to the plasma membrane (Navarro et al., 2005). Both Dlg and Lgl are cytoplasmic; Dlg is a MAGUK protein, while Lgl contains several WD40 repeats. Apical and basolateral protein complexes are mutually antagonistic in regulation of apical and basolateral membrane formation, and mutations in any of them lead to defects in epithelial polarity (Fig. 1-4; Bilder et al., 2003; Tanentzapf and Tepass, 2003). The Par/aPKC complex initiates the assembly of adherens junctions and polarization of epithelia (Harris and Peifer, 2005). The Scrib complex counteracts the Par/aPKC complex to allow formation of the basolateral membrane domain, while phosphorylation of Lgl by aPKC restricts its activity to the basolateral membrane (Fig. 1-4; Betschinger et al., 2003; Bilder and Perrimon, 2000; Hutterer et al., 2004). In addition, the Crb complex is necessary to maintain the apical membrane domain by inhibition of the Scrib complex (Bilder et al., 2003; Tanentzapf and Tepass, 2003).

In addition to differences in the protein composition apical and basolateral membrane domains have a distinct lipid composition. The apical membrane is enriched in PI(4,5)P₂, while PI(3,4,5)P₃ is more abundant at the basolateral plasma membrane (Gassama-Diagne et al., 2006; Martin-Belmonte et al., 2007). PI(4,5)P₂ in turn recruits Cdc42 via Annexin II to the apical plasma membrane and therefore promotes establishment of apical plasma

membrane domain (Martin-Belmonte et al., 2007).

1.2.2. Endocytosis in regulation of cell polarity

The balance between the apical and basolateral polarity complexes is essential to maintain proper epithelial polarity. This balance is regulated on one hand by delivery of newly synthesized proteins to the cell membrane, and on the other hand by endocytosis of excess of proteins from the plasma membrane (Leibfried and Bellaiche, 2007).

Adherens junctions are crucial for the function of epithelial cells and maintenance of their polarity. E-cadherin is a core component of adherens junctions and ensures interaction between two epithelial cells by homophilic binding between two E-cadherin molecules. Regulation of E-cadherin by endocytosis has been widely investigated in mammalian cells. E-cadherin trafficking is important in regulation of cell-cell contact dynamics (Le et al., 1999). After uptake in early endosomes E-cadherin can follow two routes through the endocytic pathway (Delva and Kowalczyk, 2009). E-cadherin can be delivered back to the plasma membrane via the recycling endosome. This results in reinforcement of cell-cell contacts at tight junctions. Rab11 activity is necessary for efficient E-cadherin recycling. If Rab11 is mutated, E-cadherin is lost from the plasma membrane and polarity of the cells is disrupted (Desclozeaux et al., 2008). Alternatively, E-cadherin can be sent for degradation in lysosomes, thus decreasing the number of E-cadherin molecules at the cell surface. As a result, cell-cell contacts become weaker. Upon excessive removal of E-cadherin from plasma membranes the cells lose adherens junctions and finally undergo epithelial-mesenchymal transition (Lu et al., 2003; Palacios et al., 2005).

In the *Drosophila* embryo, uptake of E-cadherin from adherens junctions by endocytosis is especially active during embryonic development, when rapid cell movement and tissue remodeling takes place (Emery and Knoblich, 2006). Expression of dominant negative Rab11 leads to defects in the recycling of E-cadherin and Crb and their loss from the plasma membrane (Roeth et al., 2009). Interestingly, Crb becomes mislocalized first, suggesting that Crb might be either more sensitive towards defects in recycling, or mislocalization of E-cadherin might be caused by loss of Crb.

Defects in early endocytosis can also lead to loss of cell polarity. Deletion of *Rab5* or *avalanche*, a protein involved in early endosome formation, leads to accumulation of Crb at the apical membrane (Lu and Bilder, 2005). Upon defects in early steps of endocytosis excess of Crb cannot be removed from the plasma membrane. The epithelial cells lose their

polarity, and begin to overproliferate, leading to tumorous overgrowths. Also defects in later steps of endocytosis can affect cell polarity. Erupted (Ept) and Vps25 are components of the ESCRT machinery and are needed for the transition from early to late endosome. Loss of *ept* and *vps25* leads to defects in Crb localization, apicobasal polarity of epithelial cells and tissue overgrowth (Moberg et al., 2005; Thompson et al., 2005; Vaccari et al., 2005). In addition, mutations in Scrib complex genes also lead to expansion of the apical membrane domain and tumors, indicating that defects in polarity can promote tissue overproliferation (Bilder et al., 2000).

Investigations in both mammalian and *Drosophila* systems indicate that endocytosis is an important mechanism in regulation of cell polarity. The regulation of cell polarity via endocytosis depends on degradation and recycling of the polarity complexes. Disruption of any of the steps along the endocytic pathway results in overaccumulation or loss of polarity proteins and ultimately to defects in the polarity and function of epithelial cells.

1.2.3. The Par/aPKC complex in regulation of endocytosis

As discussed in the previous chapter, endocytosis is involved in regulation of cell polarity complexes. Recent discoveries show that some of the polarity proteins also participate in regulation of endocytosis. In a genetic screen in *C.elegans* the Par/aPKC complex was found to regulate endocytosis (Balklava et al., 2007). According to the results of the screen, Par/aPKC complex proteins seem to act on several steps in endocytosis – they promote clathrin-dependent endocytosis and maintain functional recycling endosomes. It is still unknown which effector proteins mediate the function of the Par/aPKC complex in endocytosis in *C.elegans*.

In *Drosophila*, the Par/aPKC complex regulates the uptake of adherens junction proteins like E-cadherin and of apical markers like Crb in early endosomes (Gerogiou et al. 2008; Harris and Tepass 2008; Leibfried et al. 2008). Interestingly, the localization of basolateral proteins was not affected by mutations of the Par/aPKC complex proteins, indicating that different mechanisms regulate their turnover (Harris and Tepass, 2008; Leibfried et al., 2008). In *Drosophila* pupal epithelium, Cdc42 promotes endocytosis of E-cadherin. When Cdc42, Par6 or aPKC is lost, E-cadherin cannot be efficiently endocytosed, leading to destabilization of adherens junctions (Gerogiou et al. 2008; Leibfried et al. 2008). The effect of the Par/aPKC complex on early steps of endocytosis is mediated by the Cdc42 effector Cip4 (Leibfried et al., 2008). Cip4 binds to dynamin and promotes vesicle

formation and scission (Leibfried et al., 2008). Cip4 also interacts with the Arp2/3 complex, which initiates actin polymerization and thus links vesicle fission and transport (Leibfried et al., 2008; Fricke et al., 2009). In contrast, studies in *Drosophila* embryonic ectoderm show that dominant negative Cdc42 leads to loss of E-cadherin and Crb from the plasma membrane, suggesting that active Cdc42 slows down endocytosis of these proteins (Harris and Tepass, 2008). Also studies in mammalian cells provide contradictory data about the role of Cdc42 in early endocytosis. Active Cdc42 has been proposed to inhibit uptake of dimeric E-cadherin at adherens junctions (Izumi et al., 2004), while another study shows that active Cdc42 is involved in ubiquitination and lysosome targeting of E-cadherin (Shen et al., 2008). In line with the latter observation that active Cdc42 promotes endocytosis, a Cdc42 GAP has been shown to reduce uptake of apical proteins by inactivating Cdc42 (Wells et al., 2006).

Par/aPKC complex proteins also regulate delivery of apical proteins to late endosomes via an unknown mechanism (Harris and Tepass, 2008). Dominant negative Cdc42 induces loss of Crb and Par/aPKC complex proteins from the plasma membrane and accumulation in Hrs positive endosomes. Similarly, deletion of the ESCRT protein Ept impairs transition to late endosomes and causes accumulation of Crb in early endosomes (Gilbert et al., 2009; Moberg et al., 2005). The role of other members of the Par/aPKC complex in late endosome formation is not clear so far. Although the phenotypes of *ept* loss of function and Cdc42 dominant negative flies are similar with regard to Crb trafficking, the effect of aPKC in these two genetic backgrounds was cardinally different. While constitutively active aPKC rescued the dominant negative Cdc42 phenotype (Harris and Tepass, 2008), dominant negative aPKC was able to rescue the Crb mislocalization phenotype caused by loss of *ept* (Gilbert et al., 2009).

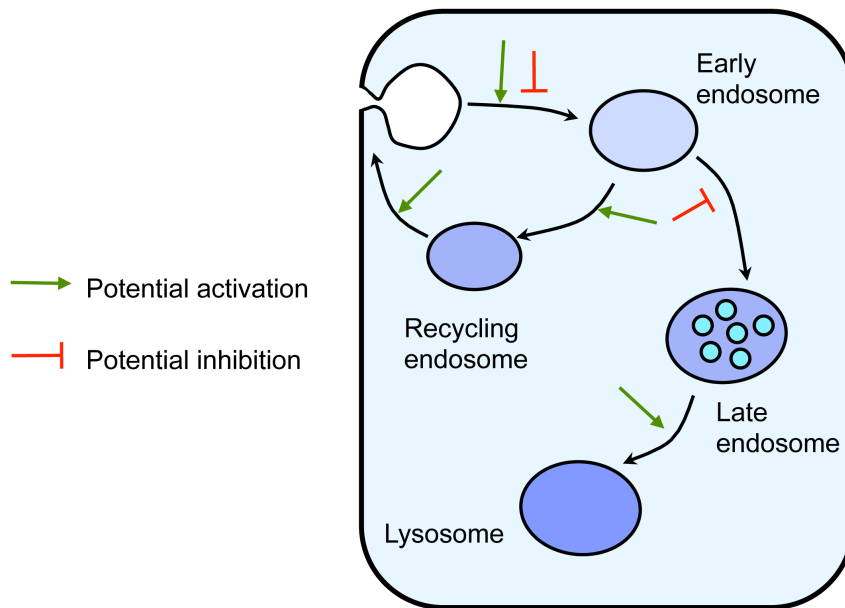


Figure 1-5. Possible effects of the Par/aPKC complex on endocytosis of Crb and E-cadherin. Endocytosed Crb and E-cadherin can be either recycled back to the plasma membrane or degraded in lysosomes. The places at which the Par/aPKC complex proteins may affect the trafficking are indicated with arrows.

Analysis of the role of Par/aPKC complex proteins in trafficking in *Drosophila* epithelia has revealed a complex picture. The effect of Cdc42 is so far best characterized. It seems that Cdc42 and other Par/aPKC complex members can act on different steps of endocytosis, and often the results show opposing effects (Fig. 1-5). Therefore further research will be needed to clarify the role of the Par/aPKC complex in endocytosis.

1.3. Rush – a new endosomal protein

Although the role of Par/aPKC complex proteins in regulation of endocytosis has been shown in a number of studies, the observed effects have been contradictory. In addition effectors of the Par/aPKC complex in endocytosis, especially at later stages, are largely unknown. In order to gain further insight in the function of the Par/aPKC complex, a yeast two-hybrid screen was conducted using the N-terminus of Baz as a bait. One of the isolated potential interaction partners of Baz was the product of the predicted gene *CG14782* (Egger-Adam, 2005). *CG14782* encodes a so far uncharacterized *Drosophila* protein with high sequence similarity along the full sequence length with homologs in other organisms from *C. elegans* to vertebrates (74,6 % sequence identity between *D. melanogaster* and *Homo sapiens*). We named the gene *rush hour* (*rush*) due to its

phenotype, which is described in the Results chapter. Rush consists mainly of two domains that are implicated in interaction with phosphoinositides - a PH (pleckstrin homology) domain and a FYVE (Fab1p, YOTB, Vac1p, EEA1) domain (Fig. 1-6). The FYVE domains have been described to bind exclusively to PI(3)P, while PH domains can interact with a broader set of phosphoinositides (Kavran et al., 1998; Lemmon, 2008). Most of FYVE domain containing proteins localize to endosomes (Gillooly et al., 2001), suggesting that Rush might be involved in endocytosis.

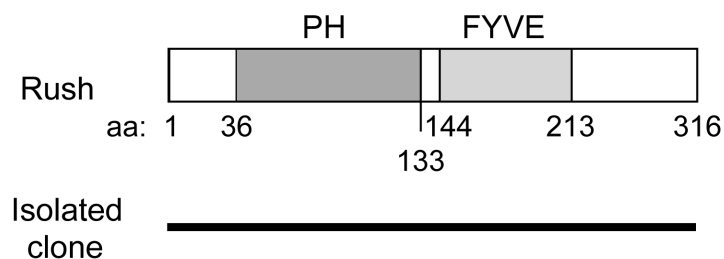


Figure 1-6. Protein structure of Rush. PH and FYVE domains are indicated. The black box depicts the cDNA clone, isolated in the yeast two-hybrid experiment. Adapted from Egger-Adam, 2005.

Rush has two human homologs, Phafin1 and Phafin2, with the highest similarity to Phafin2. The role of these proteins in human cells is poorly characterized. Both Phafin1 and Phafin2 were proposed to promote TNF α -induced apoptosis (Chen et al., 2005, Li et al., 2007, Li et al., 2008). Upon apoptosis-inducing stimulus, Phafin1 translocates to lysosomes and promotes permeabilization of lysosomal membranes (Chen et al., 2005, Li et al., 2008), while Phafin2 promotes endoplasmic reticulum-mediated apoptotic response (Li et al., 2007). In contrast to these results, a recent study proposed a role of Phafin2 in endocytosis (Lin et al., 2010). Expression of Phafin2 in the HepG2 human liver cancer cell line resulted in formation of enlarged endosomes, possibly due to activation of Rab5. Interestingly, Phafin2 is overexpressed in several cancer types like human hepatocellular carcinoma and breast cancer (Chen et al., 2002; Lin et al., 2010; Weisz et al., 2004).

The aim of this work was to investigate the role and function of Rush in *Drosophila* development. To this end I generated a *Rush* null allele and analyzed effects of Rush loss and overexpression in different epithelial systems. According to the domain structure of Rush and the function of the human homolog (Lin et al., 2010), Rush could act in regulation of endocytosis. To investigate this possibility colocalization of Rush with markers of the endosomal pathway as well as the effect of Rush deletion and

overexpression on endocytosis was analyzed. It was especially intriguing to determine whether Rush plays a role in endocytosis of polarity proteins or Par/aPKC-regulated endocytosis. For this purpose I performed genetic interaction experiments in a Cdc42 dominant negative background. The effect of dominant negative Cdc42 on endocytosis has been previously described (Harris and Tepass, 2008). Finally I used pulldown experiments with putative interaction partners deduced from genome-wide screens in yeast and mammals to gain an insight in the mechanism of Rush function.

2. Materials and Methods

2.1. Materials

2.1.1. Chemicals and enzymes

All chemicals were of analytical grade and purchased from following companies: Biomol (Hamburg, Germany), Bio-Rad (Munich, Germany), Biozym (Oldendorf, Germany), Difco (Detroit, USA), Fluka (Buchs, Switzerland), Gibco/BRL Life Technologies (Karlsruhe, Germany), Merck (Darmstadt, Germany), Polysciences (Eppelheim, Germany), Roth (Karlsruhe, Germany), Serva (Heidelberg, Germany), Sigma-Aldrich (Steinheim, Germany), Macherey-Nagel (Düren, Germany).

Solutions were prepared in distilled water and sterilized by autoclaving or sterile filtration. Enzymes for molecular biology methods were purchased from Bioline (Luckenwalde, Germany), Fermentas (St. Leon-Rot, Germany), Genecraft (Lüdingshausen, Germany), Promega (Madison, USA), Roche (Mannheim, Germany).

2.1.2. Primers

Primers were designed using DNA-Star Lasergene V6 program (DNASTAR Inc., Madison, USA). Primer synthesis was done by companies Biotez (Berlin, Germany) and Metabion (Martinsried, Germany). Primers used in this work are listed in Table 2-1.

Table 2-1. List of oligonucleotides

Name	Sequence 5' -> 3'	Description
EG-N-for	CACCGTGGACCGTCTGGTCAACTCG	Cloning of <i>rush</i> in pENTR
EG-N-rev	TCAACAGTGGCTGCCCCGTCGTCG	Cloning of <i>rush</i> in pENTR
EG-C-for	CACCATGGTGGACCGTCTGGTCAACTCG	Cloning of <i>rush</i> in pENTR
EG-C-rev	ACAGTGGCTGCCCCGTCGTCG	Cloning of <i>rush</i> in pENTR

Materials and Methods

CG1418 Ngatefor	CACCGCACACACTGGCGGGAACC	Cloning of <i>CG1418</i> in pENTR
CG1418 Ngaterev	TCAGACAACCTGGGCGAGGAAACC	Cloning of <i>CG1418</i> in pENTR
GDI Ngatefor	CACCAATGAGGAATACGATGCGATTG	Cloning of <i>GDI</i> in pENTR
GDI Ngaterev	TTACTGCTCCTCGTCACCCAACTCG	Cloning of <i>GDI</i> in pENTR
M13 for	GTAAAACGACGGCCAG	Sequencing of inserts in pENTR vector
M13 rev	CAGGAAACAGCTATGAC	Sequencing of inserts in pENTR vector
EGFP-C- for	CAAAGACCCCAACGAGAAG	Sequencing of destination vectors
EGFP-N- rev	CGGACACGCTGAACTTGTG	Sequencing of destination vectors
GST for	CAGCAAGTATATAGCATGGC	Sequencing of destination vectors
MBP for	GCGTGCTGAGCGCAGGTATTAACGCCGC	Sequencing of destination vectors
UASPf	GGCAAGGGTCGAGTCGATAG	Sequencing of destination vectors
CG gst for	CAGGATCCGTGGACCGTCTGGTCAACTCG	Cloning of <i>rush</i> in pGEX-4T-1
CG gst rev	GAGAATTCTCAACAGTGGCTGCCCCGTCG	Cloning of <i>rush</i> in pGEX-4T-1
FYVE gst for	CTGGATCCAACCACGCCGCCGTTTGGG	Cloning of Rush FYVE domain in pGEX-4T-1
FYVE gst rev	GTGAATTCTCAGTGCTTCAAGCGCTCGTAGC	Cloning of Rush FYVE domain in pGEX-4T-1

PH gst for	GAGGATCCCTGGTGGGCGAGGGC	Cloning of Rush PH domain in pGEX-4T-1
PH gst rev	GAGAATTCTCACAGGTCCTCCACGCAC	Cloning of Rush PH domain in pGEX-4T-1
FYR176Gf	GCATCACTGCGGCAACTGCGGCGCTGTTG	Point mutation R176G in Rush FYVE domain
FYR176Gr	CAACAGCGCCGCAGTTGCCGCAGTGATGC	Point mutation R176G in Rush FYVE domain
PH DN for	CCAAGATGTGTCGCGAGCGGCCCAAGTCG	Point mutation K48E in Rush PH domain
PH DN rev	CGACTTGGGCCGCTCGCGACACATCTTGG	Point mutation K48E in Rush PH domain
CG UTR down	GTATTTCTCCAAGTATTGCTGCCAGC	Verification of <i>rush</i> deletion
Sta rev	GTACATTGTTGTGGTAGTTACAGATGG	Verification of <i>rush</i> deletion
UP	GACGGGACCACCTTATGTTATTTTCATCATG	Verification of <i>rush</i> deletion

2.1.3. Vectors

Table 2-2. List of vectors

Plasmid	Description	Reference or source
pHSI-65	cDNA clone, containing <i>Rush</i> sequence	Egger-Adam, 2005
pENTR/D-TOPO	Entry vector for Gateway cloning, kanamycin resistance	Invitrogen, Carlsbad, Germany
pTGW	Expression vector, UAS _t promoter, N-terminal GFP tag, ampicilin resistance	Murphy lab, Baltimore, USA
pTWG	Expression vector, UAS _t promoter, C-terminal GFP tag, ampicilin resistance	Murphy lab, Baltimore, USA
pPWR	Expression vector, UAS _p promoter, C-terminal RFP tag, ampicilin resistance	Murphy lab, Baltimore, USA

Materials and Methods

pAHW	Expression vector, Actin5C promoter, N-terminal 3x HA tag, ampicillin resistance	Murphy lab, Baltimore, USA
pAWH	Expression vector, Actin5C promoter, C-terminal 3x HA tag, ampicillin resistance	Murphy lab, Baltimore, USA
pAGW	Expression vector, Actin5C promoter, N-terminal GFP tag, ampicillin resistance	Murphy lab, Baltimore, USA
pAWG	Expression vector, Actin5C promoter, C-terminal GFP tag, ampicillin resistance	Murphy lab, Baltimore, USA
pWAGAL4	GAL4 expression vector, Actin promoter	Y. Hiromi, unpublished
pGGWA	Destination vector for expression of GST fusion proteins in <i>E. coli</i> , ampicillin resistance	Murphy lab, Baltimore, USA
pMGWA	Destination vector for expression of MBP fusion proteins in <i>E. coli</i> , ampicillin resistance	Murphy lab, Baltimore, USA
pGEX-4T-1	Vector for expression of GST fusion proteins in <i>E. coli</i> , ampicillin resistance	Amersham Pharmacia Biotech, Buckinghamshire, England

2.1.4. Bacterial strains

Table 2-3. List of bacterial strains

Strain	Genotype	Application	Source
DH5 α	$\phi 80dlacZAM15$, $\Delta(lacZYA-argF)U169$, <i>deoR</i> , <i>recA1</i> , <i>endA1</i> , <i>hsdR17</i> ($r_K^- m_K^+$), <i>phoA</i> , <i>supE44</i> , λ^- , <i>thi-1</i> , <i>gyrA96</i> , <i>relA1</i>	Amplification of plasmid DNA	Invitrogen
BL21	F $^-$, <i>ompT</i> , <i>hsdS_B</i> (r_B^- , m_B^-), <i>dcm</i> , <i>gal</i> , λ (DE3)	Expression of recombinant proteins	Invitrogen
TOP10	F $^-$, <i>mcrA</i> , $\Delta(mrr-hsdRMS-mcrBC)$, $\phi 80dlacZAM15$, $\Delta lacX74$, <i>deoR</i> , <i>recA1</i> , <i>araD139</i> , $\Delta(ara, leu)7697$, <i>galK</i> , <i>rpsL</i> (<i>strr</i>), <i>endA1</i> , <i>nupG</i>	Cloning of PCR fragments in pENTR vector	Invitrogen
XL1-Blue	<i>endA1</i> , <i>gyrA96</i> (nal^R), <i>thi-1</i> , <i>recA1</i> , <i>relA1</i> , <i>lac</i> , <i>glnV44</i> , F $^+$ [$::Tn10$ proAB $^+$ <i>lacI^q</i> $\Delta(lacZ)M15$], <i>hsdR17</i> ($r_K^- m_K^+$)	Site-directed mutagenesis	Stratagene

2.1.5. Antibodies

Table 2-4. List of primary antibodies

Epitope	Animal	Dilution	Designation	Reference, source
Actin	Rabbit	1:1000	A2066	Sigma
Bazooka	Rabbit	1:1000	DE99646-2	Wodarz et al., 2000
Bazooka	Rat	1:1000	DE99647-1	Wodarz et al., 1999
Rush C-term	Rabbit	1:1000	DE03410, affinity purified, EP033850	Egger-Adam, 2005
Crb	Mouse	1:50	Cq 4	Developmental Studies Hybridoma Bank, University of Iowa, USA
DE-Cadherin	Rat	1:2	DCAD 2	Developmental Studies Hybridoma Bank, University of Iowa, USA
FasIII	Mouse	1:20	7G10	Developmental Studies Hybridoma Bank, University of Iowa, USA
GDI2	Rabbit	1:1000	AV13037	Sigma-Aldrich
GFP	Mouse	1:1000	# 11 814 460 001	Roche
GFP	Mouse	1:1000	# A11120	Invitrogen
GFP	Rabbit	1:1000	# A11122	Invitrogen
GST	Rabbit	1:20 000	G7781	Sigma-Aldrich
HA	Mouse	1:1000	#11 583 816 001	Roche
HA	Rat	1:1000	# 11 867 423 001	Roche
Hrs	Guinea pig	1:1000		Lloyd et al., 2002
Lva	Rabbit	1:1000		Sisson et al., 2000
Orb	Mouse	1:20	4H8	Developmental Studies Hybridoma Bank, University of Iowa, USA
Par6	Guinea pig	1:1000	DE02639 SA172	Kim et al., 2009
Rab5	Rabbit	1:1000		Tanaka and Nakamura, 2008
Rab7	Rabbit	1:1000		Tanaka and Nakamura, 2008
Rab11	Rabbit	1:1000		Tanaka and Nakamura, 2008

Table 2-5. List of secondary antibodies

Epitope	Animal	Tag	Dilution	Source
Mouse IgG	Goat	HRP	1:10 000	Dianova
Rabbit IgG	Goat	HRP	1:10 000	Dianova
Rat IgG	Goat	HRP	1:10 000	Dianova
Guinea pig IgG	Donkey	Cy3	1:200	Dianova
Guinea pig IgG	Donkey	Cy5	1:200	Dianova
Mouse IgG	Donkey	Cy2	1:200	Dianova
Mouse IgG	Donkey	Cy3	1:200	Dianova
Rabbit IgG	Goat	Cy2	1:200	Dianova
Rabbit IgG	Donkey	Cy3	1:200	Dianova
Rabbit IgG	Goat	Cy5	1:200	Dianova
Rat IgG	Goat	Cy5	1:200	Dianova

2.2. Molecular biology methods

2.2.1. Polymerase chain reaction (PCR)

Amplification of DNA fragments was done with the PCR method (Mullis and Faloona, 1987) according to a standard procedure (Sambrook and Russel, 2001). PCR reactions were done in 50 µl total reaction volume. Per reaction 20-50 ng of plasmid DNA or 200 ng of fly genomic DNA were mixed with 200 nM of forward/reverse primer (Table 2-1), 250 µM of each dNTP (Bioline, Luckenwalde, Germany) and 1U of polymerase in the corresponding reaction buffer. Depending on the aim of DNA amplification, Taq polymerase (Genecraft, Lüdingshausen, Germany) or Pfu polymerase (Bioline, Luckenwalde, Germany) were used. Pfu polymerase was used to amplify DNA fragments for cloning due to its higher proof-reading activity.

A standard PCR program is shown in Table 2-6. PCR programs were run on Master Cycler Personal (Eppendorf, Hamburg, Germany). PCR products were purified either directly from the PCR reaction mixture or after agarose gel electrophoresis (see 2.2.3.) by cutting out of the gel the DNA band of correct size. In both cases NucleoSpin Extract II kit (Macherey-Nagel, Düren, Germany) was used according to manufacturer's instructions. PCR products were eluted in 30 µl distilled H₂O.

Table 2-6. Standard PCR program

Step	Temperature	Duration
1) Initial denaturation	95 °C	5 min
2) Denaturation	95 °C	30 sec
3) Annealing	50-70 °C depending on primer pair	30 sec
4) Elongation	72 °C	Depending on construct length (1min/kb)
Repeat steps 2-4 34 times		
5) Final elongation	72 °C	5 min
6) End of the reaction	4 °C	∞

2.2.2. Long template PCR

Expand Long Template PCR System (Roche, Mannheim, Germany) was used to amplify PCR fragments longer than 3 kb. To verify deletion of *Rush* genomic region in flies, long template PCR reactions were set up according to manufacturer's instructions. The PCR reaction mix used to amplify *Rush* genomic region is shown in Table 2-7. PCR program for long template PCR is shown in Table 2-8.

Table 2-7. PCR mix for verification of *Rush* deletion.

Component	Volume (µl)
Template genomic DNA	1-2 µl (300 ng)
10x Buffer 2	5 µl
Long template enzyme mix	0,75 µl
dNTP (25 mM each)	1 µl
CG UTR down primer (50 µM)	0,3 µl
Sta rev primer (50 µM)	0,3 µl
Water	Fill up to 50 µl

Table 2-8. PCR program for long template PCR.

Step	Temperature	Duration
1) Initial denaturation	94 °C	2 min
2) Denaturation	94 °C	10 sec
3) Annealing	60 °C	30 sec
4) Elongation	68 °C	4 min
Repeat steps 2-4 10 times		
5) Denaturation	94 °C	15 sec
6) Annealing	60 °C	30 sec
7) Elongation	68 °C	4 min + 20 sec for each cycle
Repeat steps 5-7 10 times		
8) Final elongation	68 °C	7 min
9) End of the reaction	4 °C	∞

2.2.3. Agarose gel electrophoresis

To analyze DNA fragments produced in PCR or enzymatic digestion of DNA, horizontal agarose gel electrophoresis system Power Pac Basic (Bio-Rad, Munich, Germany) was used. 1% agarose gels were used (1% w/v agarose, 40 mM Tris, 10 mM EDTA). Ethidium bromide (0,5 µg/ml) was added to the solution before pouring the gel. Ethidium bromide intercalates between the base pairs of a DNA molecule. Illumination with UV light ($\lambda=302$ nm) causes fluorescence of ethidium bromide and thereby visualizes DNA.

The samples were mixed with 1/6 volume of loading dye solution (Fermentas, St. Leon-Rot, Germany) and loaded in the pockets of the gel. To determine the size of separated DNA fragments, 5 µl of GeneRuler 1kb DNA Ladder (Fermentas, St. Leon-Rot, Germany) were loaded in a separate pocket. Gels were run at 100 V for 20-30 min in TAE buffer (40 mM Tris, 10 mM EDTA). The DNA bands were visualized and photographed with BioDoc-It UV transilluminator (Ultra Violet Products, Upland, USA).

2.2.4. Estimation of DNA concentration

Concentration of DNA was determined by the absorption at 260/280 nm with BioPhotometer spectrophotometer (Eppendorf, Hamburg, Germany). Double-stranded DNA has an absorption maximum at 260 nm, while contamination of the sample with

proteins can be determined by absorption at 280 nm. Absorption quotient $A_{260/280}=1,8$ corresponds to a pure DNA solution.

2.2.5. Gateway cloning technology

The Gateway cloning method allows fast cloning of the gene of interest from the entry vector into diverse destination vectors. A wide range of destination vectors is available that allow expression of the protein of interest under control of different promoters and with different N-terminal and C-terminal tags. Gateway cloning employs sequence-specific recombination, done by DNA recombination enzymes from λ phage.

TOPO cloning

Rush was amplified with primers EG-N-for/EG-N-rev (without Start codon to generate N-terminally tagged protein) or EG-C-for/EG-C-rev (without Stop codon to generate C-terminally tagged protein) from plasmid pHSI65 (Table 2-2). *GDI* and *CG1418* were amplified from wild type fly cDNA (prepared by Gang Zhang) with primers GDI Ngatefor/GDI Ngaterev and CG1418 Ngatefor/CG1418 Ngaterev accordingly (Table 1). Purified PCR products were introduced into the pENTR/D-TOPO vector using the pENTR/D-TOPO Cloning kit (Invitrogen, Carlsbad, Germany) according to the manufacturer's protocol. During the reaction the Topoisomerase I cleaves the vector DNA, leaving a 5' overhang, complementary to the CACC sequence in the 5' end of the forward primers, used for amplification of the gene (Table 2-1). These sequences anneal and lead to the cloning of the gene into the vector in the correct orientation. 1 μ l of the cloning reaction was used to transform *E. coli* cells. The success of transformation was determined with a treatment with restriction nucleases (Fermentas, St. Leon-Rot, Germany) according to manufacturer's instructions. The sequence of the insert was verified by sequencing using the M13 for and M13 rev primers (Table 2-1).

Gateway LR recombination into expression vectors

Rush, *GDI* and *CG1418* were transferred from the pENTR/D-TOPO vector into destination vectors (Table 2-2) in the LR recombination reaction. λ phage recombination enzymes recognize *attL1* and *attL2* sequences in the entry vector, cut the gene out and ligate it into

the destination vector between *attR1* and *attR2* sequences, forming the expression clone (Fig. 2-1). Due to sequence differences between *attL1* and *attL2* as well as between *attR1* and *attR2*, the gene is inserted in a correct orientation. Gene *ccdB*, coding for a toxic protein, is transferred in the same way from the destination vector to the entry vector, forming a by-product of the reaction. The LR recombination reaction was performed with LR Clonase Enzyme Mix (Invitrogen, Carlsbad, Germany) according to the manufacturer's protocol, using 100 ng of pENTR vector and 150 ng of the destination vector. 1 µl of the reaction mix was used for transformation of *E. coli* cells. As *ccdB* codes for a toxic compound, the cells that are transformed with the destination vector or the by-product plasmid do not form colonies. *E. coli* cells that contain the expression clone were selected by their resistance to ampicillin.

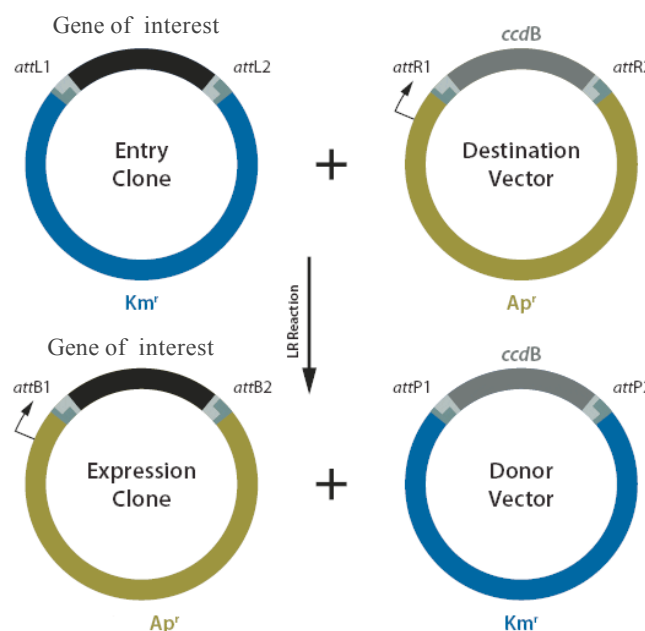


Figure 2-1. Gateway recombination reaction. λ phage recombination enzymes recognize *attL1* and *attL2* sequences in the entry vector, cut the gene of interest out from the entry clone and ligate it into the destination vector between *attR1* and *attR2* sequences. The obtained expression clone contains the gene of interest fused to the selected tag. The product of *ccdB* is toxic and eliminates cells, transformed with the by-product of the recombination reaction (Adapted from Invitrogen).

2.2.6. Cloning of inserts into pGEX-4T-1 vector

To express GST-tagged proteins in *E. coli* cells, full Rush sequence or its PH and FYVE domains alone were amplified with primers that contain *EcoRI* and *BamHI* recognition

sites (Table 2-1). Purified PCR products and pGEX-4T-1 vector were digested with EcoRI and BamHI. pGEX-4T-1 vector was dephosphorylated with Shrimp Alkaline Phosphatase (Roche, Mannheim, Germany). PCR products were ligated with the dephosphorylated pGEX-4T-1 vector using T4 DNA Ligase (Fermentas, St. Leon-Rot, Germany). 2 µl of ligation reactions were transformed into *E. coli* cells. Success of cloning was verified by sequencing of clones.

2.2.7. Transformation of chemically competent *E. coli* cells

E. coli strains used in this work are listed in Table 2-3. In brief, chemically competent *E. coli* cells were transformed as follows: cells were thawed on ice, approx. 100 ng of plasmid DNA was added, gently mixed and incubated on ice for 15 min. Then the cells were heat-shocked at 42 °C for 30 sec in a water bath. The cells were briefly cooled down on ice, 250 µl of room temperature SOC medium (2% tryptone, 0,5% yeast extract, 10mM NaCl, 2,5mM KCl, 10mM MgCl₂, 10mM MgSO₄, 20mM glucose) was added and the cells were incubated at 37 °C for 1 h with shaking at 200 rpm. Then the cells were plated on LB agar plates (1% tryptone, 0,5% yeast extract, 1% NaCl, 1% agar) with an appropriate antibiotic (kanamycin 50 µg/ml or ampicillin 100 µg/ml) for selection of transformed cells.

2.2.8. Purification of plasmid DNA

To purify plasmid DNA from *E. coli* cells in smaller amounts, plasmid DNA was purified according to a modified plasmid purification method from Qiagen, Hilden, Germany. Briefly, a single colony of transformed *E. coli* cells was inoculated in 1 ml LB medium and incubated overnight at 37 °C at 200 rpm. Then cells were pelleted by centrifugation for 1 min at 13000 rpm. The pellet was resuspended in 200 µl of buffer P1 (50mM Tris-HCl, pH 8,0, 10mM EDTA, 100 µg/ml RNase A). Afterwards 200 µl of buffer P2 (200mM NaOH, 1% SDS) was added, the mixture was mixed by inverting 5-6 times and incubated for 5 min at room temperature. After addition of 200 µl of buffer P3 (3M K acetate, pH 5,5) the mixture was inverted 5-6 times and centrifuged for 20 min at 13000 rpm, 4 °C. The supernatant was transferred to a fresh centrifuge tube. Then 400 µl of isopropanol were added and the mixture was centrifuged for 30 min at 13000 rpm, 4 °C. The supernatant was discarded and the pellet was washed with 500 µl ice-cold 70% ethanol. The sample was centrifuged for 5 min at 13000 rpm, the supernatant was discarded and the pellet was air-

dried at room temperature. Then purified plasmid DNA was dissolved in 20 µl H₂O.

To obtain large amounts of pure DNA for cloning and transformation, plasmid DNA was purified with Nucleobond X100 kit (Macherey-Nagel) according to the manufacturer's procedure.

2.2.9. Site-directed mutagenesis

To create point mutations in *Rush* sequence, QuikChange II Site-Directed Mutagenesis kit (Stratagene) was used according to manufacturer's instructions. In brief, pENTR vector containing *Rush* was amplified with primers PH DN for/PH DN rev for K48E mutation or FYR176Gf/FYR176Gr for R176G mutation (Table 2-1), using 20 ng of an entry clone and 125 ng of each of primers. The PCR program used for site directed mutagenesis is shown in Table 2-9. Methylated template DNA was removed by digestion with 1 µl *DpnI* for 1 h at 37 °C. XL1-Blue *E. coli* cells were transformed with 2 µl of the reaction solution. Cells were incubated on ice for 30 min, heat-shocked for 45 sec at 42 °C and afterwards cooled down on ice for 2 min. 500 µl of NZY⁺ broth (1% casein hydrolysate, 0,5% yeast extract, 0,5% NaCl, 20 mM glucose, 12,5 mM MgCl₂, 12,5 mM MgSO₄) preheated to 42 °C was added to each transformation reaction. Cells were incubated for 1 h at 37 °C with shaking at 200 rpm and plated on LB agar plates.

Table 2-9. PCR program for site-directed mutagenesis reaction

Step	Temperature	Duration
1) Initial denaturation	95 °C	30 sec
2) Denaturation	95 °C	30 sec
3) Annealing	55 °C	1 min
4) Elongation	68 °C	3,5 min
Repeat steps 2-4 16 times		
5) End of the reaction	37 °C	∞

2.2.10. Sequencing of DNA

Sequencing reaction was set up as follows: to sequence insert in a plasmid, 300 ng of plasmid DNA were mixed with 8 pmol of corresponding primer, 1,5 µl sequencing buffer

and 1,5 µl sequencing mix and filled up to 10 µl with sterile water. To sequence a PCR product, 20-30 ng of PCR product was mixed with 8 pmol of the sequencing primer, 1 µl of sequencing buffer and 1 µl sequencing mix and filled up to 10 µl with sterile water. PCR program for sequencing reactions is shown in Table 2-10. After completion of PCR program the mixture was transferred to a new tube. After addition of 1 µl of 125 mM EDTA, 1 µl of 3 M NaAc and 50 µl of 100% ethanol the sample was incubated for 5 min at room temperature. Then the sample was centrifuged for 15 min at 13000 rpm, the supernatant was removed and the pellet washed once with 70% ethanol. After centrifugation for 5 min at 13000 rpm the supernatant was removed and the pellet was air-dried. Afterwards the pellet was dissolved in 15 µl of HiDi (Applied Biosystems, Darmstadt, Germany). Analysis of sequencing reactions was done by in-house sequencing service in the Department of Developmental Biochemistry, Ernst-Caspari-Haus, GZMB, Göttingen.

Table 2-10. PCR program for sequencing reaction

Step	Temperature	Duration
1) Initial denaturation	96 °C	2 min
2) Denaturation	96 °C	20 sec
3) Annealing	55 °C	30 sec
4) Elongation	60 °C	4 min
Repeat steps 2-4 26 times		
5) End of the reaction	12 °C	∞

2.2.11. Isolation of genomic DNA from flies

To purify genomic DNA from flies, 30 flies (preferably male) were shock frozen in liquid nitrogen. Frozen flies were disrupted with a biovortexer in 400 µl of homogenization buffer (100mM HCl, pH 7,5, 100 mM EDTA, pH 8,0, 100 mM NaCl, 0,5% SDS) and incubated for 15-30 min at 65 °C. Then 228,4 µl of 5 M KAc and 571,6 µl of 6 M LiCl were added and the mixture was incubated on ice for 15 min. The mixture was centrifuged at 13000 rpm for 15 min, and 1 ml of the supernatant was transferred to a new tube. After addition of 600 µl of isopropanol the mixture was centrifuged again at 13000 rpm for 15 min. The supernatant was discarded and the DNA pellet was washed once with ice cold

70% ethanol. After centrifugation at 13000 rpm for 10 min the supernatant was discarded and DNA pellet was air dried. Purified genomic DNA was solubilized in 150 µl of sterile water and stored at 4 °C.

2.2.12. Culture and transfection of Schneider 2 cells

Schneider 2 (S2) cells, an immortalized culture of *Drosophila* embryonic cells (Schneider, 1972), were used for experiments in the cell culture system. The cells were grown at 25 °C in *Drosophila* S2 medium (Invitrogen, Carlsbad, Germany) supplemented with serum and antibiotics. S2 cells were transfected with FuGENE HD Transfection Reagent (Roche, Mannheim, Germany). 1×10^6 cells were used for each transfection reaction. The cells were harvested with centrifugation at 1000 rpm for 10 min, resuspended in S2 cell medium and transferred to a 6 well plate. 2 µg of plasmid DNA were diluted in 100 µl of sterile water. 4 µl of FuGENE transfection reagent was added in the solution and incubated for 15 min at room temperature. Afterwards the solution was added to the wells with cell suspension. After transfection cells were incubated at 25 °C for 2–3 days.

2.3. Biochemical methods

2.3.1. Protein extraction from embryos

Embryos were collected from apple juice plates in small amount of water with a paintbrush. To remove the chorion, 5% sodium hypochlorite (NaOCl) was added and embryos were incubated for 4-5 min. Then embryos were collected on a metal sieve with a vacuum pump, washed extensively with H₂O, transferred into a centrifuge tube and used immediately or shock-frozen at -70 °C.

Embryos were homogenized for 3 min on ice with a biovortexer (Roth, Karlsruhe, Germany) in five-fold volume of TNT lysis buffer (150mM NaCl, 50mM Tris, pH 8,0, 1% Triton X-100) (Willert et al., 1997). Protease inhibitors were freshly added to the lysis buffer before use (Pefabloc 200 µg/ml, Pepstatin 2 µg/ml, Aprotinin 2 µg/ml, Leupeptin 2 µg/ml (Roche, Mannheim, Germany)). After incubation on ice for 30 min the sample was centrifuged for 10 min at 13000 rpm, 4 °C. The supernatant was transferred to a new tube and protein content was determined (see 2.3.3.).

2.3.2. Protein extraction from S2 cells

S2 cells were harvested by a centrifugation at 1000 rpm for 5 min and washed 3 times with ice-cold PBS (130 mM NaCl, 270 mM KCl, 0,7 mM Na₂HPO₄, 0,3 mM KH₂PO₄, pH 7,4). The pellet was resuspended in 200 µl of TNT lysis buffer containing protease inhibitors and incubated on ice for 30 min. Afterwards the supernatant was centrifuged for 20 min at 13000 rpm, 4 °C. The supernatant was transferred to a clean tube and the protein content was measured (see 2.3.3.)

2.3.3. Determination of protein concentration

Protein concentration in samples was determined according to Bradford method with Roti-Quant reagent (Roth, Karlsruhe, Germany). 800 µl H₂O were mixed with 200 µl of the reagent and 2 µl of the protein solution was added. 2 µl of the lysis buffer were used as a blank. The absorption was measured at 600 nm with BioPhotometer spectrophotometer (Eppendorf, Hamburg, Germany). OD₆₀₀ =1 corresponds to approximately 1 mg/ml of total protein.

2.3.4. SDS-polyacrylamide gel electrophoresis

Protein samples were separated electrophoretically by means of denaturing discontinuous SDS-polyacrylamide gel electrophoresis (SDS-PAGE) essentially as described (Wodarz, 2008). 10% polyacrylamide gels were used (2,5 ml 30% acrylamide/BIS (29:1), 2,8 ml 1M Tris, pH 8,0, 38 µl 20% SDS, 2,1 ml H₂O, 30 µl 10% APS, 8 µl TEMED) with a stacking gel of following composition: 310 µl 30% acrylamide/BIS (29:1), 235 µl 1M Tris, pH 6,8, 10 µl 20% SDS, 1,3 ml H₂O, 10 µl 10% APS, 5 µl TEMED. Mini Protean system 3 (Bio-Rad, Munich, Germany) was used for pouring and running of gels.

Protein samples were mixed 1:1 with 2X SDS Loading buffer (100mM Tris, pH 6,8, 4% SDS, 0,2% Bromphenolblue, 20% glycerol, 100mM β-mercaptoethanol) and boiled for 5 min. Afterwards the samples were loaded in the pockets of the gel. 5 µl of PageRuler Prestained Protein Ladder (Fermentas, St. Leon-Rot, Germany) were loaded as a size marker. Proteins were separated at 200 V for 1 hour in SDS buffer (192 mM glycine, 2,5 mM Tris, 0,1% SDS).

2.3.5. Western blot

Proteins separated by SDS-PAGE (1.3.4.) were transferred onto a nitrocellulose membrane (Schleicher and Schuell, Dassel, Germany) with Mini Trans-Blot system (Bio-Rad, Munich, Germany) according to the manufacturer's instructions. Protein transfer was done in transfer buffer (192 mM glycine, 2,5 mM Tris, 20% methanol) at 100 V for 1 h at 4 °C. Afterwards the transfer of proteins was tested by staining with Ponceau S solution. The staining was removed by washing in TBST (20mM Tris, pH8,0, 150mM NaCl, 0,2% Tween 20). Sites of unspecific antibody binding were blocked by incubating the membrane for 1 h in the blocking buffer (1% bovine serum albumin, 3% skim milk powder in TBST). Then the membrane was incubated with a primary antibody (diluted accordingly in the blocking buffer) overnight at 4 °C. The membrane was washed with TBST three times for 20 min and then incubated with a secondary antibody (coupled to horseradish peroxidase (HRP), dilution 1:10000 in the blocking buffer) for 1 h at room temperature. Primary and secondary antibodies used for Western blot are listed in Tables 2-4 and 2-5. After incubation with secondary antibody the membrane was washed again three times for 20 min with TBST and incubated for 1 min with BM chemiluminescence blotting substrate (Roche, Mannheim, Germany). HRP activity was visualized by exposing the membrane to an X-ray film Fuji SuperRX (Fuji, Tokyo, Japan). The film was developed and fixed with Optimax X-ray film processor (Protec Medizintechnik, Oberstenfeld, Germany).

2.3.6. Coomassie staining

Polyacrylamide gels were fixed with 12% w/v trichloroacetic acid for 1 hour at room temperature. Afterwards gels were stained with colloidal Coomassie staining solution (10 % v/v phosphoric acid, 10% w/v ammonium sulfate, 0,12% w/v Coomassie Brilliant Blue G250, 20% v/v methanol) overnight at room temperature (Candiano et al., 2004). Destaining was done by consecutive washes in water.

2.3.7. GST and MBP fusion protein purification

50 ml of 2xYTA medium (16 g/l tryptone, 10 g/l yeast extract, 5 g/l NaCl, pH 8,0) was inoculated with 2 ml overnight culture of bacteria transformed with target plasmid and incubated at 37 °C till the culture reached mid log phase ($OD_{550}=0,5-1,0$). IPTG was added to a final concentration of 0,5 mM to induce the expression of recombinant protein. After

incubation with IPTG for 2 - 4 hours at 30 °C bacteria were harvested by centrifugation at 8000 rpm at 4 °C. The pellet was resuspended in 2,5 ml 1x PBS with protease inhibitors. Bacteria were disrupted either by sonication or freeze-thawing at -20 °C. Triton-X100 was added to the lysate to a final concentration of 2% and the mixture was gently mixed for 20 min at 4°C. The lysates was cleared by centrifugation at 10000 rpm for 10 min at 4 °C.

To purify GST fusion proteins 40 µl of Gluthatione Sepharose beads (GE Healthcare) were added to the lysate. After incubation for 30 min at room temperature beads were washed three times in PBS. Bound protein was eluted with elution buffer containing 20 mM reduced glutathione in 50mM Tris HCl, pH 8,0.

For purification of MBP fusion proteins 40 µl of Amylose resin (New England Biolabs, Schwalbach/Taunus, Germany) was added to the lysates. After three washing steps in PBS, MBP fusion protein was either left bound on beads or eluted with buffer containing 10 mM Tris HCl, 10 mM maltose, pH 7,2.

2.3.8. MBP fusion protein pulldown

To analyze direct interactions between proteins, MBP fusion protein pulldown was used. 2 µl of amylose resin with bound MBP fusion protein or MBP alone was washed three times with pulldown buffer (150 mM NaCl, 10 mM MgCl₂, 20 mM HEPES (4-(2-hydroxyethyl)-1-piperazineethanesulfonic acid), 1 mM EDTA, 1% Triton X-100, 5 mM DTT). The resin was then incubated with 1 µg of GST fusion protein in pulldown buffer for 1 hour at room temperature. 1 µg of GST alone was used as a negative control. The resin with bound GST fusion protein was washed three times with pulldown buffer. Then 30 µl of 2x SDS loading buffer was added and the sample was analyzed by Western blot.

2.3.9. Lipid overlay assay

To determine lipid binding specificity of Rush and its separate domains, PIP Strips (Echelon Biosciences, Salt Lake City, UT) were used according to the manufacturer's protocol. In brief, the membrane was blocked in blocking buffer (1xTBS, 0,1% Tween, 3%BSA) for 1 hour. After blocking, the membrane was incubated for 1 hour with 0,2 µg/ml GST fusion protein in blocking buffer. 0,25 µg/ml of PIP2 Grip™ protein (Echelon Biosciences, Salt Lake City, UT) or GST alone were used as a control. The membrane was washed three times in TBS with 0,1% Tween and incubated with anti-GST antibody for 30

min. Afterwards the membrane was washed as previously and incubated for 1 hour with HRP-coupled secondary antibody. The membrane was washed three times and bound protein detected by a chemiluminescence reaction.

2.3.10. Endosome fractionation assay

Early and late endosomes were separated from S2 cell or embryo protein extracts by a sucrose gradient as described in Torres et al. (2008). S2 cells were harvested by centrifugation at 1000 rpm, 4 °C, washed once in 10 ml of ice cold PBS and resuspended 1:4 in homogenization buffer. Cells were homogenized by passing 10 times through a 26-gauge needle in a 1 ml syringe. Post nuclear supernatant (PNS) was separated by centrifugation for 15 min at 3500 rpm, 4 °C. PNS was diluted 2:3 with 60% sucrose in homogenization buffer (250mM sucrose, 3mM imidazole, pH7,5) to achieve final sucrose concentration of 40,6%. A sucrose gradient was prepared by sequentially overlaying 1 ml of PNS, 40,6% sucrose with 2 ml of 35% sucrose in 3mM imidazole, pH 7,5, 1,5 ml of 25% sucrose in 3mM imidazole, pH 7,5 and 400 µl of homogenization buffer (8% sucrose) in a Beckman 5 ml centrifuge tube. Gradient was centrifuged at 40000 rpm (125.000 x g) at 4 °C in Optima MAX ultracentrifuge (Beckman Coulter, Fullerton, USA). Early endosomes were collected at the 35/25% sucrose interface and late endosomes at the 8/25% sucrose interface. Protein distribution in endosomal fractions was analyzed by Western blot.

To prepare endosome fractions from fly embryos, embryos were devitellinized as described in 2.3.1., homogenized for 3 min on ice with a biovortexer (Roth, Karlsruhe, Germany) and resuspended 1:4 in homogenization buffer. The embryo lysate was further prepared similarly as described for S2 cells.

2.4. Immunohistochemistry

2.4.1. Fixation of embryos

Embryos from overnight egg collection cages were used for staining with antibodies. Before the staining embryos were fixed to permeabilize the tissue and make it accessible for antibodies as well as to preserve the tissue and inhibit protease activity.

Embryos were collected like described before (see 2.3.1.) and after washing with H₂O transferred into scintillation glasses with 1:1 mixture of fixation solution and heptane. For

most stainings 4% formaldehyde in PBS was used as a fixation solution. Steffanini solution (440 µl 37% formaldehyde, 660 µl pikric acid, 660 µl 0,5M PIPES (piperazine-1,4-bis-2-ethanesulfoic acid), pH 7,5, 2,34 ml sterile water) was used as a fixation solution for stainings with antibody against Rush. Embryos were fixed for 20 min with shaking. Afterwards the lower aqueous phase that contains formaldehyde was discarded and 1 volume of methanol was added. Embryos were strongly shaken for approx. 30 sec to remove the vitelline envelope. Devitellinized embryos were transferred into a fresh tube, washed two times with methanol and stored at -20 °C or stained immediately.

2.4.2. Immunostaining of embryos

Fixed embryos were washed 3x 20 min with PBT (1x PBS, 0,1% Tween 20) on a shaker. Unspecific binding sites were blocked by incubation in a blocking solution (5% normal horse serum (NHS) in PBT) for 1 h. Embryos were incubated with a primary antibody diluted in blocking solution overnight at 4 °C or 2 h at room temperature. Then embryos were washed 3x 20 min with PBT, incubated with a dilution of secondary antibody in blocking solution for 2 h at room temperature. Used antibodies are listed in Tables 2-4 and 2-5. After a repeated washing step with PBT (3x 20 min) embryos were transferred to a microscopy slide and embedded in Mowiol/DABCO.

Mowiol: 5 g Elvanol/Mowiol (Höchst, Frankfurt, Germany) were dissolved in 20 ml PBS, pH7,4. 10 ml of glycerol were added and mixed for 16 h. The solution was centrifuged for 15 min at 12000 rpm and the supernatant stored at -20 °C. Few flakes of DABCO (Diazabicyclo(2.2.2)octane) were added 30 min before embedding and mixed with overhead rotor.

2.4.3. Fixation and immunostaining of ovaries

Wild type flies were put on apple juice agar plates three to four days before preparation of ovaries to stimulate egg development. Ovaries were prepared in PBS. Egg chambers were separated from each other by pipetting up and down with a pipette, saturated in NHS. Then ovaries were transferred to a centrifuge tube and fixed for 20 min in fixation solution (see 2.4.1.). After washing 3x 10 min with PBT ovaries were blocked in PTX (5% NHS, 0,5% Triton X-100 in PBS) for 3 h at room temperature or overnight at 4 °C. Staining with

antibodies was done as described in 2.4.2.

2.4.4. Fixation and immunostaining of S2 cells

S2 cells were fixed in chamber slides coated with 0,01% L-polylysine. Cells were allowed to adhere to the slide for 2 h at 25 °C and washed once with PBS. Fixation solution containing 4% formaldehyde in PBS was added for 10 min at room temperature. Fixed cells were washed twice with PBS.

For immunostaining the cells were incubated for 1 h in the blocking solution containing 5% NHS in PBT. Subsequently the cells were incubated for 1 h with primary antibody (see Table 2-4 for a list of used primary antibodies) diluted in blocking solution. The cells were washed three times with PBT and incubated for 1 h with the secondary antibody (Table 2-5) diluted in blocking solution. Afterwards the cells were washed three times with PBT and embedded in Mowiol/DABCO.

2.4.5. Staining of DNA

Staining of DNA in fixed preparations was done with DAPI (Dianova). DAPI was added in 1:2000 dilution in PBT during the first washing step after incubation with secondary antibody.

2.4.6. Staining of lysosomes with LysoTracker

Staining of lysosomes was done essentially as described in Hou et al. (2008). Ovaries were dissected in PBS and incubated with 50 µM LysoTracker DND-99 (Invitrogen, Carlsbad, Germany) in PBS for 3 min in the dark. Then the ovaries were washed three times for 5 min each in PBS and fixed for 10 min in 4% formaldehyde in PBS. The ovaries were washed again three times for 5 min in PBS and mounted on microscope slides in Mowiol/DABCO.

2.4.7. Staining of actin microfilaments

To stain actin microfilaments, Cy3-conjugated phalloidin (Invitrogen, Carlsbad, Germany) was used. 5 µl of phalloidin were vacuum-dried, resuspended in 10 µl of PBT and added to the sample during the incubation with secondary antibodies.

2.4.8. Dextran uptake assay

Third instar larval wing discs were dissected in serum free S2 medium and incubated with 1 mg /ml Alexa Fluor 594 conjugated dextran (lysine fixable, MW10000; Invitrogen Molecular Probes) for 10 minutes. After three washing steps in ice cold S2 medium for 10 min each, discs were fixed for 20 min with 4% formaldehyde in PBS. Then discs were washed three times for 20 min in PBT and incubated with blocking solution (10% NHS in PBT) for 2 hours in room temperature. Discs were incubated with first antibody in blocking solution overnight at 4 °C and washed three times with PBT for 20 min. Secondary antibody was added for 2 hours at room temperature, and after three washing steps in PBT imaginal discs were mounted on microscope slides in Mowiol/DABCO.

2.4.9. Confocal microscopy, image acquisition and statistical analysis

Images of immunohistochemistry stainings were acquired with LSM 510 Meta confocal laser scanning microscope (Carl Zeiss, Jena, Germany) with 45x 0,8 NA Plan Neofluar and 63x 1,4 NA Plan Apochromat objectives using LSM 510 software (Carl Zeiss, Jena, Germany). Single images were processed with Adobe Photoshop CS2 (Adobe Systems, San Jose, USA) software.

For measurements of the size and number of vesicles images were analyzed with ImageJ software (National Institutes of Health, Bethesda, USA). Images were first converted to 8-bit grayscale, inverted and processed with automatic thresholding. Mean particle size and particle number of each image were measured with the analyze particles function. Statistical significance was calculated with Student's t-test.

2.5. Fly genetics

2.5.1. Fly breeding

The fly stocks used in the work were kept at 18 °C, room temperature or 25 °C on standard medium (Ashburner, 1989). For collection of embryos, flies were kept in egg collection

cages on apple juice plates. To stimulate egg laying, small amount of yeast paste was applied at the center of the apple juice plate.

Standard medium: 712 g cornmeal, 95 g soya flour, 168 g dry yeast, 450 g malt extract, 150 ml 10% Nipagin (700 ml 99% ethanol, 300 ml H₂O, 100 g Nipagin (C₈H₈O₃)), 45 ml propionic acid, 50 g agar, 400 g sugar beet sirup, add 9,75 l H₂O

Apple juice plates: 40 g agar, 1 l H₂O, 340 ml apple juice, 17 g sugar, 20 ml 10% nipagin

2.5.2. Fly stocks

Table 2-11. List of fly stocks.

Stock	Genotype	Description	Reference
Wild type Oregon R	wild type	Red eyes	A. Wodarz lab stock collection
<i>white⁻</i>	<i>w¹¹¹⁸</i>	White eyes	Bloomington #5905
P(EP) <i>rush</i>	<i>y¹ P{EPgy2}<i>rush</i>^{EY04997} w^{67c23}</i>	P{EP} element insertion in 5' UTR of <i>rush</i> gene, UAS reporter line.	Bloomington #19697
P(XP)d03799	P{XP} <i>rush</i> ^{d03799}	P-element insertion upstream of <i>rush</i>	Exelixis Collection, Harward
PBac(WH)f03712	PBac{WH}f03712	PiggyBac insertion downstream of <i>sta</i>	Exelixis Collection, Harward
<i>rush</i>	<i>rush⁴</i> ; Tr1	<i>rush</i> null allele	This work
<i>arm</i> -Gal4	<i>w[*]</i> ; P{GAL4- <i>arm</i> .S}11	GAL4 driver line, ubiquitous expression in <i>armadillo</i> gene pattern, 2nd chromosome	Bloomington #1560
<i>act</i> -Gal4	<i>y¹w[*]</i> ; P{ <i>Act5C</i> -Gal4}25FO1/CyO, <i>y⁺</i>	GAL4 driver line, ubiquitous expression, 2nd chromosome	Bloomington #4414

<i>Cu2</i> -Gal4	P{Gal4- <i>Cu2</i> }	Gal4 driver line, expression in follicle cells from stage 8, 2nd chromosome	Trudi Schüpbach
<i>da</i> -Gal4	<i>w</i> [*] ; P{GAL4- <i>da</i> .G32}UH1	Gal4 driver line, ubiquitous expression in <i>daughterless</i> gene pattern, 3rd chromosome	Bloomington #5460
<i>pnr</i> -Gal4	<i>y</i> ^l <i>w</i> ¹¹¹⁸ ; P{GawB} <i>pnr</i> ^{MD237} /TM3, P{UAS- <i>y</i> .C}MC2, <i>Ser</i> ^l	Gal4 driver line, expression in <i>pannier</i> gene pattern, 3rd chromosome	Bloomington #3039
P{GawB}109C1	P{GawB}109C1, <i>y</i> ^l <i>w</i> [*]	Gal4 driver line, expression in polar cells and follicle epithelium, 1st chromosome	Bloomington #7020
Cdc42DN	<i>w</i> [*] ; P{UAS- <i>Cdc42</i> .N17}3	<i>Cdc42</i> dominant negative construct	Bloomington #6288
YFP-Rab5	<i>y</i> ^l <i>w</i> [*] ; P{UASp-YFP. <i>Rab5</i> }02	Wild type <i>Rab5</i>	Bloomington #24616
YFP-Rab5CA	<i>y</i> ^l <i>w</i> [*] ; P{UASp-YFP. <i>Rab5</i> .Q88L}l(2)k16918 ₂₄	<i>Rab5</i> constitutively active construct	Bloomington #9774
Rab5DN-GFP	<i>w</i> ; UAS- <i>Rab5</i> S43N-GFP/TM3, <i>Sb</i>	<i>Rab5</i> dominant negative construct	Entchev et al., 2000
Rab5DN-GFP	<i>w</i> ; UAS- <i>Rab5</i> S43N-GFP/CyO	<i>Rab5</i> dominant negative construct	Entchev et al., 2000
YFP-Rab7	<i>y</i> ^l <i>w</i> [*] ; P{UASp-YFP. <i>Rab7</i> }21/SM5	Wild type <i>Rab7</i>	Bloomington #23641
Tr1	C(1)DX, <i>y</i> <i>f</i> / <i>sta</i> ^{l13} / Y; Tr1	<i>sta</i> rescue construct	Melnick et al., 1993
P(70FLP)	<i>w</i> ¹¹¹⁸ ; <i>noc</i> ^{Sco} /SM6b, P{70FLP}7	Stock for heat dependent flipase expression	Bloomington #6876

Binsinscy	Df(1)Exel8196 <i>w¹¹¹⁸</i> /Binsinscy	First chromosome balancer line	Bloomington #7769
FM7(<i>Twist</i> GFP)	FM7 { <i>twi</i> -GFP}	First chromosome balancer line, expresses GFP in <i>Twist</i> pattern	Benni Shilo, Weizmann Institute of Science, Rehovot, Israel
FM7(<i>lacZ</i>)	<i>y¹arm⁴w*</i> /FM7c, P{ <i>ftz/lacC</i> }YH1	First chromosome balancer line, ubiquitously expresses <i>lacZ</i>	Bloomington #616
<i>Gla</i> /CyO	<i>w⁻</i> ; <i>Gla</i> /CyO, P{ <i>ftz::lacZ</i> }	Second chromosome balancer line, curly wings	A. Wodarz lab stock collection
TM3/TM6B	<i>w*</i> ; TM3, <i>Sb¹ Ser¹</i> /TM6B, <i>Tb¹</i>	Third chromosome balancer line	Bloomington #2537

2.5.3. The UAS-GAL4 system

The UAS-GAL4 system (Brand and Perrimon, 1993) is used to ectopically overexpress the gene of interest in a time and tissue specific manner. The method makes use of a yeast transcription factor GAL4 that binds to an upstream activating sequence (UAS), therefore activating gene expression. In UAS reporter flies the gene of interest is placed under the control of UAS. Another fly stock, so called GAL4 driver line, contains the GAL4 gene under the control of a promoter or enhancer of a gene with a known expression pattern. When the two fly stocks are crossed, GAL4 activates the expression of the gene of interest. By choosing different GAL4 driver lines, the gene can be expressed in a wide variety of tissues and developmental stages. GAL4 driver lines and UAS reporter flies used in this work are described in Table 2-11.

2.5.4. Generation of transgenic flies

To generate transgenic flies, transgenic constructs inserted in P-element based vectors were injected into the posterior end of syncytial blastoderm embryos together with a helper plasmid that contains transposase DNA. Transposase activity mediates integration of the P-element including transgenic construct into genomic DNA. Transgenic flies that have

undergone successful integration of the P-element can be recognized by red eye color, since vectors used for injection contain the *mini-white* gene. The protocol for transgenic fly generation was adapted from Bachmann and Knust (2008). In brief, 20 µg of plasmid DNA was mixed with 5 µg of helper plasmid and 5 µl of 10 x injection buffer (5mM KCl, 0,1 mM sodium phosphate, pH 6,8) in final volume of 50 µl. Dechorionated *white⁻* embryos were arranged on coverslips and after 15-20 min of drying covered with 10S Voltalef oil (Prolabo, Paris, France). The plasmid mixture was injected to the posterior ends of the embryos by micromanipulator InjectMan NI2 (Eppendorf, Hamburg, Germany). After injection embryos were kept in 10S Voltalef oil at 18°C for 48 hr before the hatched larvae were collected. Hatched flies were single-crossed to *w⁻*; *Gla/CyO* flies for the transgenic fly selection and insertion site analysis. A list of transgenic constructs used for injection in flies is shown in Table 2-12.

Table 2-12. Transgenic constructs used for injection in flies.

Gene	Vector	Promoter	Tag
<i>rush</i>	pTWG	UAS _t	GFP
<i>rush^{K48E}</i>	pTWG	UAS _t	GFP
<i>rush^{R176G}</i>	pTWG	UAS _t	GFP
<i>rush^{K48E R176G}</i>	pTWG	UAS _t	GFP
<i>CG1418</i>	pTGW	UAS _t	GFP
<i>GDI</i>	pTGW	UAS _t	GFP

2.5.5. FLP/FRT mediated gene deletion

To generate a deletion of *rush*, FLP/FRT mediated gene deletion described in Parks et al. (2004), was used. The method makes use of the ability of FLP recombinase to mediate recombination between two FRT sites located on homologous chromosomes. This way a deletion of a genomic region flanked by two transposons that contain FRT sites can be achieved. In case of *rush* two transposon insertion lines were available – P(XP)d03799 is located in the 5' UTR of *rush*, while a piggyBac insertion line pBac(WH)f03712 is located in the 5' UTR of *sta*, a gene positioned downstream of *rush* (Fig. 2-2 A). Upon induction of FLP recombinase the genomic region between two FRT sites is deleted, leaving a single transposon at the deletion site. As FLP mediated recombination is more efficient in *cis*, excision of the UAS sequence of the P(XP) element takes place before recombination in

trans. In this case successful recombination between the two FRT sites in *trans* can be detected by loss of red eye color, since *white* genes on both transposons are deleted together with the genomic region.

Crosses used to delete the *rush* gene are shown in Fig. 2-2 B. First, virgin females of the P(XP)d03799 insertion line were crossed with males of a stock carrying a heat-inducible FLP recombinase on the second chromosome. FLP recombinase coding sequence in this stock is inserted in the balancer chromosome SM6b, allowing to select flies that carry FLP recombinase gene by curly wings. Male progeny of this cross that had curly wings were crossed to pBac(WH)f03712 virgin females. Progeny of this cross were heat shocked for two hours at 37 °C for two days in second instar larval stage. Curly winged virgin females heterozygous for P(XP)d03799 and pBac(WH)f03712 from this generation were crossed with Binsinscy balancer males and the progeny were screened for white eyes. Recombination caused a simultaneous deletion of the neighboring *sta* gene, which is essential for *Drosophila* development (Melnick et al., 1993). Therefore a *sta* rescue construct Tr1 was crossed in. Tr1 contains a complete *sta* sequence, but not *rush*, and has been shown to fully rescue loss of *sta* (Melnick et al., 1993).

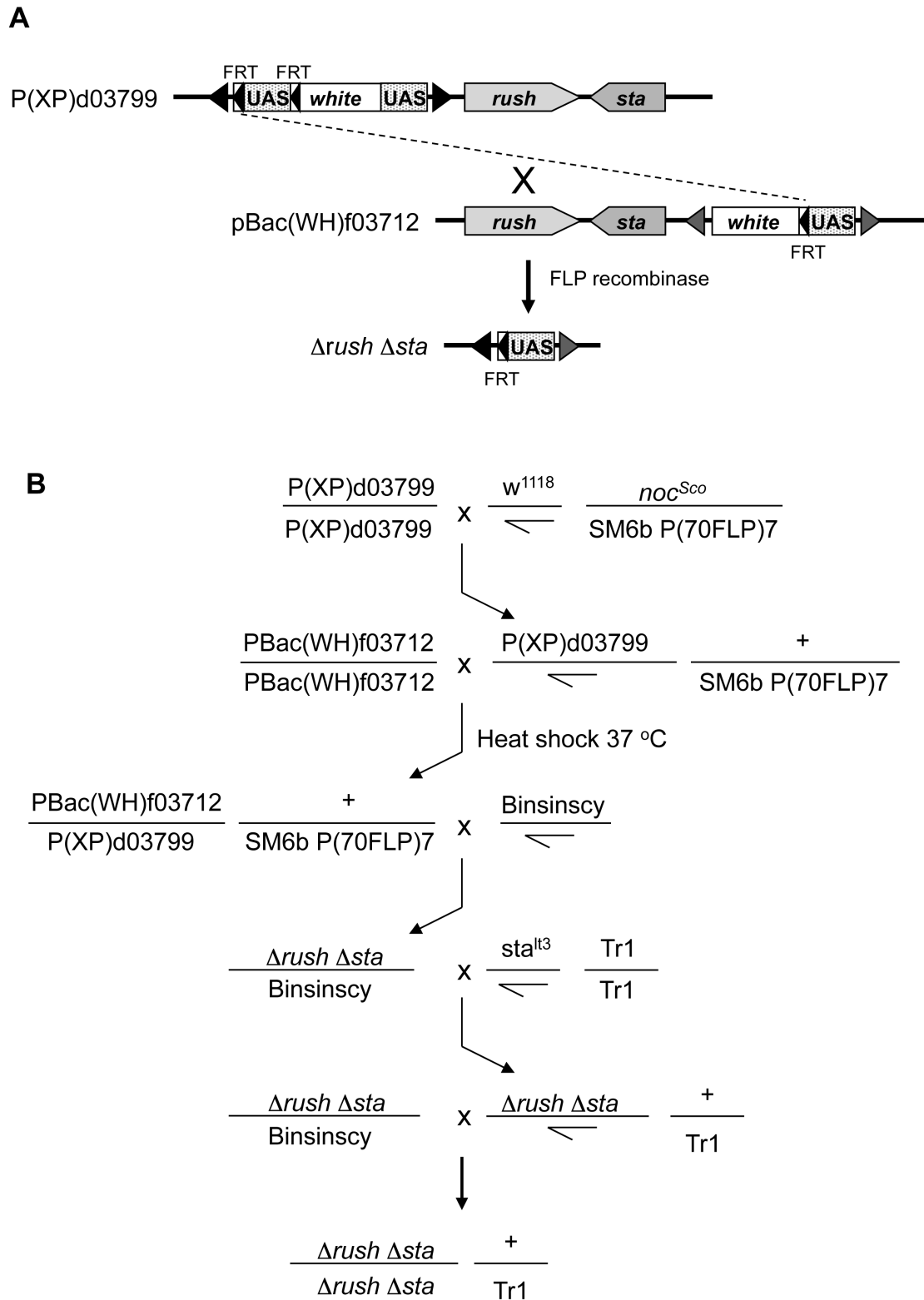


Figure 2-2. FLP/FRT mediated deletion of *rush* gene. **A** – Recombination induced by FLP recombinase can be used to delete genomic region between two transposons that contain FRT sites. In this case, P(XP)d03799 and pBac(WH)f03712 insertion lines were used to delete *rush* gene. **B** – Crossing scheme to obtain *rush* deletion line using FLP/FRT mediated gene deletion method.

3. Results

3.1. Localization of Rush

3.1.1. Colocalization of Rush with polarity markers

The *rush* gene is localized on the first chromosome and codes for a protein with a predicted length of 316 amino acids (Fig. 3-1). To determine the expression and subcellular localization of Rush during embryonic development, the embryos were stained with an affinity purified antibody against the C-terminus of Rush. Rush was ubiquitously expressed in embryos (Fig 3-2 A, B). Rush localized to the apical plasma membrane already in the stage 5 embryo (Fig 3-2 A), suggesting that Rush is maternally contributed. To test the specificity of the antibody staining, I overexpressed endogenous Rush by using a UAS sequence-containing P-element P(EP)EY04997. The P(EP)-element is inserted in the 5' UTR of *rush*, 632 base pairs before the start codon (Fig. 3-1). Expression of Rush was driven by expression of *prd*-Gal4. *prd* is a pair rule gene and is expressed in seven stripes in alternating segments. Antibody staining showed an increase of Rush signal in *prd* pattern (Fig. 3-2 C), indicating that the antibody is specific for Rush. As the staining of Rush in wild type embryos was weak, subcellular localization of Rush was analyzed in embryos that overexpress Rush under the control of the *prd* promoter (*prd*>Rush). In the *prd*>Rush embryonic ectoderm Rush was localized at the plasma membrane with accumulations in the cytosol (Fig. 3-2 D). At the plasma membrane Rush colocalized with E-cadherin (Fig 3-2 D'').

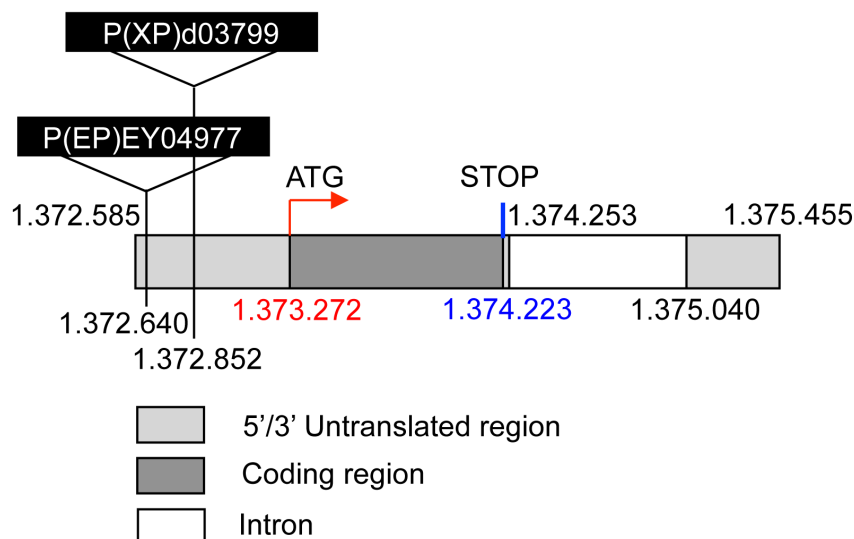


Figure 3-1. The localization and structure of *rush*. The *rush* gene is located on the first chromosome and contains two exons (1669 bp and 415 bp long). The coding region is located in the first exon. Positions of start and stop codons are denoted with red and blue letters, respectively. The numbers denote base pairs in the *Drosophila* genome. Insertion positions of two P-elements in the 5' UTR of *rush* are shown. P-element size is not shown in scale.

Due to difficulties to analyze localization of wild type Rush in embryos, I stained wild type ovaries with anti-Rush antibody. Rush was expressed both in the germline (Fig. 3-3 A, white arrow in Fig. 3-3 B) and in the follicle epithelium (Fig. 3-3). In the follicle epithelium, similarly as in the embryonic ectoderm, Rush localized to the plasma membrane as well as in cytoplasmic puncta (Fig. 3-3). Rush localized mainly at the lateral domain of the plasma membrane with accumulations at the apical side (Fig. 3-3 A, D, E). Similarly as in the embryonic ectoderm, Rush colocalizes with E-cadherin at the lateral plasma membrane of the follicle epithelium (Fig. 3-3 B, C). We co-stained wild type ovaries with antibodies against Baz and Par6 to determine whether Rush colocalizes with the Par/aPKC complex proteins. Baz and Par6 localize at the subapical region of the lateral plasma membrane (Fig. 3-3 D, E). Rush partially colocalizes with Baz and Par6 at the apical part of the lateral plasma membrane, however, the accumulations of Rush are localized slightly more basally than Baz and Par6 (Fig. 3-3 D, E).

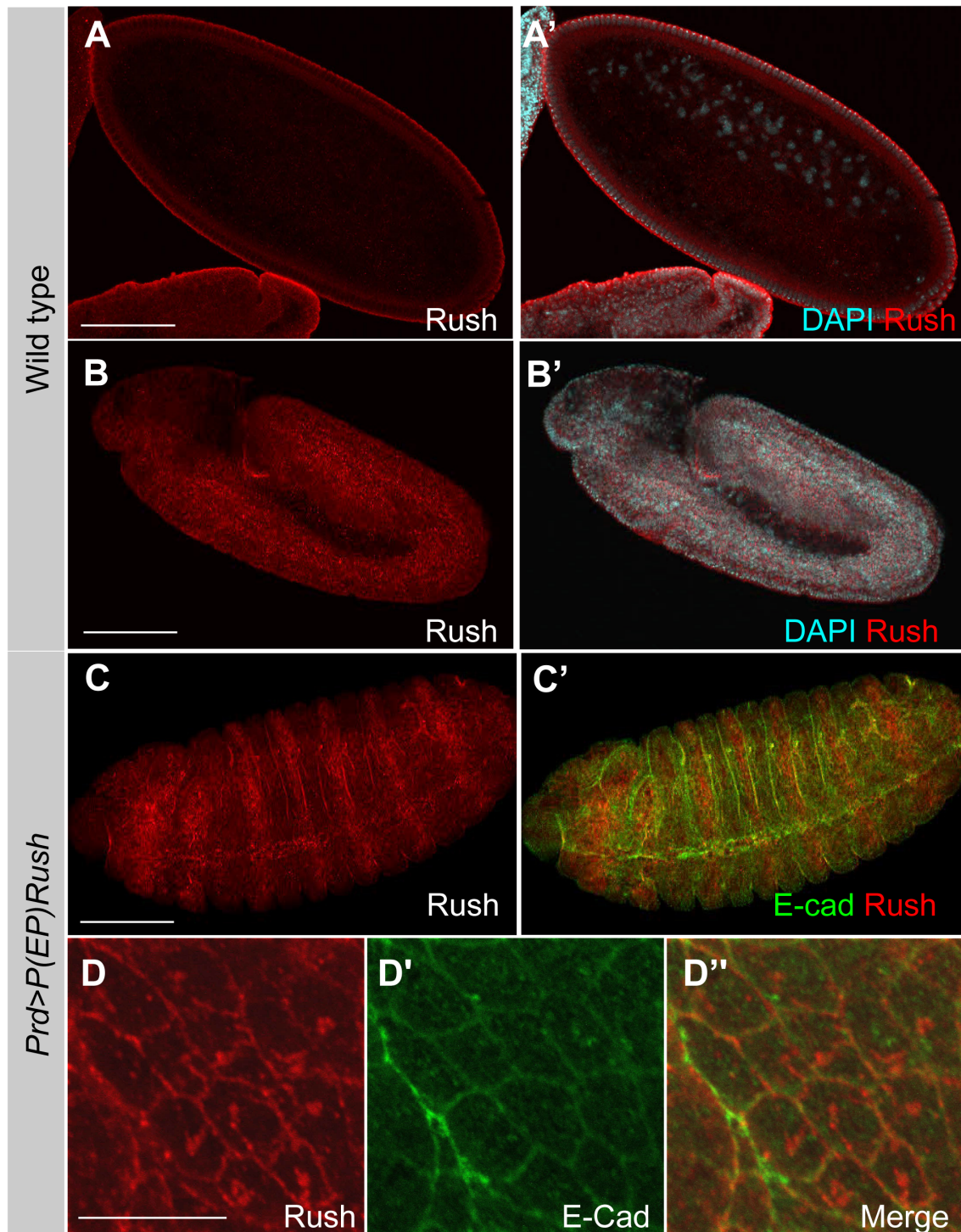


Figure 3-2. Localization of Rush in embryos. **A, B** - Wild type embryos were stained with an antibody against C-terminus of Rush. **A** - stage 5 embryo, **B** - stage 11 embryo. **C, D** - overexpression of wild type Rush in a *prd* pattern. **C** - stage 15 embryo. **D** - Subcellular localization of Rush in the ectoderm of a stage 15 embryo. Rush colocalizes with E-cadherin at the plasma membrane. to the plasma membrane and forms accumulations in the cytoplasm. Scale bars: **A, B, C** = 100 μ m, **D** = 10 μ m. In **A, B, C** anterior is to the left.

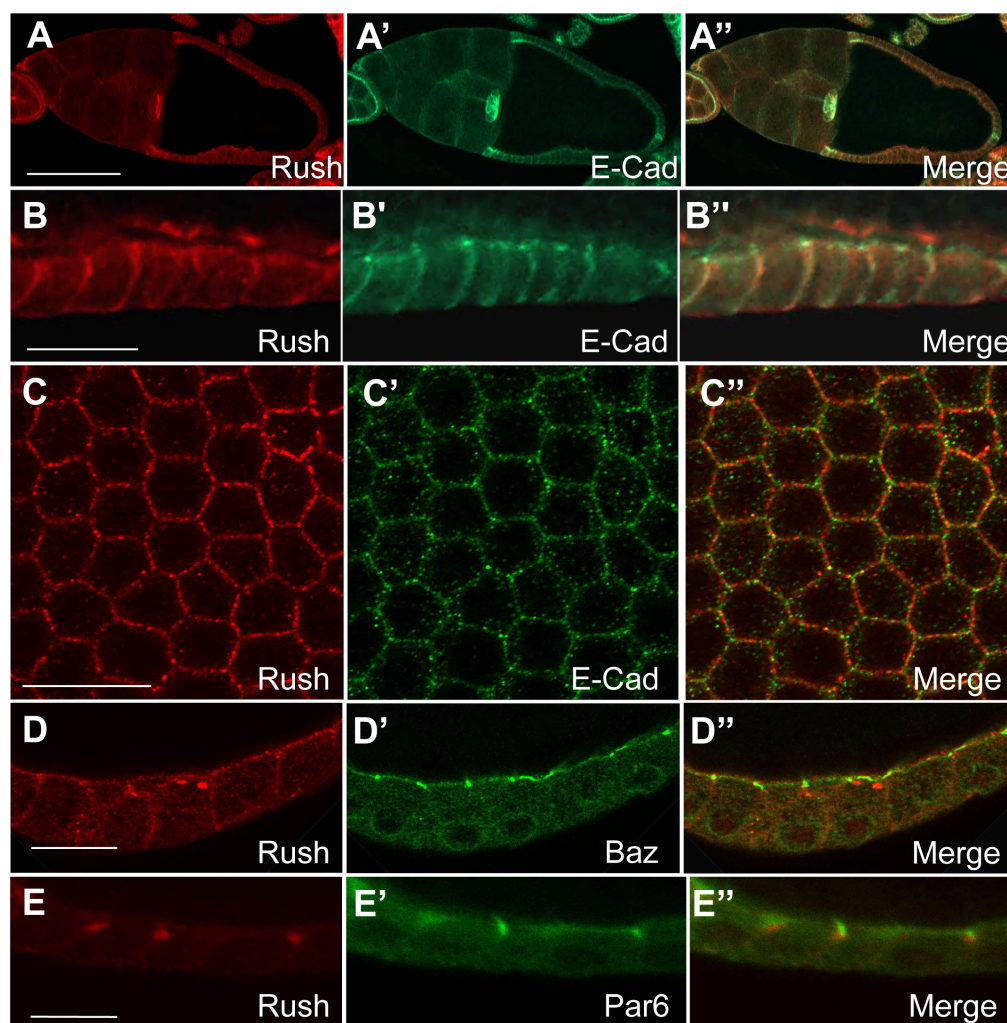


Figure 3-3. Localization of Rush in wild type ovaries. Ovaries were stained with antibodies against Rush and cell polarity markers. All panels show stainings of stage 10 egg chambers. **A** – Rush is expressed both in the germline and in the follicle epithelium. **B** – Cross section of the follicle epithelium. Rush localizes to the lateral plasma membrane with apical accumulations and colocalizes with E-cadherin. **C** – Tangential view of the follicle epithelium. Rush colocalizes with E-cadherin at the cell-cell contacts. **D** – Cross section of the follicle epithelium. Rush partially colocalizes with Baz. **E** – Cross section of the follicle epithelium. Rush partially colocalizes with Par6 at the subapical region. In panel A anterior is to the left. In panels B, D, E apical is to the top. Scale bars: A = 50 μ m, B, C, D, E = 10 μ m.

3.1.2. Rush associates with endosomes

Both in the embryonic ectoderm and in the follicle epithelium a fraction of Rush was found in dot-like accumulations in the cytoplasm. Rush contains a FYVE domain (Fig. 1-6), which has been described to localize proteins to endosomal compartments (Gillooly et al., 2001). Therefore these dot-like structures could be endosomes. To investigate this possibility, I analyzed the colocalization of Rush with markers of the endocytic pathway.

Results

In the wild type follicle epithelium, cytoplasmic puncta of Rush colocalized with Hrs (Fig 3-4 A), a FYVE domain-containing protein that regulates the transition between early and late endosomes (Lloyd et al., 2002). Rab proteins are widely used as markers of different endocytic compartments. As it was not possible to stain simultaneously for Rush and Rabs in wild type tissue, since all available antibodies were generated in rabbits, I expressed YFP-tagged versions of wild type Rab5, Rab7 and a constitutively active mutant of Rab11 (Rab11CA) to mark early, late and recycling endosomes, respectively. Rush showed good colocalization with YFP-Rab7 (Fig. 3-4 B), but colocalized less extensively with YFP-Rab5 and YFP-Rab11CA (Fig. 3-4 C-D). Therefore Rush seems to associate with the late endosome and/or the transition intermediate between early and late endosomes.

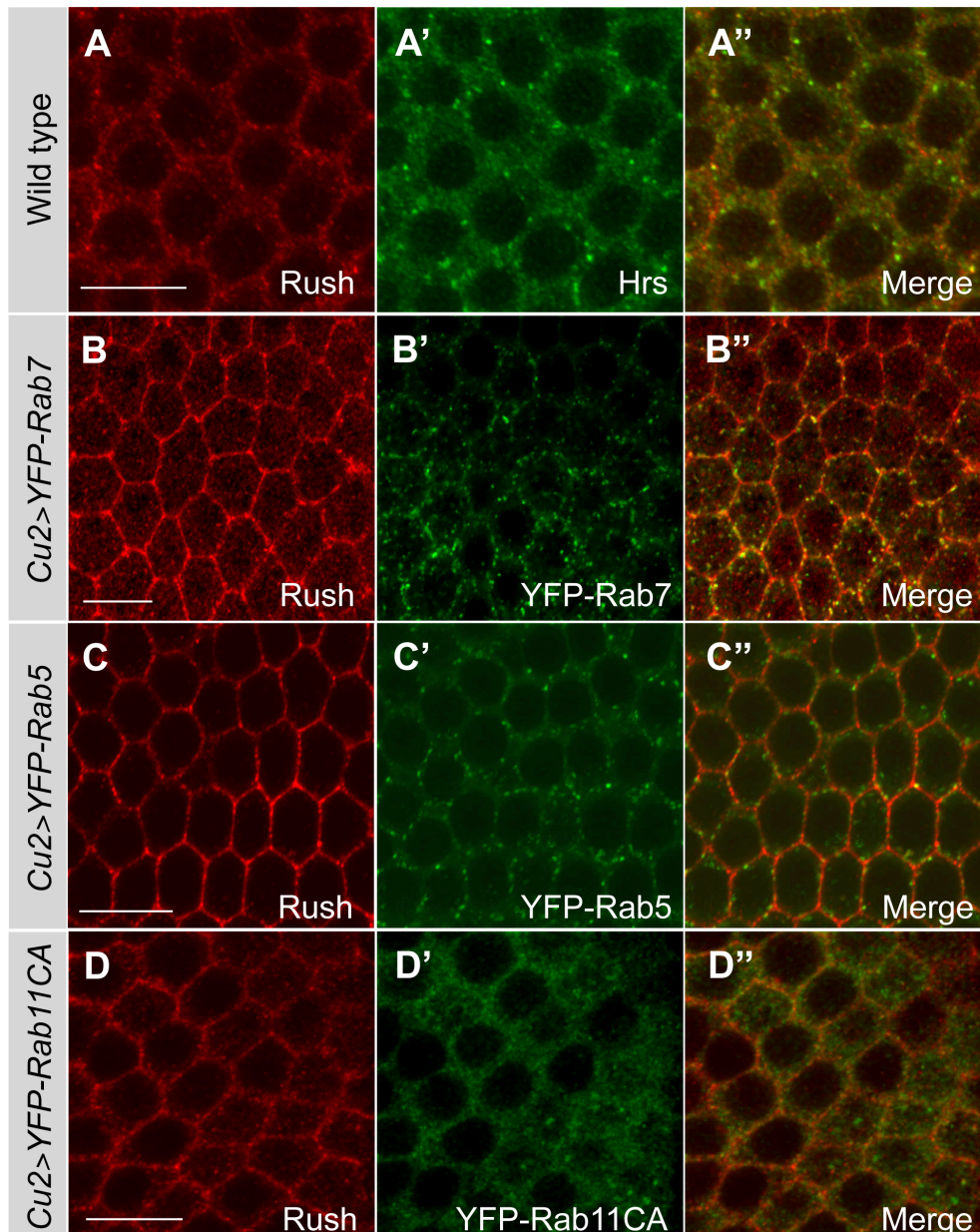


Figure 3-4. Colocalization of Rush with endosome markers. Ovaries of the indicated genotype were stained against Rush and different endosome markers. All panels show tangential sections of stage 8-10 egg chambers. **A** – Rush colocalizes with Hrs in cytoplasmic puncta. **B** – Rush colocalizes with YFP-Rab7, a marker of late endosomes. Less colocalization was observed between Rush and YFP-Rab5 (**C**) and YFP-Rab11CA (**D**). Scale bars = 10 μ m.

The oocyte is a cell with highly active endocytic pathways due to the active uptake of yolk protein precursors (DiMario and Mahowald, 1987). Endocytic markers have been described to have a dynamic localization during oocyte maturation (Tanaka and Nakamura, 2008). In stage 7-8 egg chambers Rush accumulated in the centre of the oocytes (Fig. 3-5). Hrs accumulated in the centre of wild type oocytes together with Rush, indicating that these accumulations have an endocytic origin (Fig. 3-5 A). YFP-Rab7, when expressed in the germline under the control of the actin promoter, also accumulates in the centre of the oocyte (Fig. 3-5 B). Rush colocalizes with YFP-Rab7 in these accumulations. A similar localization of endocytic compartments to the centre of the oocyte in stage 7-8 egg chambers has been described before (Januschke et al., 2007; Tanaka and Nakamura, 2008). Thus Rush colocalizes with late endosomes both in the follicle epithelium and in the oocyte.

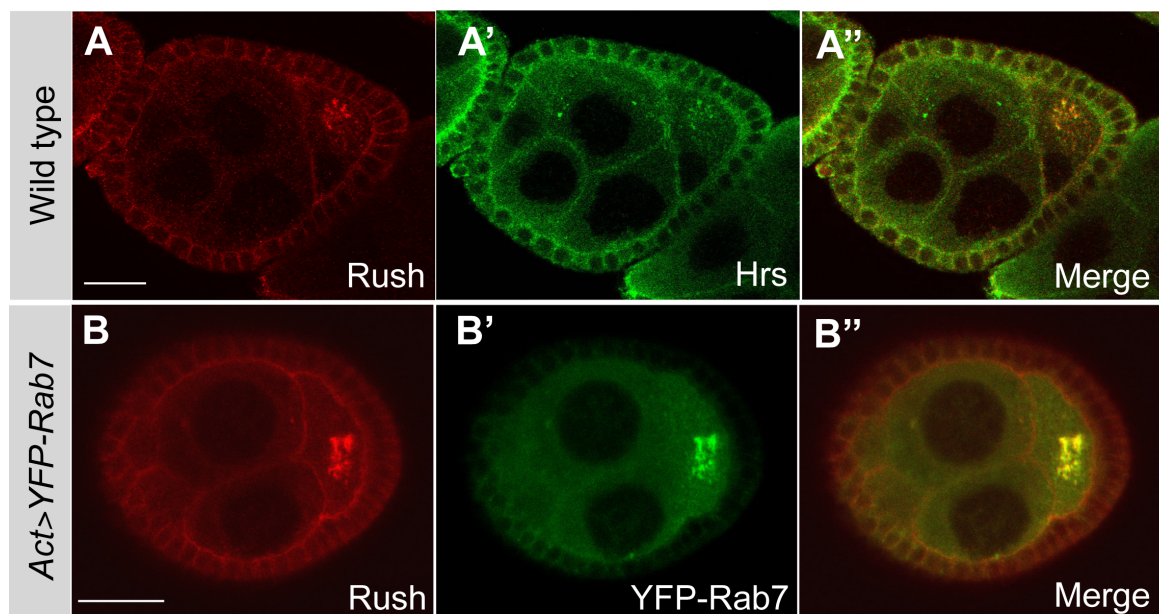


Figure 3-5. Rush colocalizes with endosome markers in the oocyte. **A** – Rush accumulates and colocalizes with Hrs in the oocyte of a wild type stage 8 egg chamber. **B** - YFP-Rab7 was overexpressed under the control of an ubiquitous actin promoter. In the stage 7 egg chamber YFP-Rab7 accumulates in the centre of the oocyte and colocalizes with Rush. Scale bars = 20 μ m.

Results

To verify the association of Rush with endosomes, I performed cell fractionation experiments. Wild type S2 cell lysates were separated on a sucrose gradient and early and late endosome fractions were separated. Rush was found to fractionate together with endosome markers Rab5 and Rab7, but not in the fraction that contains Rab7 alone (Fig. 3-6).

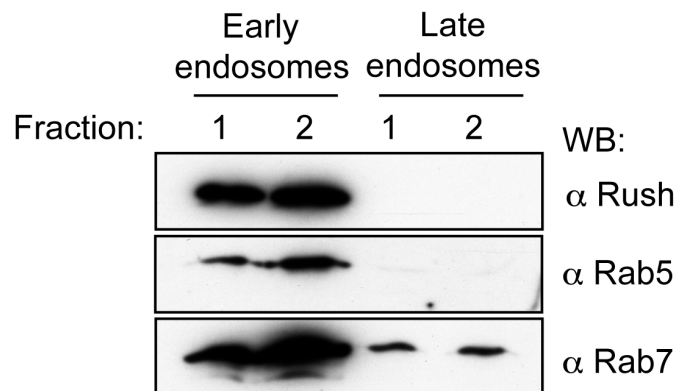


Figure 3-6. Rush cofractionates with endosomal markers. Wild type S2 cell lysates were fractionated on a sucrose gradient and the fractions corresponding to the early and late endosomes were analyzed with Western blotting. Rush co-fractionated with Rab5 and Rab7, but not Rab7 alone.

3.1.3. Effect of Rush overexpression on endocytic compartments

To further analyze association of Rush with endosomes, I generated a Rush fusion protein with a C-terminally attached GFP tag. When overexpressed in the follicle epithelium under the control of *Cu2*-Gal4, Rush-GFP localized to the lateral plasma membrane and in dot-like structures in the cytoplasm (Fig. 3-7 C''), similar to the wild type protein (Fig. 3-4 A). To test whether overexpression of Rush affects polarity of epithelial cells, the *Cu2*>Rush-GFP ovaries were stained against the polarity markers Baz and Par6. The localization of Baz and Par6 to the apical plasma membrane and the subapical region in *Cu2*>Rush-GFP follicle epithelium cells was similar as in the wild type cells (Fig. 3-7 C). Localization of E-cadherin was not affected either (Fig. 3-7 B, D). Therefore overexpression of Rush does not disrupt follicle cell polarity.

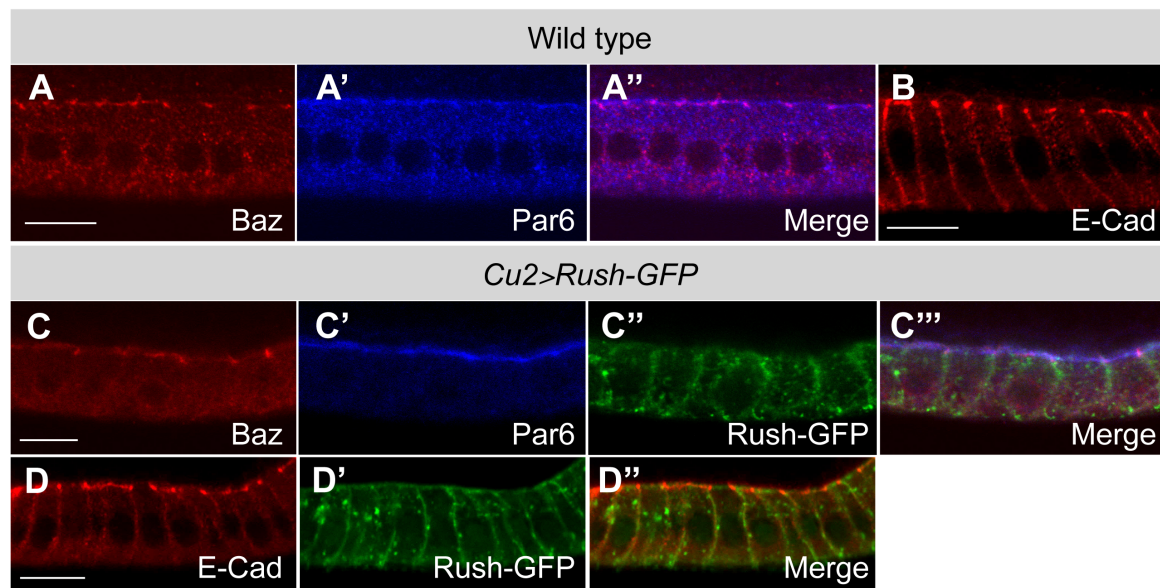


Figure 3-7. Overexpression of Rush-GFP does not affect localization of polarity markers. Expression of UAS-Rush-GFP in the follicle epithelium was driven by *Cu2*-Gal4. Ovaries were stained against Rush and polarity proteins Baz, Par6 and E-cadherin. Cross sections of follicle epithelia of stage 10 egg chambers are depicted. **A** – In the wild type follicle epithelium Baz and Par6 localize to the apical membrane and the subapical region. **B** - Localization of E-cadherin in the wild type follicle epithelium. **C** – overexpression of Rush-GFP does not change localization of Baz and Par6. **D** - overexpression of Rush-GFP does not affect localization of E-cadherin. Apical is to the top. Scale bars = 10 μ m.

To investigate whether the cytoplasmic accumulations of Rush-GFP represent endocytic compartments, I stained the ovaries that overexpress Rush-GFP in the follicle epithelium with antibodies against endosomal markers. Similarly as in the wild type tissue, Rush-GFP colocalized with Hrs and Rab7 (Fig. 3-8 A, B). Rush-GFP did not colocalize with Rab5, which localizes to early endosomes (Fig. 3-8 C), or Rab11, the marker of recycling endosomes (Fig. 3-8 D). Interestingly, overexpression of Rush-GFP led to formation of enlarged late endosomes, as marked by Rab7 staining, in comparison with wild type cells (Fig. 3-8 E). The observed large late endosomes could be induced by the activity of Rush, for example, in promoting transition between early and late endosomes or in a blockage of transport to lysosomes. Another possibility would be that the overproduction of Rush causes its increased degradation and leads to an increase in the endosome size. To test whether the cytoplasmic puncta of Rush-GFP represent functional endosomes, I performed dextran uptake experiments. Fluorescent dextran is endocytosed together with the fluid phase and can be used to track the endocytic pathway. Dextran uptake has been analyzed in detail in epithelium of wing discs of wandering third instar larvae (Boekel et al., 2006; Lu and Bilder, 2005), therefore I used this epithelial tissue for analysis of Rush-GFP

endosomes.

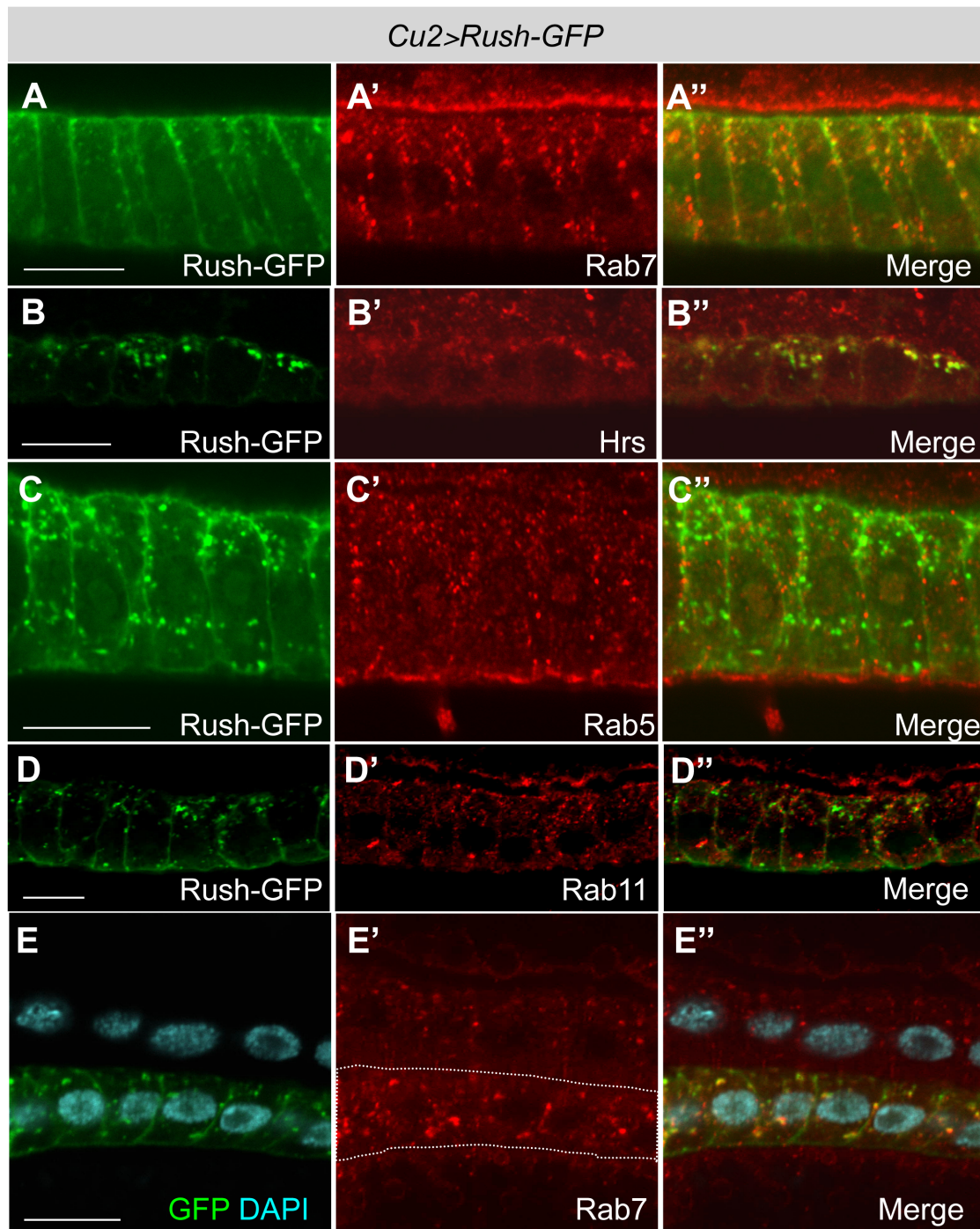


Figure 3-8. Rush-GFP colocalizes with late endosome markers. Ovaries that overexpress Rush-GFP were stained with antibodies against Rab proteins. Cross sections of follicle epithelia of stage 10 egg chambers are shown. Cytoplasmic puncta of Rush-GFP colocalize with Rab7 (A) and Hrs (B), but not with the early endosome marker Rab5 (C) or recycling endosome marker Rab11 (D). E - Rab7 vesicles are enlarged in Rush-GFP expressing follicle epithelium (marked with dotted line) in comparison with the wild type follicle cells. Apical is to the top. Scale bars = 10 μ m.

Immunofluorescence staining of wing discs with antibodies against Rush and Hrs confirmed that also in this tissue endogenous Rush and Rush-GFP colocalize with Hrs, while Hrs-positive structures are larger in the wing discs that overexpress Rush-GFP (Fig. 3-9 A, B). When incubated with fluorescent dextran, wing disc epithelial cells take up dextran molecules together with the fluid phase. After incubation of wing discs that overexpress Rush-GFP with dextran for 10 min, dextran was found in puncta inside of cells (Fig. 3-9 C'). Endocytosed dextran partially colocalized with Rush-GFP (Fig. 3-9 C), indicating that the endosomes that are marked by Rush-GFP are functional and receive freshly endocytosed material.

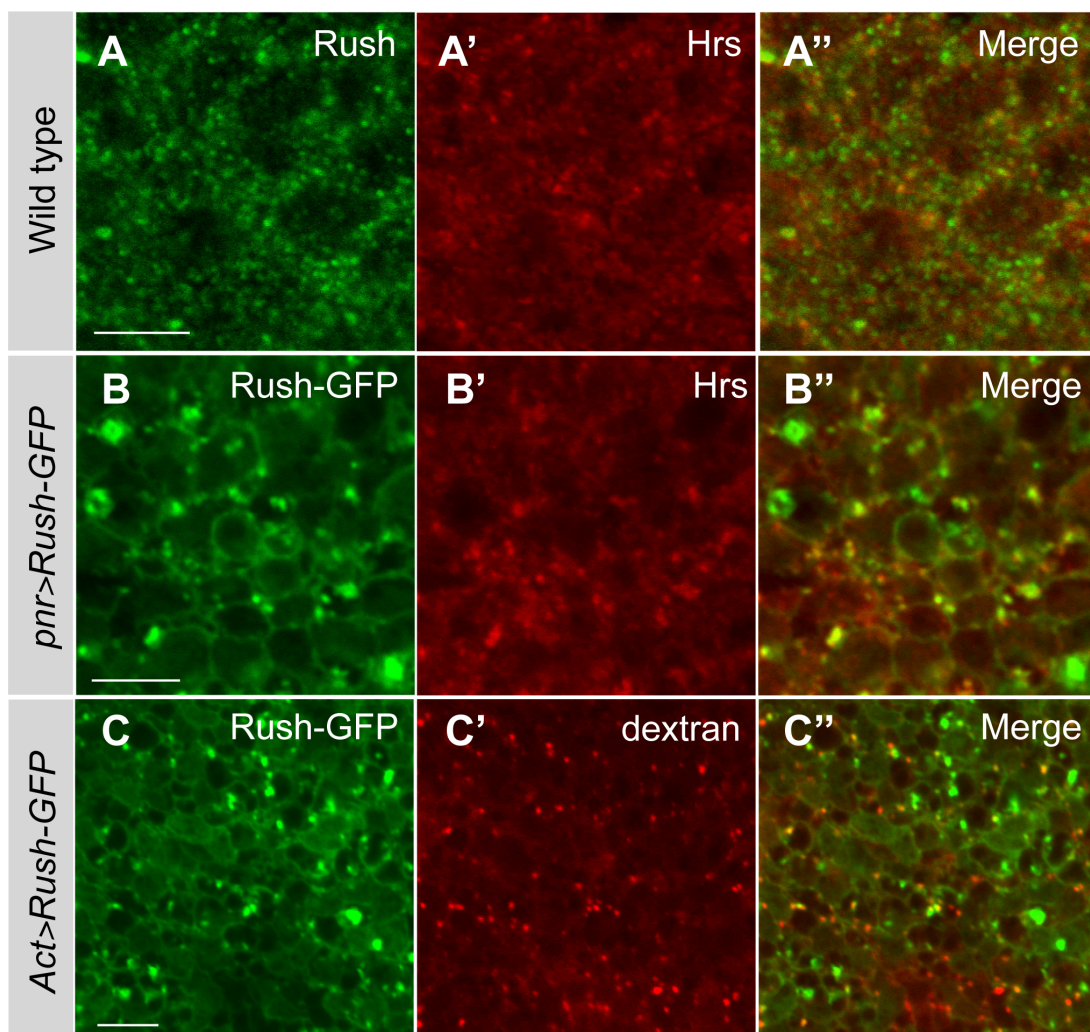


Figure 3-9. Rush colocalizes with Hrs and endocytosed dextran in wing discs. A – endogenous Rush colocalizes with Hrs in wild type wing discs. B – Rush-GFP colocalizes with Hrs in enlarged endocytic compartments. C – Rush-GFP marked endosomes are functional as shown by colocalization of endocytosed dextran. Scale bars = 5 μ m.

Results

Since Rush overexpression caused formation of enlarged late endosomes, I wondered whether the endocytic pathway downstream of late endosomes was affected. For this purpose I stained wild type egg chambers and egg chambers that overexpress Rush-GFP in the follicle epithelium with LysoTracker (LTR). LTR stains acidic intracellular compartments and especially lysosomes. LTR staining was brighter in wild type follicle epithelium than in the follicle epithelium of *Cu2>Rush-GFP* ovaries (Fig. 3-10). Therefore it is possible that trafficking from the late endosome to lysosome is slowed down in Rush overexpressing cells, and thus leads to an increase in late endosome size.

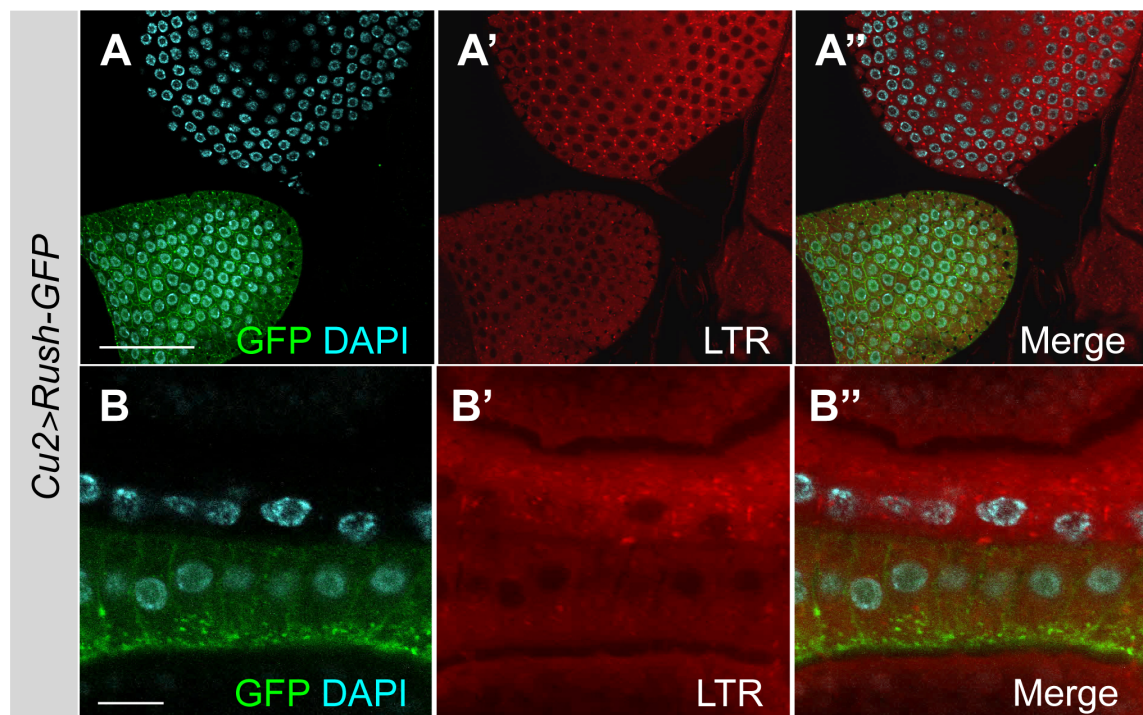


Figure 3-10. LTR staining is decreased in Rush-GFP overexpressing follicle epithelium. Wild type ovaries and ovaries with Rush-GFP expressed in follicle cells under the control of *Cu2*-Gal4 were incubated with LTR for 3 min. **A** – Follicle epithelium of stage 10 egg chambers after incubation with LTR. LTR signal is weaker in the Rush-GFP expressing follicle epithelium. **B** – Higher magnification of wild type and Rush-GFP follicle epithelium. Scale bars: A = 50 μ m, B = 10 μ m.

Unexpectedly, overexpression of UAS-Rush-GFP in the follicle epithelium under the control of the *Cu2* promoter in some cases induced apoptosis of germline cells (Fig. 3-11 A-C). Germline cells of *Cu2>Rush-GFP* egg chambers exhibited the hallmarks of apoptosis - condensed and fragmented nuclei. Interestingly, in most cases the follicle cells that express Rush-GFP were not apoptotic (Fig. 3-11 B). Expression of *Cu2*-Gal4 begins in stage 8 egg chambers. The observed apoptotic egg chambers usually had reached stage 10

in the oogenesis (Fig. 3-11 A-C), possibly due to higher Rush-GFP levels after a longer expression period. To test whether the cell-non-autonomous apoptotic effect of Rush overexpression is specific to stage 10 chambers, I overexpressed Rush-GFP under the control of the P{GawB}109C1 enhancer trap line, which drives Gal4 expression in polar cells and follicle cells starting from early stages of oogenesis. Also in this case egg chambers with apoptotic germline cells were observed (Fig. 3-11 D). When Rush-GFP was expressed in the follicle epithelium starting from early stages, egg chambers underwent apoptosis earlier, indicating that the apoptosis is not specific to a stage in oogenesis, but rather to Rush-GFP levels.

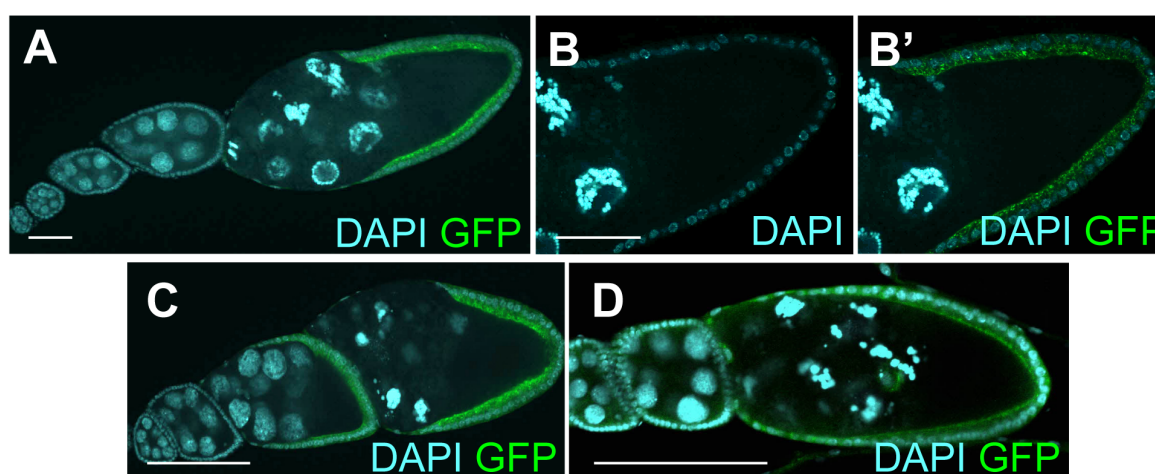


Figure 3-11. Overexpression of Rush-GFP in the follicle epithelium causes germline apoptosis. A, B, C – overexpression of UAS-Rush-GFP in the follicle epithelia under the control of the *Cu2*-Gal4 driver leads to germline apoptosis. B – A magnification of the stage 10 egg chamber shown in A. D – expression of UAS-Rush-GFP under the control of the P{GawB}109C1 enhancer trap line also induces germline apoptosis. Apoptotic stage 9 egg chamber is shown. Anterior is to the left. Scale bars: A, C, D = 100 μ m, B = 50 μ m.

3.2. Rush modifies the shape of Rab5-induced early endosomes

As Rush localizes both to the plasma membrane and to late endosomes, we wondered whether Rush associates also with early endosomes. It is possible that I could not observe colocalization between Rab5 and Rush due to weak antibody staining in wild type epithelium. For this purpose I decided to analyze Rush localization in flies that express Rab5Q88L, which is unable to hydrolyze GTP and is therefore constitutively in its active state (Rab5CA). Rab5 in the active state promotes fusion of endocytic vesicles with early endosomes and the homotypic fusion of separate early endosomes (Gorvel et al., 1991;

Rubino et al., 2000). When expressed alone, Rush-GFP does not significantly colocalize with Rab5 in the follicle epithelium (Fig. 3-12 A). Expression of YFP-Rab5CA in the follicle epithelium led to formation of enlarged early endosomes (Fig. 3-12 B), as described previously (Bucci et al., 1992). Interestingly, Rush colocalized with Rab5CA vesicles (Fig. 3-12 B). Co-expression of Rush-GFP together with YFP-Rab5CA resulted in striking changes of the Rab5-marked endosome morphology. Rab5-induced large endosomes changed their shape and seemed to consist of smaller interconnected vesicles (Fig. 3-12 C, inset in Fig. 3-12 C''). Rush was also localized to these large vesicle clusters (Fig. 3-12 D).

Rush-GFP-marked vesicles are distributed more or less uniformly in the cytoplasm of follicle cells (Fig. 3-13 A). In contrast, enlarged early endosomes that form in Rab5CA-expressing cells are localized at the apical side of cells (Fig. 3-13 B). Interestingly, when I co-expressed Rush-GFP together with YFP-Rab5CA, Rush changed its localization and was now found only in apical endosomes (Fig. 3-13 C).

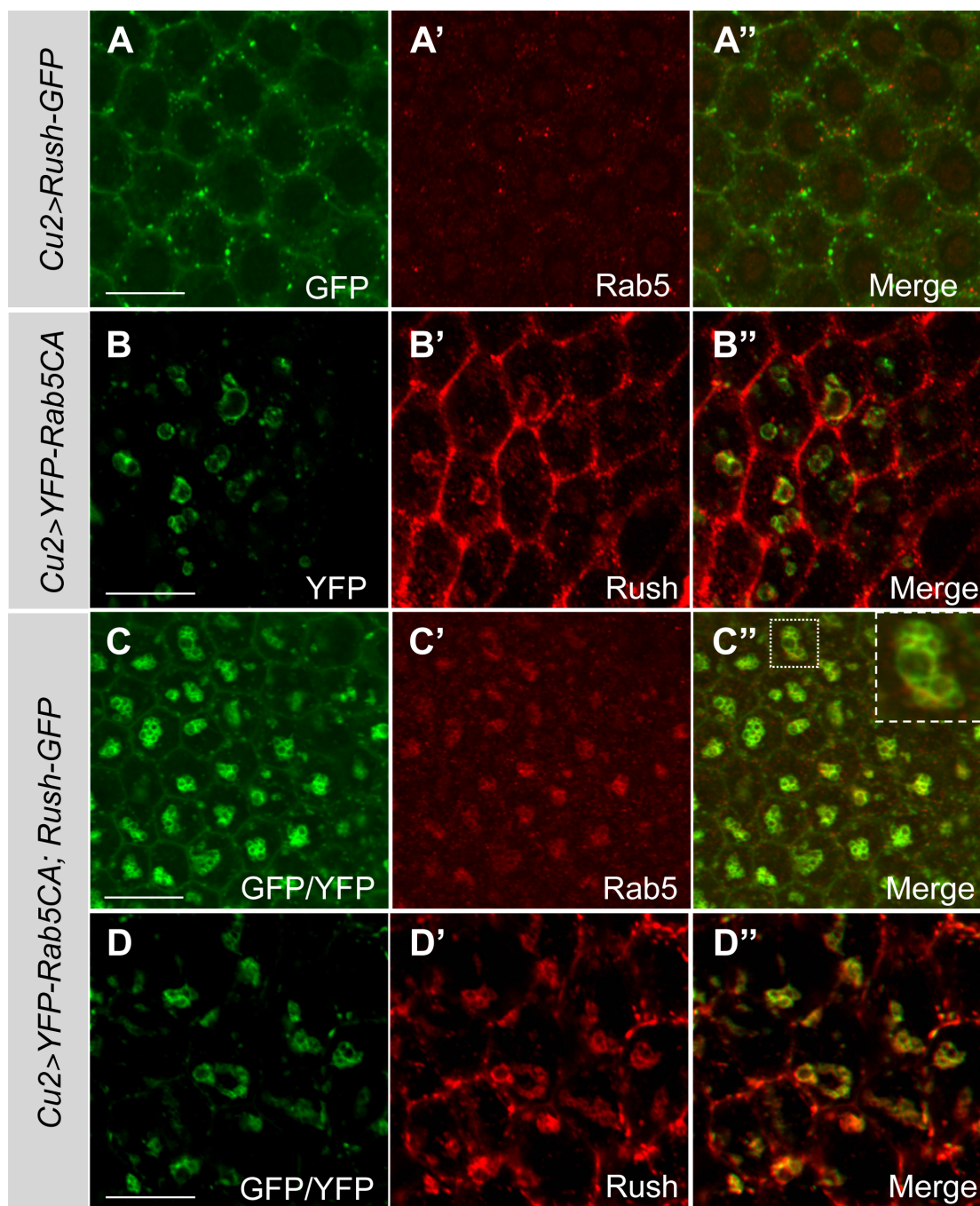


Figure 3-12. Rush-GFP changes the shape of Rab5CA-induced endosomes. Rush-GFP and/or YFP-Rab5CA were overexpressed in the follicle epithelium with *Cu2>Gal4*. All panels depict tangential sections of stage 10 egg chamber follicle epithelium. **A** – Rush-GFP does not colocalize with Rab5. **B** – Expression of YFP-Rab5CA results in formation of large endosomes that colocalize with Rush. **C, D** – co-expression of Rush-GFP and YFP-Rab5CA leads to fractionation of the large endosomes. Inset in C'' represents the area marked by the white rectangle. Scale bars = 10 μ m.

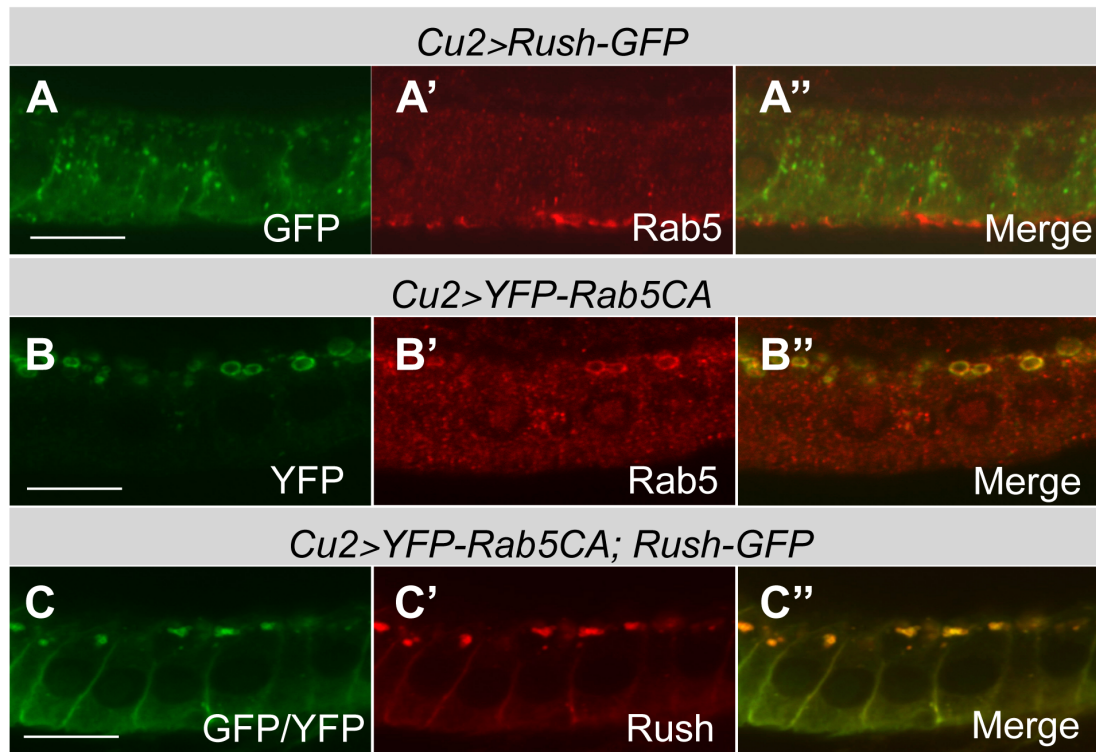


Figure 3-13. Rab5CA expression changes the localization of Rush-GFP. All panels show cross sections of the follicle epithelium of stage 10 egg chambers. **A** – Rush-GFP localization in follicle epithelium. **B** – Rab5CA causes formation of large apical endosomes. **C** – When co-expressed with Rab5CA, Rush-GFP changes its localization and localizes apically. Apical is to the top. Scale bars = 10 μ m.

Rush-GFP, when expressed alone, colocalizes with Rab7, a marker for late endosomes (Fig. 3-14 A). As expression of Rab5CA leads to relocation of Rush to early endosomes, I tested whether Rab5CA affects localization of other late endosomal proteins like Rab7. I found that Rab7 also became associated with Rab5CA-positive large endosomes (Fig. 3-14 B). Rab7 is also recruited to the clusters of endosomes that are formed due to simultaneous overexpression of Rush-GFP and YFP-Rab5CA (Fig. 3-14 C).

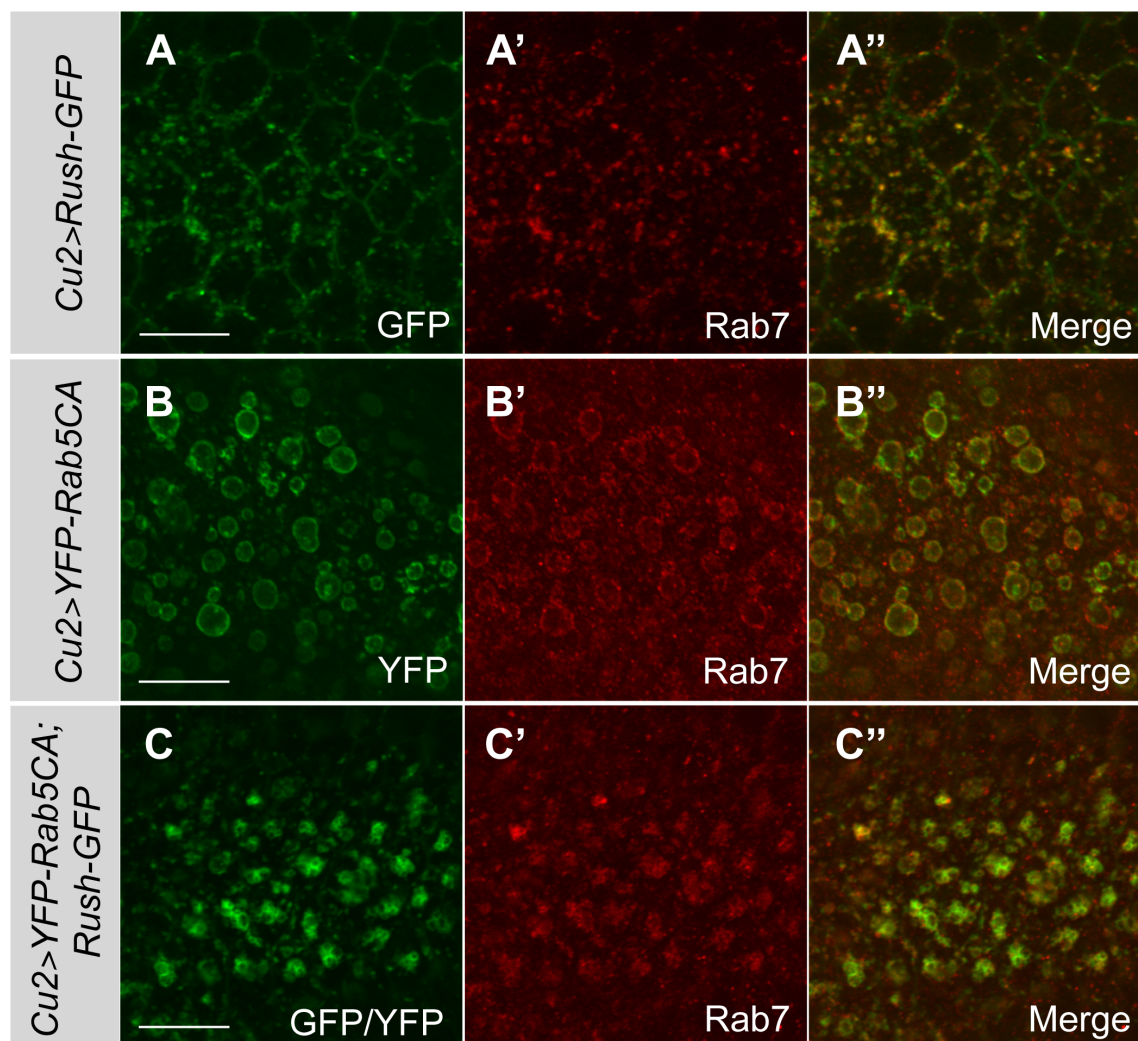


Figure 3-14. Rab7 localizes to Rush-GFP and YFP-Rab5CA vesicles. **A** – Rush-GFP colocalizes with Rab7. **B** – Rab7 localizes to Rab5CA-induced large endosomes. **C** – Rab7 colocalizes with large vesicle clusters in follicle cells that co-express Rush-GFP and YFP-Rab5CA. All panels show tangential sections of stage 10 egg chamber follicle epithelium. Scale bars = 10 μ m.

As Rab5CA caused relocation of late endosome proteins to the Rab5-positive compartment, I performed stainings against Rab11 to see if the distribution of the recycling endosome proteins is affected. Rab11 does not colocalize with Rush-GFP vesicles (Fig. 3-15 A) and Rab5CA vesicles (Fig. 3-15 B). In the cells that express Rush-GFP and YFP-Rab5CA, Rab11 signal is slightly increased in the clustered endosomes (Fig. 3-15 C). Taken together, expression of Rab5CA leads to association of late endosome proteins and Rush with enlarged early endosomes, most probably due to inability of early endosomes to transit to a late endosome state. Overexpression of Rush together with Rab5CA changed the morphology of the enlarged early endosomes, leading to their fragmentation.

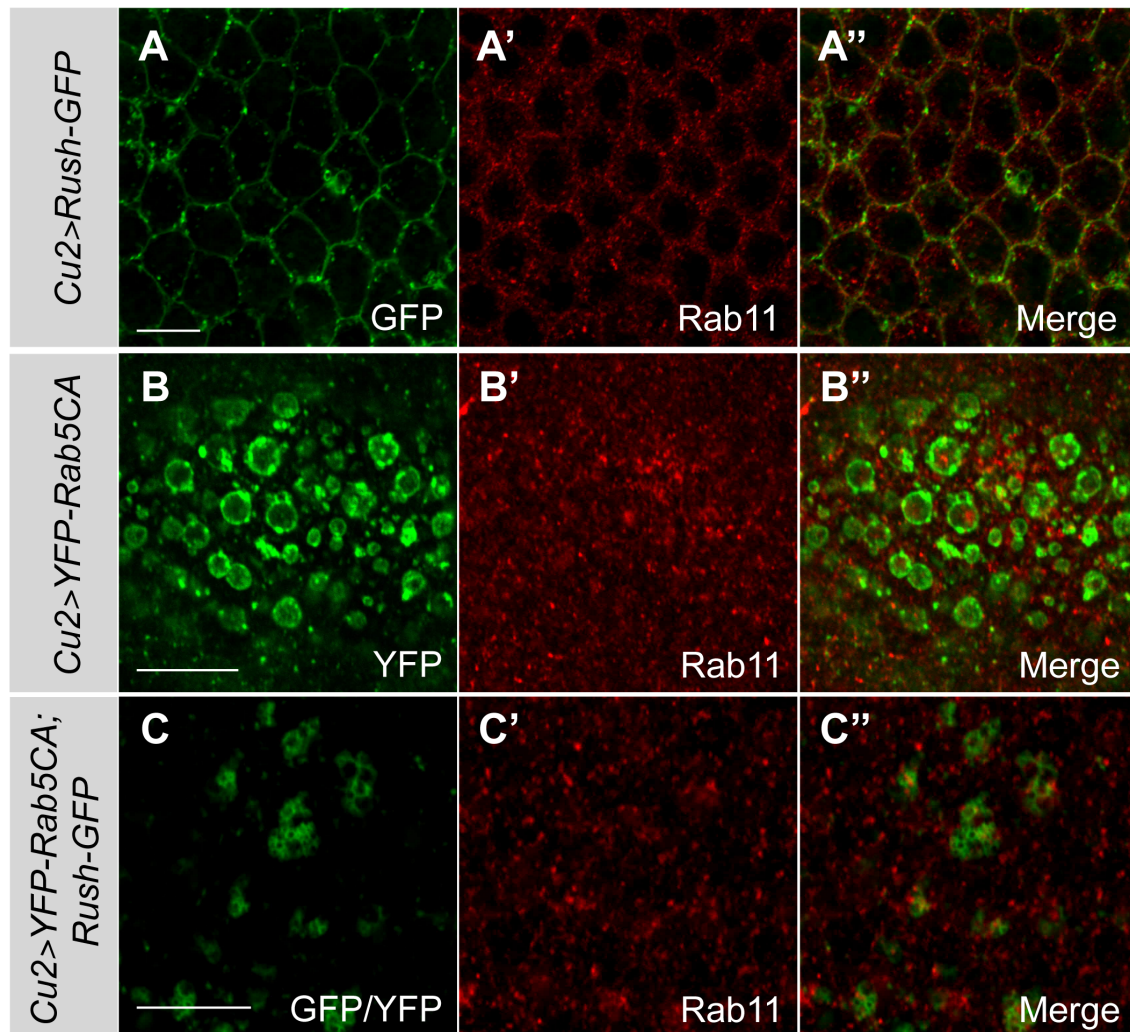


Figure 3-15. Localization of Rab11 in Rush-GFP and/or YFP-Rab5CA expressing follicle epithelium. **A** – Rab11 shows very limited colocalization with Rush-GFP. **B** - Rab11 does not colocalize with Rab5CA. **C** - Rab11 staining is slightly increased at Rush-GFP, Rab5CA-induced clustered endosomes. All panels are tangential sections through the follicle epithelium of stage 10 egg chambers. Scale bars = 10 μ m.

3.3. Lipid binding properties of Rush

Rush contains two lipid binding domains, a PH and a FYVE domain (Fig. 1-6, Fig. 3-16 A). Both FYVE and PH domains interact with phosphatidylinositol phosphates (PIPs), but differ in their affinity for PIPs. FYVE domains have been described to bind specifically to PI(3)P, a phosphoinositide found on early endosomes and multivesicular bodies (van Meer et al., 2008). PH domains of different proteins have diverse affinities to PIPs, e.g. the PH domain of phospholipase C δ 1 (PLC δ 1) binds preferentially to PI(4,5)P₂, while 3-phosphoinositide-dependent kinase 1 (PDK1) interacts with PI(3,4)P₂ and PI(3,4,5)P₂ (Varnai et al., 2002; Currie et al., 1999). Rush localizes to the plasma membrane and

endosomes. Lipid binding domains of Rush could mediate its membrane association. Therefore I aimed to determine whether the lipid binding domains of Rush are functional and which lipids they bind to. For this purpose I performed lipid overlay assays with GST-tagged full length Rush and its separate domains (Fig. 3-16 A). As both domains have been described to interact with PIPs, GST fusion proteins were incubated with phospholipids that are immobilized on a nitrocellulose membrane (PIP Strips). A scheme of the distribution of phospholipids on the membrane is shown in Fig. 3-16 B. The results of the lipid overlay assay are shown in Fig. 3-16 C. The PH domain of Rush interacted most strongly with PI(3,4)P₂ and PI(4)P and had a weaker interaction with PI(3)P. The FYVE domain, as expected, interacted exclusively with PI(3)P. Full length Rush interacted most strongly with PI(3)P, but also bound to a lesser extent with PI(4)P, PI(5)P, PI(3,4)P₂, PI(4,5)P₂ and PI(3,4,5)P₃. Thus, the lipid binding domains of Rush are able to interact with PIPs and Rush has the highest affinity towards PI(3)P, a lipid specific for early endosomes (van Meer et al., 2008).

To analyze how the two lipid binding domains affect the subcellular localization of Rush, I aimed to eliminate lipid binding properties of each of the domains. Single amino acid exchange mutations that abolish lipid binding of PH and FYVE domains have been described before (Kutateladze, 2006; Yagisawa et al., 1998). In both domains basic amino acid residues are responsible for the interaction with phospholipids. In the FYVE domain the core motif RR/KHHCR is responsible for the interaction of the domain with PI(3)P. Mutations in any of the arginine or histidine residues in this motif leads to disruption of the lipid binding (Gaullier et al., 2000). Based on these findings, I exchanged the Arg¹⁷⁶ residue of Rush with Gly using site-directed mutagenesis (Fig. 3-16 A). A Lys³² exchange with Glu in the phospholipase C PH domain abolished the ability of the protein to interact with P(4,5)P₂ (Yagisawa et al., 1998). The homologous residue Lys⁴⁸ in the PH domain of Rush was identified based on an alignment with the phospholipase PH domain and mutated to Glu (Fig. 3-16 A). The lipid binding abilities of the mutated domains and the full length Rush are shown in Fig. 3-16 D. The PH domain with the K48E mutation lost its ability to interact with PIPs, as well as the FYVE domain with the R176G mutation (amino acid numbering according to their position in full length Rush). The full length Rush^{K48E} interacted only with PI(3)P due to the activity of the FYVE domain. Rush^{K48E R176G} was not able to interact with PIPs and exhibited only background interaction levels. Interestingly, also Rush^{R176G} lost its affinity to PIPs, although one would expect a similar affinity to PIPs as for the PH domain alone. This effect might be caused by conformational changes in the

Results

protein caused by the mutation. It is also possible that in a full length protein an interaction between the PH and FYVE domains is necessary for lipid association of Rush.

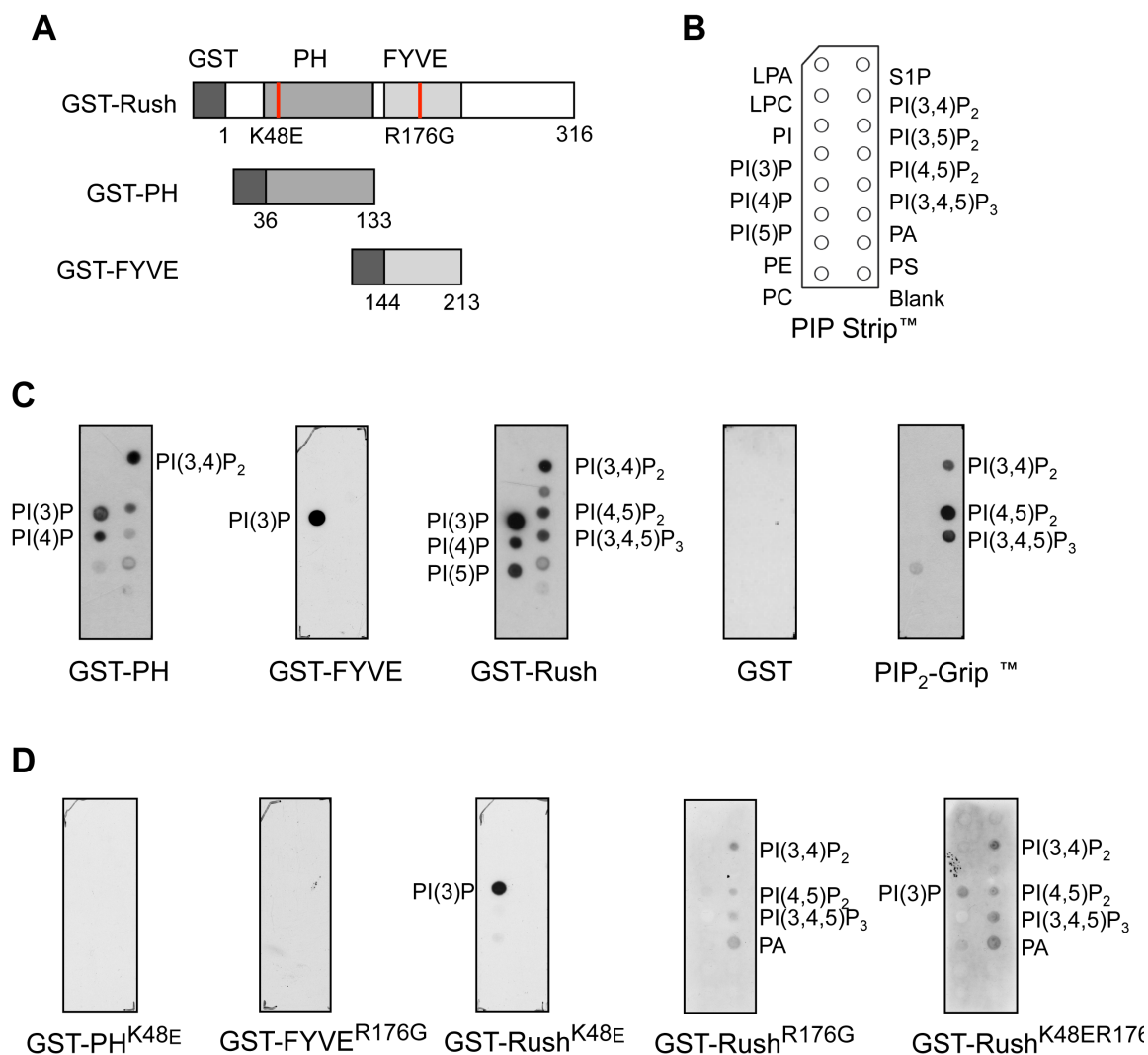
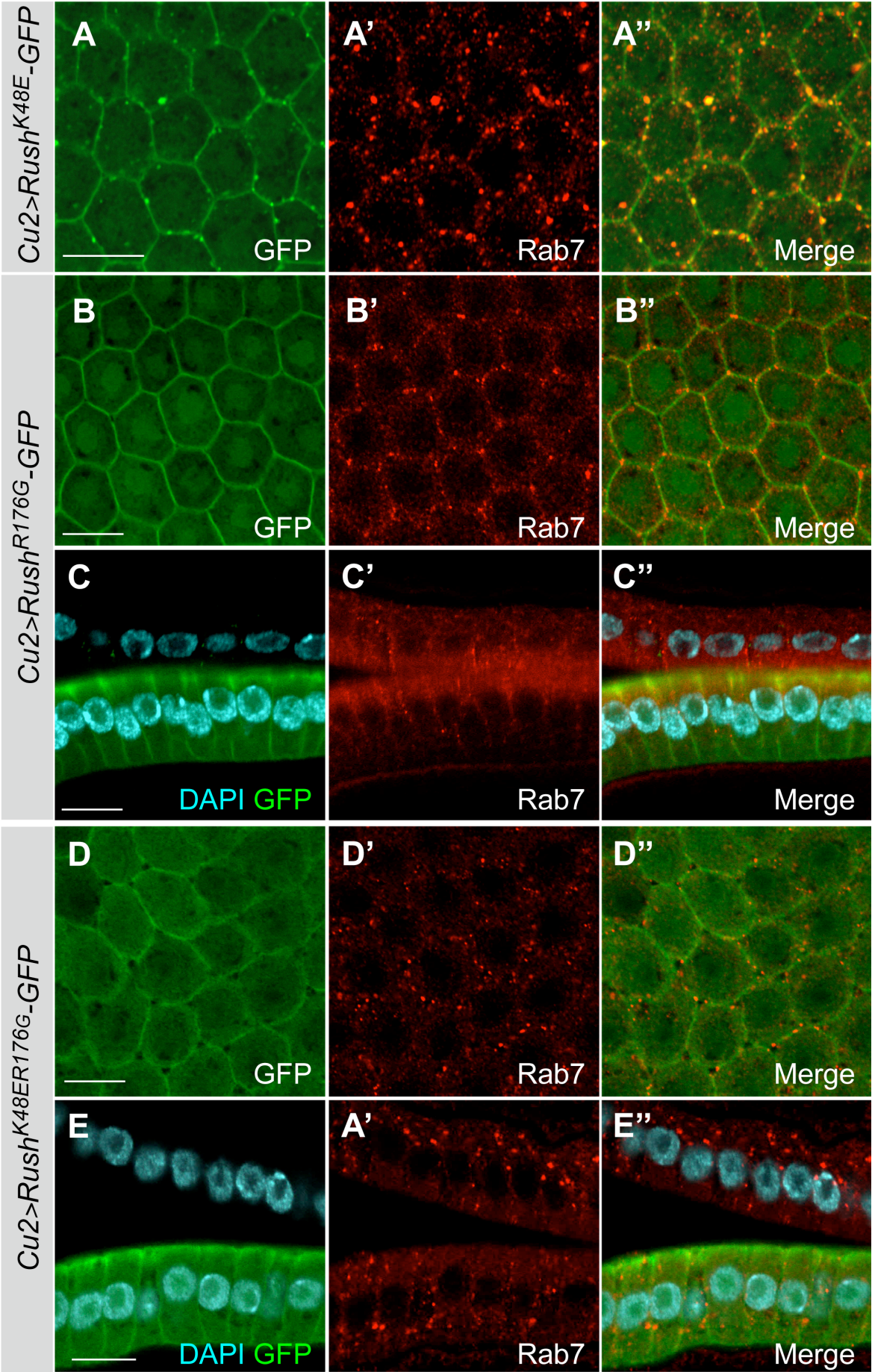


Figure 3-16. Lipid binding specificity of Rush. **A** – A scheme of GST fusion constructs that were used in lipid overlay assays. Red bars indicate the amino acid residues that were mutated to abolish lipid binding abilities of the respective domain. **B** – Scheme of a PIP Strip showing the lipid composition of dots. **C** – Binding of Rush and its lipid binding domains to different PIPs. PIP Strips were incubated with GST fusion proteins and lipid-bound proteins were detected with anti-GST antibody. GST only and PIP₂-Grip were used as controls. PIP₂-Grip is a GST-tagged PH domain with the highest affinity towards PI(4,5)P₂. **D** – Single amino acid mutations in PH and FYVE domains of Rush abolish their ability to bind with PIPs.

To observe how the mutations in lipid binding domains affect the localization of Rush in cells, transgenic flies expressing mutated full length Rush proteins tagged with GFP were created. When expressed in the follicle epithelium, Rush^{K48E}-GFP could still localize to the plasma membrane and endosomes, indicating that the FYVE domain of Rush is sufficient

for membrane localization of Rush (Fig. 3-17 A). Unexpectedly, Rush^{R176G}-GFP was detected at the plasma membrane (Fig. 3-17 B), although no significant affinity of Rush^{R176G} towards PIPs could be detected in the lipid overlay assay (Fig. 3-16 D). Rush^{R176G}-GFP did not colocalize with cytoplasmic Rab7 puncta, indicating that the FYVE domain of Rush is needed for the association with endosomes (Fig. 3-17 B). Rush^{K48ER176G}-GFP, as expected from the lipid overlay assay, did not bind to membranes and was distributed in the cytoplasm (Fig. 3-17 D). Overexpression of Rush^{K48E}-GFP led to formation of large Rab7-positive endosomes (Fig. 3-17 A), similarly as expression of wild type Rush-GFP (Fig. 3-8 E). Overexpression of either Rush^{R176G}-GFP or Rush^{K48ER176G}-GFP did not enlarge the size of late endosomes (Fig. 3-17 E), suggesting that the FYVE domain of Rush is responsible for its effect on the late endosome size.

Figure 3-17. Subcellular localization in Rush lipid binding defective mutants. **A** – Rush^{K48E}-GFP localizes to the plasma membrane and Rab7-positive endosomes similarly as the wild type Rush. Rush^{K48E}-GFP mutant also causes formation of enlarged Rab7-positive endosomes. **B** - Rush^{R176G}-GFP localizes to the plasma membrane and does not localize to Rab7 vesicles. **C** - The size of Rab7 endosomes is not increased in Rush^{R176G}-GFP expressing follicle cells in comparison to the wild type epithelium. **D** – Rush^{K48ER176G}-GFP has lost its ability to associate with membranes and is cytoplasmic. **E** – Rush^{K48ER176G}-GFP overexpression does not cause formation of enlarged late endosomes. Wild type follicle epithelium is shown for comparison. Scale bars =10 μ m.



3.4. Generation of *rush* mutant allele

To further investigate the function of Rush, a *rush* null allele was generated. For this purpose the full coding sequence of *rush* was removed via FLP/FRT-mediated excision. This method makes use of the ability of FLP recombinase to cause a recombination between two FRT sites positioned on two complementary chromosomes (in *trans*). Two transposon insertion lines that contain FRT sites were available from the Harvard stock collection. These transposons are inserted upstream and downstream of the *rush* locus. The P(XP)d03799 element is located in the 5' UTR of *rush* (Fig. 3-1, Fig. 3-18 A), while pBac(WH)f03712 element is inserted in the 5' UTR of *sta*, a gene located downstream of *rush* (Fig. 3-18 A). The FLP recombinase-induced deletion of the genomic region between the two FRT sites was used to remove the *rush* coding region. The *sta* gene downstream of *rush* was also removed during the recombination. *sta* is an essential gene, therefore a rescue construct containing a full coding sequence of *sta* including the upstream regulatory sequences was crossed in after the recombination. Mutant flies were selected by the white eye phenotype, since the recombination removed *mini-white* genes carried by the transposons. Obtained white-eyed flies were homozygous viable, and healthy stocks could be established.

As the obtained putative *rush* deletion lines were homozygous viable, the loss of *rush* gene was tested by several methods. The deletion of *rush* genomic region was verified by PCR on genomic fly DNA (Fig. 3-18 B, C). PCR with the primer pair that encompasses the whole deleted region leads to formation of a 5105 bp long fragment in wild type flies, while only a shorter 2442 bp fragment is obtained from the genomic DNA of *rush* deletion lines (Fig. 3-18 B). This shorter fragment represents the residual transposon that is left at the deletion site after the recombination has taken place. Primers that are complementary to the N-terminus and C-terminus of *rush* produce a 951 bp fragment in wild type flies (Fig. 3-18 C). No PCR product is formed in the *rush* deletion flies, showing that the whole coding region of *rush* is deleted. To prove that the obtained mutant lines represent a *rush* null allele, we performed Western blot with protein extracts from the flies of original transposon insertion lines and the *rush* mutant flies (Fig. 3-18 D). Blotting with the antibody against the C-terminus of Rush resulted in a band of approximately 40 kD that corresponds to the full length Rush in the extracts from original transposon insertion stocks. In comparison, no signal for Rush was detected in the *rush*⁴ embryo extract,

indicating that *rush*⁴ is indeed a null allele.

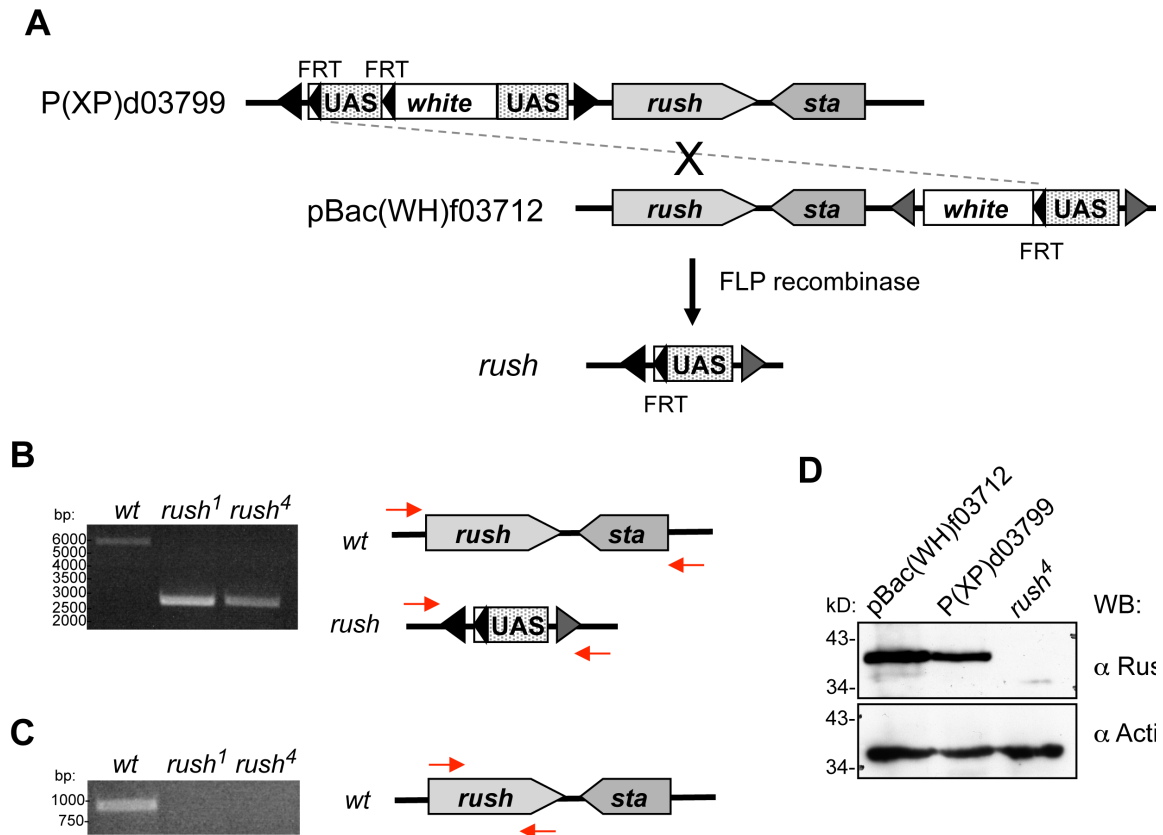


Figure 3-18. Generation of *rush* null allele. **A** – The scheme of generation of *rush* deletion via FLP/FRT recombination. Two transposons that contain FRT sites are inserted upstream and downstream of *rush* and its neighboring gene *sta*. Induction of FLP recombinase expression leads to recombination between FRT sites. The recombination in *cis* happens first, thus removing the UAS sequence of the P(XP)d03799 element and leaving one FRT site. The recombination in *trans* (shown with a dotted line) leads to removal of the genomic sequence between the two FRT sites. After the recombination a residual transposon is left at the deletion site. A rescue construct for *sta* was crossed in after the recombination. **B**, **C** – Verification of the deletion of the *rush* gene by PCR on adult fly genomic DNA. **B** – PCR with primers upstream and downstream of the whole deletion site. In case of the wild type stock, a DNA fragment of 5105 bp that includes *rush* and *sta* genes is obtained. In *rush* deletion lines a shorter DNA fragment of 2442 bp forms that covers the residual transposon after the deletion. **C** – PCR with *rush* specific primers. In wild type flies a PCR product of 951 bp length, which covers the full coding sequence of *rush*, is obtained. No product could be obtained in the *rush* deletion lines. Results from two deletion lines are depicted. **D** – Protein extracts from the flies of original transposon stocks and a *rush* deletion line were blotted with an antibody against Rush C-terminus. No Rush protein was detected in the extract from *rush*⁴ flies. Antibody against actin was used as a loading control.

3.5. Characterization of *rush* null allele

Flies with *rush* deletion were homozygous viable and did not show obvious phenotypic defects. To test whether loss of Rush leads to defects in cell polarity I stained ovaries of *rush*⁴ flies with antibodies against Baz and Rush. Localization of Baz at the cell-cell contacts in *rush*⁴ mutant follicle epithelium was the same as in the wild type cells (Fig. 3-19). No signal for Rush could be detected in *rush*⁴ follicle epithelium (Fig. 3-19 B). Optical sections in Fig. 3-19 were taken through the apical side of epithelial cells to detect Baz, while Rush localizes at the plasma membrane slightly below Baz and colocalizes with E-cadherin (Fig. 3-3). Therefore Rush staining in Fig. 3-19 A is detected mainly in cytoplasmic puncta.

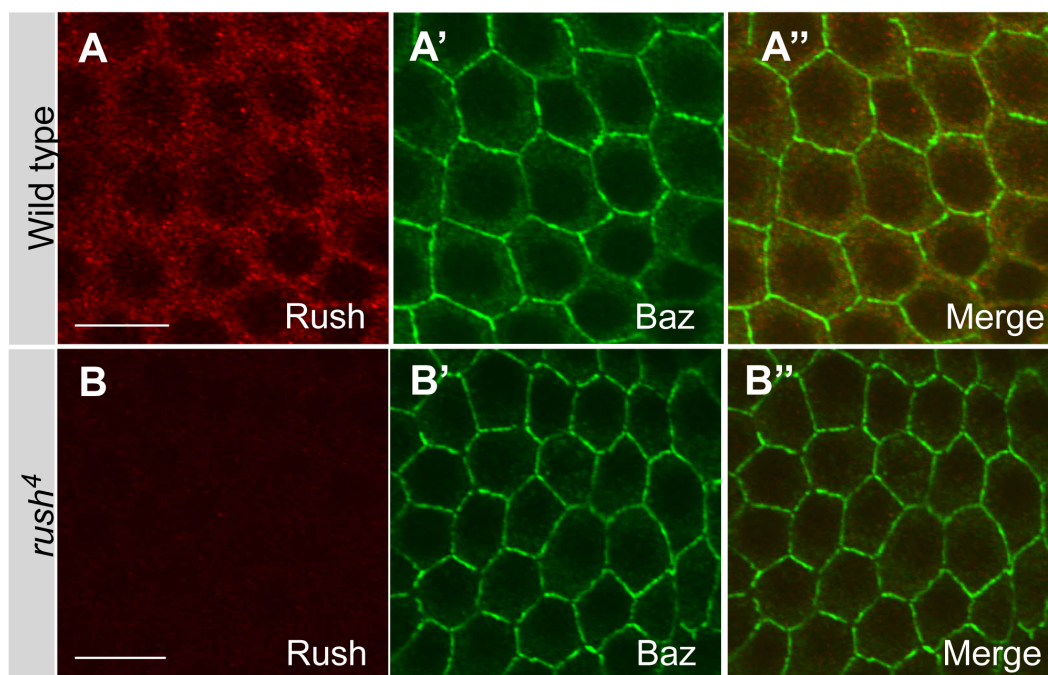


Figure 3-19. Loss of Rush does not affect localization of Baz. Wild type and *rush*⁴ fly ovaries were stained with antibodies against Rush and Baz. Tangential sections of stage 10 follicle epithelia are shown. No Rush staining was detected in the mutant epithelia (**B**) in comparison to wild type ovaries (**A**). Baz is located at the cell-to-cell contacts in the wild type follicle epithelium (**A**). **B** – Localization of Baz in *rush*⁴ mutant follicle epithelium is the same as in the wild type. Scale bars = 10 μ m.

In a low number of cases abnormally large *rush*⁴ egg chambers were observed (Fig. 3-20 A, B). In contrast to wild type egg chambers that are comprised of 16 cells and have one oocyte (Fig. 3-20 C), these egg chambers are formed by 32 cells and often have two oocytes (Fig. 3-20 D). Increased number of nuclei in an egg chamber can be caused by two reasons. First, an increased number of germline stem cell divisions can lead to an abnormal cell number. Second, a fusion of two egg chambers might have taken place. The second

possibility is supported by the double number of cells and the presence of two oocytes. Egg chambers are separated from each other by stalk cells. Formation of stalk cells is induced by differentiated follicle cells, so called polar cells. In wild type egg chambers, two pairs of polar cells are specified at the anterior and posterior end of the egg chamber (Fig. 3-20 H', white arrows). If differentiation of polar cells is impaired, stalks do not form. Lack of stalk cells can lead to fusion of two neighboring egg chambers. To test this possibility, I stained *rush*⁴ ovaries with antibody against FasIII, a protein that is expressed in all follicle cells of newly formed egg chambers and specifically marks polar cells in later stages. In *rush*⁴ ovaries, some of the enlarged egg chambers have three clusters of polar cells (Fig. 3-20 E - H, white arrowheads). Therefore it is possible that the fusion of *rush*⁴ egg chambers is caused by defects in polar cell differentiation, which then leads to fusion of egg chambers. Polar and stalk cells differentiate from a common pool of progenitor cells, therefore defects in formation of polar cells often affect the number of stalk cells (Grammont and Irvine, 2001). To test whether stalk formation is affected in *rush* mutants, I counted the number of stalk cells in *rush*⁴ and wild type ovarioles. The average number of stalk cell was increased in *rush* ovarioles (Fig. 3-20 I). Thus the differentiation of both polar and stalk cells is affected in *rush* mutant ovaries.

As wild type Rush localized to endosomes and Rush overexpression increased late endosome size, I tested *rush*⁴ mutant flies for changes in compartments of the endocytic pathway. For this purpose I stained *rush*⁴ ovaries with antibodies against Rab7 and Rab11 for analysis of late and recycling endosomes respectively. Staining of the pBac(WH)f03712 insertion stock (marked as f03712 in Fig. 3-21) was used as a control. Rab7 staining in the follicle epithelium of *rush*⁴ ovaries was often weaker than in the epithelium of the control ovaries (Fig. 3-21 A, B). To find out whether the observed difference in Rab7 signal was due to changes in endosome formation, I compared the size and number of Rab particles in the samples using ImageJ software. Interestingly, Rab7 vesicles were smaller in *rush*⁴ epithelia (2,21 μ m) than in control sample (2,48 μ m). This size difference was highly statistically significant ($p < 0,0001$; Fig. 3-21 C). In comparison, the size of Rab11 marked recycling endosomes in both samples did not differ to a statistically significant level (Fig. 3-21 C). The number of the Rab7 and Rab11 endosomes did not significantly differ between the two samples (Fig. 3-21 D, E). Thus loss of *rush* decreases the size of late, but not recycling, endosomes.

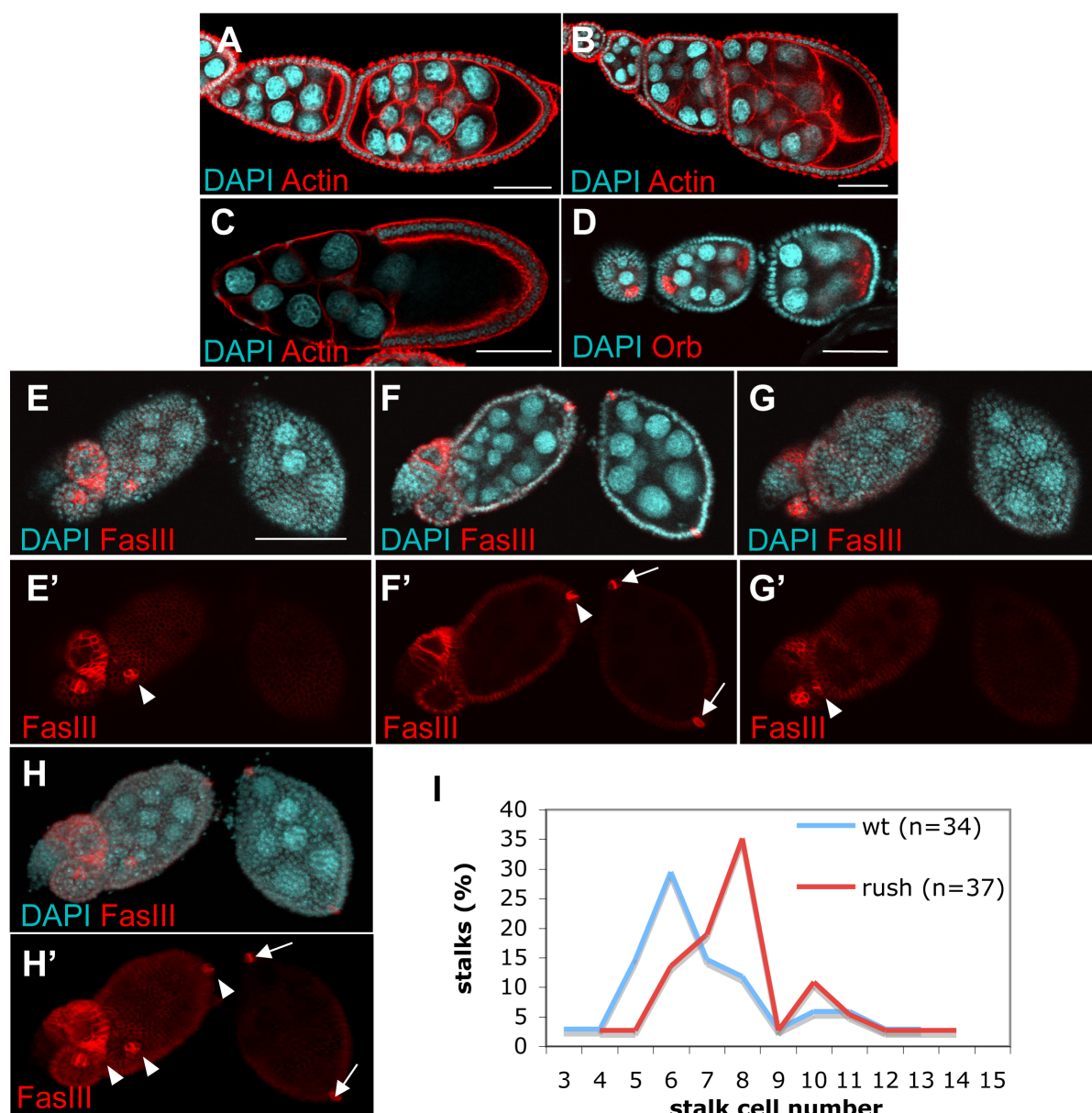


Figure 3-20. Egg chambers of *rush*⁴ flies display defects in oogenesis. The ovaries of *rush*⁴ flies were stained with phalloidin to mark actin cytoskeleton and DAPI. In some cases fused egg chambers comprised of 32 cells were observed (A, B). A normal wild type egg chamber contains 16 cells (C). D – Fused egg chambers contain two oocytes, marked by Orb staining (in the middle). In comparison, only one Orb-positive oocyte is found in normal egg chambers. E, F, G, H – *rush*⁴ ovaries were stained with the antibody against polar cell marker FasIII. Panels E–G represent z sections through the enlarged egg chamber. H – projection of z-stacks taken through the egg chambers. H' – Wild type egg chambers have two pairs of polar cells that are positioned at the anterior and posterior end of the egg chamber (marked with white arrows). In the fused egg chamber three clusters of polar cells are marked by FasIII (white arrowheads). Anterior is to the left. Scale bars = 50 μ m. I – The average stalk length is increased in *rush*⁴ ovarioles in comparison to the wild type.

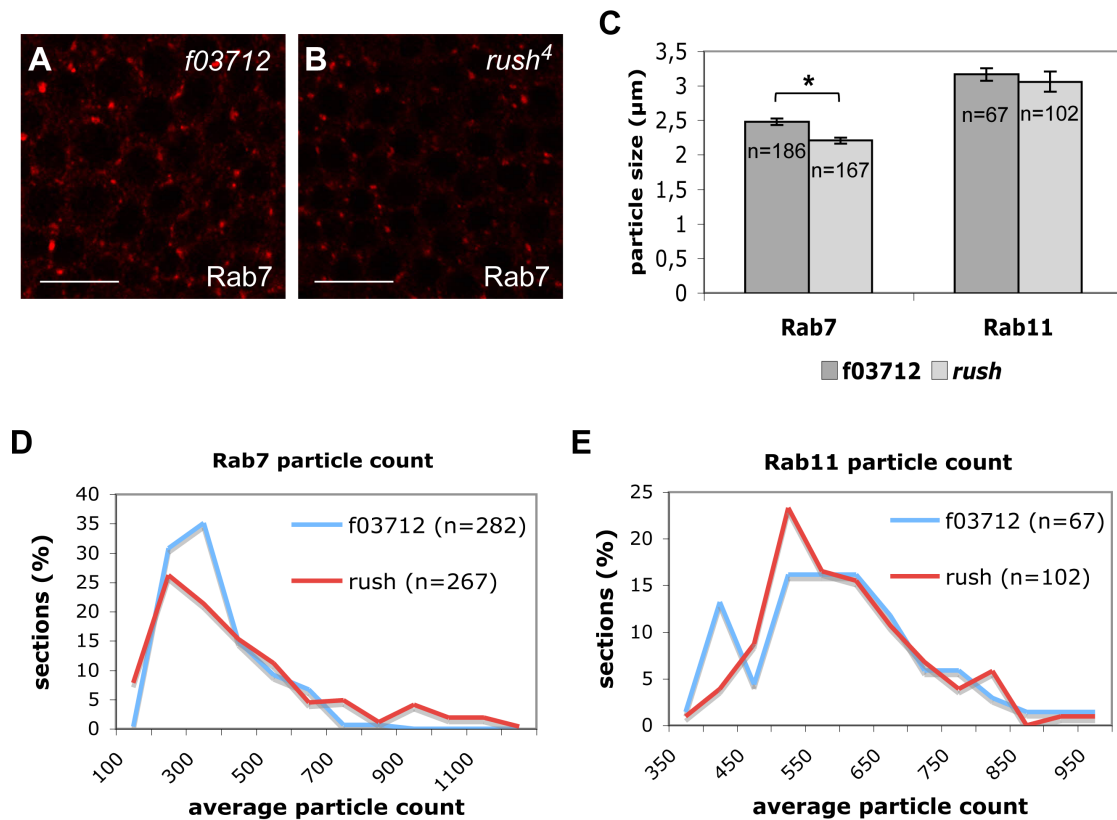


Figure 3-21. The effect of *rush* deletion on endosomal compartments. **A, B** - The ovaries of *rush*⁴ and original transposon insertion stock (f03712) flies were stained against Rab7. Middle sections of the follicle epithelium of stage 8 egg chambers are shown. Scale bars = 10 μm. **C** - Rab7 and Rab11 particle size was measured from z-stacks taken through the follicle epithelium of individual stage 8 egg chambers (mean ± SE [error bars]). Average size of Rab7 particles was significantly smaller in *rush*⁴ epithelium than in the wild type ($p < 0,0001$). The difference between Rab11 particle size in *rush*⁴ and wild type cells was not statistically significant. The number of Rab7 (**D**) and Rab11 (**E**) particles was measured in the same z-sections of *rush*⁴ and pBac(WH)f03712 follicle epithelia as in **C**.

To check whether the loss of *rush* affects formation of early endosomes, I stained wild type and *rush* mutant ovaries with anti-Rab5 antibody. Unfortunately the staining did not give a strong signal that would allow a comparison of early endosome size between the samples. To overcome this problem, I expressed YFP-Rab5CA transgene in the follicle epithelium with the *Cu2-Gal4* driver. No significant difference in formation of Rab5CA-induced large early endosomes in the *rush*⁴ or wild type cells was observed (Fig. 3-22).

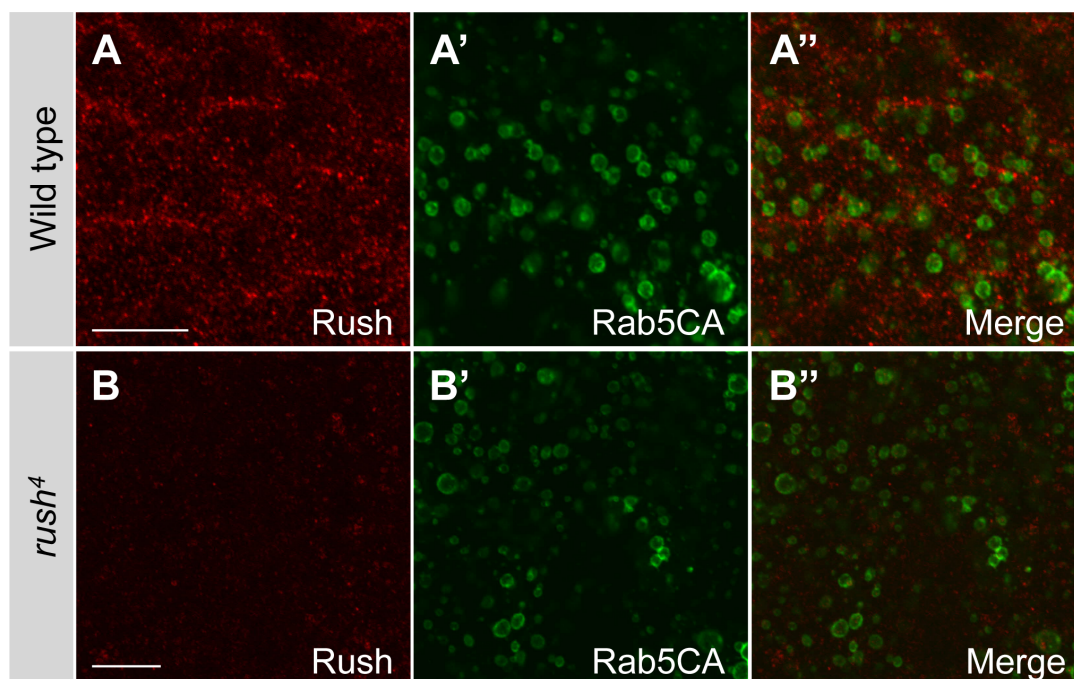


Figure 3-22. Formation of early endosomes is not affected in *rush* mutant cells. UAS-YFP-Rab5CA was expressed under the control of *Cu2-Gal4* driver in the ovaries of wild type (A) and *rush* mutant (B) flies. Tangential sections of the follicle epithelium of stage 10 egg chambers are shown. Scale bars = 10 μ m.

3.6. *rush* genetically interacts with *cdc42*

Although loss or overexpression of Rush did not cause defects in cell polarity, I tested whether Rush-induced enlarged endosomes participate in trafficking of polarity proteins. Crb is localized apically in epithelial cells and determines apical character of the plasma membrane (Wodarz et al., 1995). Regulation of Crb endocytosis by several factors, including Cdc42, has been described recently (Georgiou et al., 2008; Harris and Tepass, 2008; Leibfried et al., 2008). I investigated Crb endocytosis in Rush-GFP-overexpressing epithelial cells. As I was not able to obtain good Crb staining in the follicle epithelium, I overexpressed UAS-Rush-GFP in the embryonic ectoderm under control of the *tub-Gal4* driver (*tub>Rush-GFP*). In the embryonic ectoderm, similarly as in the follicle epithelium, overexpression of Rush-GFP leads to formation of large Rush-GFP vesicles (Fig. 3-23 A'). Crb colocalizes with Rush-GFP in these vesicles (Fig. 3-23 A). As Rush-GFP overexpression caused an increase in the endosome size, I wondered if it also increases the endocytic uptake of Crb. In comparison to *tub>Rush-GFP* embryos, cytoplasmic puncta of Crb were smaller in wild type embryos (Fig. 3-23 B). I quantified the size of Crb cytoplasmic puncta in wild type and *tub>Rush-GFP* embryonic ectoderm (Fig. 3-23 C). The quantification revealed that the average size of Crb-containing vesicles is increased

approximately two-fold in *tub>Rush-GFP* embryos (0,60 μm) in comparison to the wild type (0,37 μm). Although the endocytosis of Crb seems to be increased in *tub>Rush-GFP* embryos, I did not observe loss of Crb from the apical plasma membrane (Fig. 3-23 A, B). It might be explained by the activity of recycling endosomes that ensure the delivery of Crb back to the plasma membrane.

Expression of dominant negative Cdc42 (Cdc42DN) in the embryos has been described to result in accumulation of Crb in large Hrs-positive endosomes (Harris and Tepass, 2008). This phenotype is similar to the Rush-GFP overexpression phenotype, therefore it was interesting to determine whether Rush interacts with Cdc42 in Crb endocytosis. First, to verify the effect of Cdc42DN on Crb localization, I expressed UAS-Cdc42DN in the embryos under the control of *arm-Gal4* (*arm>Cdc42DN*). In the ectoderm of wild type embryos Crb and E-cadherin are localized to the cell-cell contacts (Fig. 3-24 A). In the embryonic ectoderm of *arm>Cdc42DN* embryos, Crb was lost from the plasma membrane and localized to cytoplasmic punctate structures (Fig. 3-24 B'). The localization of E-cadherin was less affected, although loss of E-cadherin at the plasma membrane in the ventral ectoderm was observed (Fig. 3-24 B''). These observations are in line with the effects of Cdc42DN on the Crb and E-cadherin localization, described by Harris and Tepass (2008).

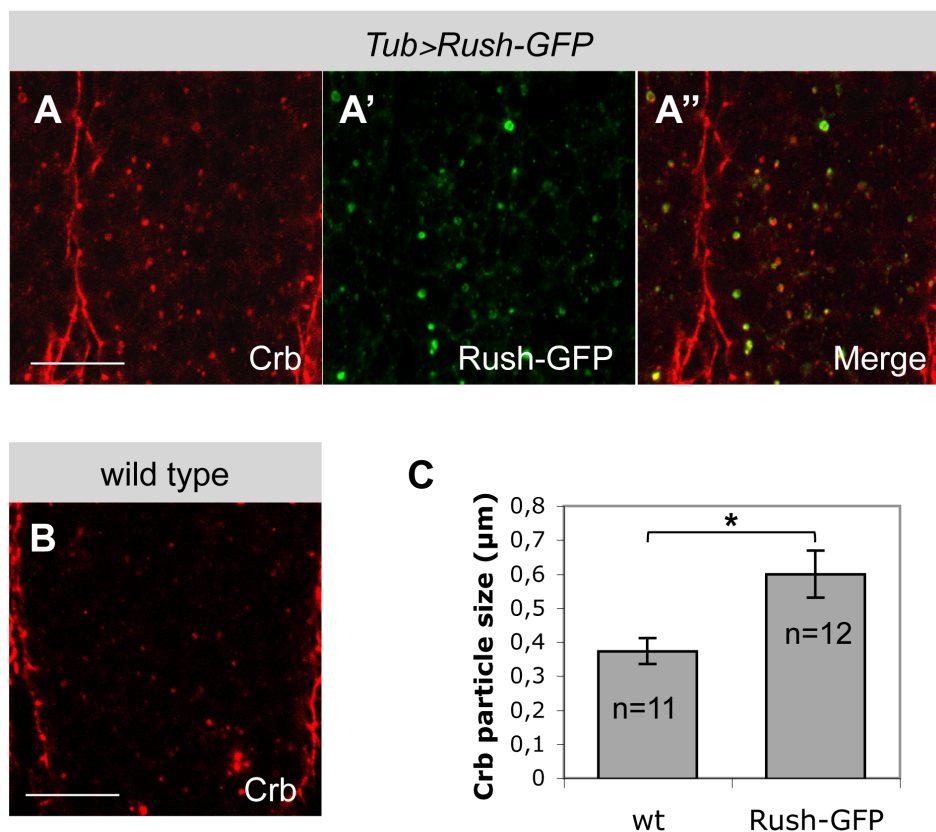
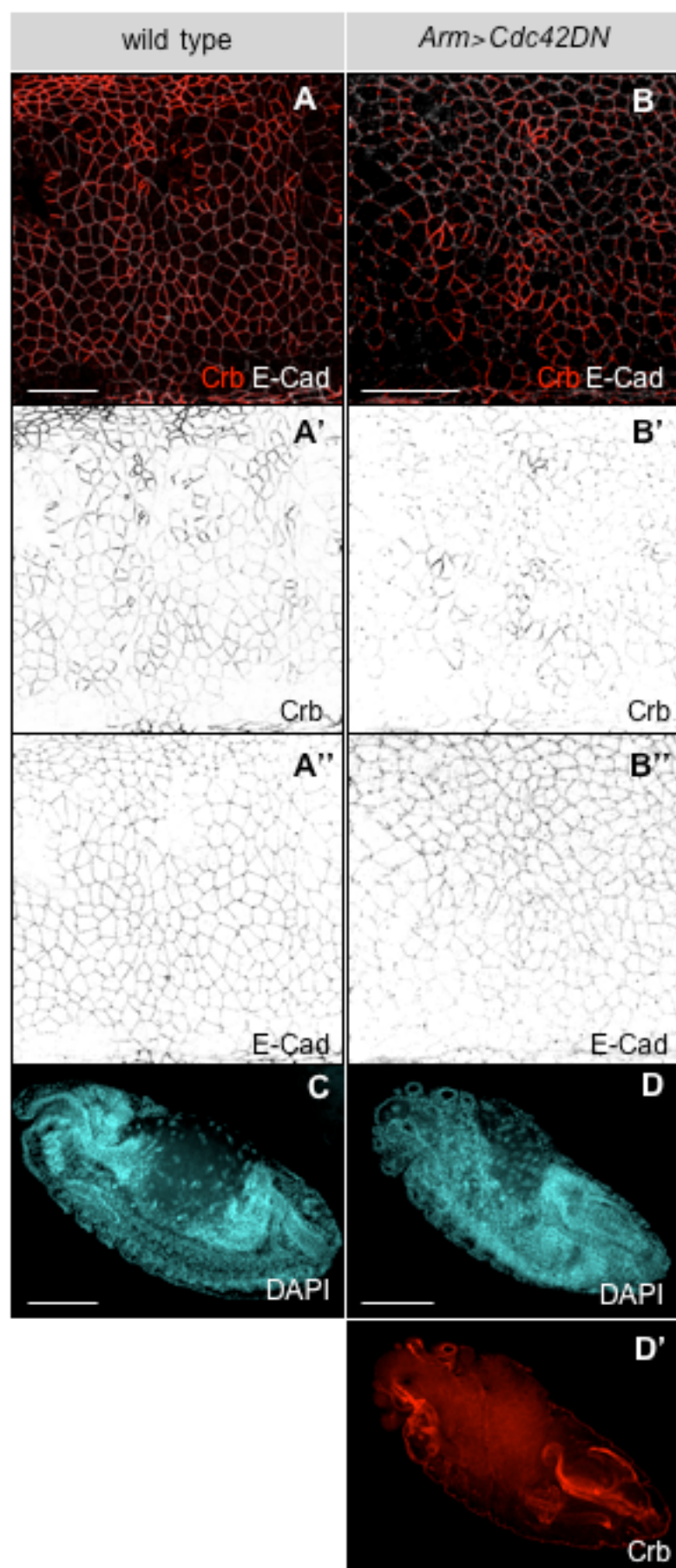


Figure 3-23. Overexpression of Rush-GFP in embryonic ectoderm leads to an increase in Crb endocytosis. Wild type and *tub>Rush-GFP* embryos were stained with an anti-Crb antibody. **A, B** - Tangential sections of the ectoderm of stage 12 embryos. **A** - Large Rush-GFP vesicles colocalize with Crb in *tub>Rush-GFP* ectodermal cells. **B** - Cytoplasmic Crb puncta are smaller in the wild type ectoderm. Scale bars = 10 μm. **C** - The size of Crb vesicles is significantly increased upon Rush-GFP overexpression (mean ± SEM [error bars]), $p < 0,05$.

Expression of *arm>Cdc42DN* was lethal. In the early stages of development *arm>Cdc42DN* embryos do not have obvious morphological defects (data not shown). In later stages of embryonic development morphological defects of embryos become apparent (Fig. 3-24 D). Epithelial sheets of the embryos bulge out, most probably due to loss of cell polarity caused by mislocalization of polarity complexes. Interestingly, head structures were most heavily affected (Fig. 3-24 D).

Figure 3-24. Cdc42DN causes mislocalization of Crb and E-cadherin. **A** - In wild type embryonic ectoderm Crb and E-cadherin localize to cell-cell contacts. **B** - In *arm>Cdc42DN* embryos Crb is lost from the plasma membrane and localizes in dots in the cytoplasmic puncta (**B'**). E-cadherin is lost from the plasma membrane in the ventral ectoderm (**B''**). Ectoderm of stage 11 embryos is shown. **C** - wild type stage 15 embryo. **D** - *arm>Cdc42DN* stage 15 embryo. Head structures are deformed and epithelial bulges can be observed. Anterior is to the left, dorsal is to the top. Scale bars A, B = 20 μm, C, D = 100 μm.



To test whether Cdc42DN affects formation of late endosomes in other tissues, I expressed Cdc42DN in the follicle epithelium under control of *Cu2-Gal4*. In early egg chambers expression of *Cu2-Gal4* takes place in patches, offering a possibility to compare neighboring cells that differ in the expression of the transgene. Follicle epithelial cells that express Cdc42DN had elevated levels of Rab7 in comparison to their neighbors that had not yet started to express the transgene (Fig. 3-25 A). In stage 8, when the expression of the transgene takes place in the whole follicle epithelium, follicle cells that express Cdc42DN have increased Rab7 staining in comparison to the cells of wild type chambers (Fig. 3-25 B).

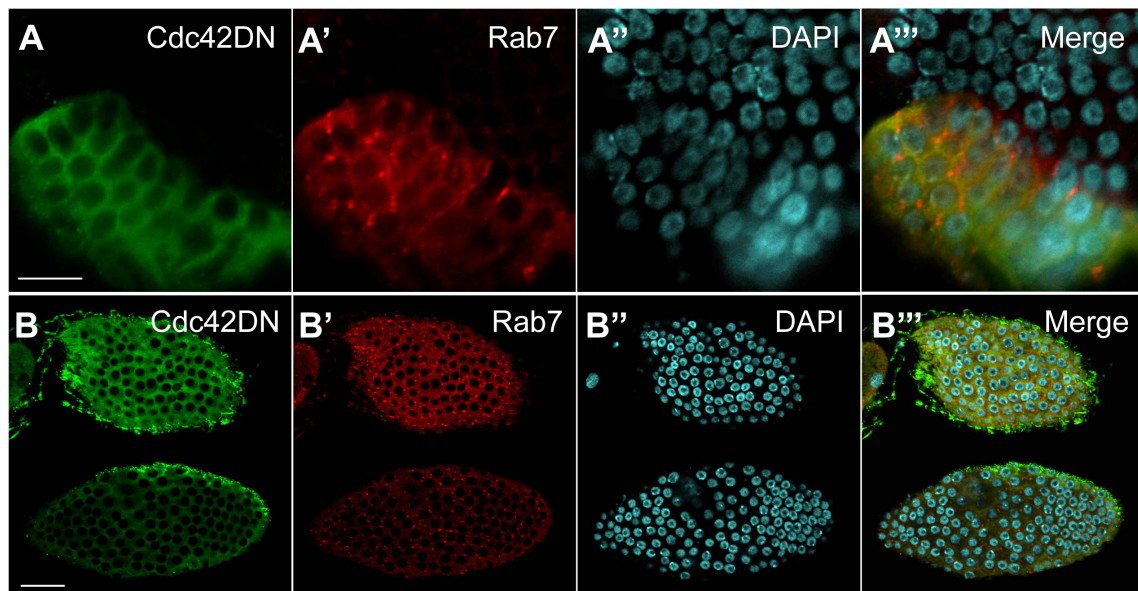


Figure 3-25. Cdc42DN causes formation of enlarged Rab7 endosomes. Expression of Cdc42DN in the follicle epithelium under the control of *Cu2-Gal4*. **A** - The follicle epithelium of stage 7 egg chamber. **B** - Stage 8 egg chambers. Scale bar A = 10 μm ., B = 20 μm .

As overexpression of Rush and disruption of Cdc42 function lead to a similar phenotype regarding late endosome formation and Crb endocytosis, I wondered whether loss of Rush could reverse the effect of Cdc42DN expression. For this purpose I analyzed *rush*⁴; *arm*>Cdc42DN embryos. Loss of *rush* decreased the frequency of late embryonic defects (Fig. 3-26 A) and the lethality of Cdc42DN-expressing embryos (Fig. 3-26 B). Adult *rush*⁴; *arm*>Cdc42DN flies exhibited several defects, including clefts in abdominal segments (Fig. 3-26 D), incomplete rotation of male genitalia (Fig. 3-26 G) and ectopic wing crossveins (Fig. 3-26 J). Formation of extra wing crossveins in result of disruption of

Results

Cdc42 function has been described previously (Baron et al., 2000; Genova et al., 2000). Interestingly, UAS-Rush-GFP overexpression with an ubiquitous *da*-Gal4 driver leads to similar abdominal defects in adult flies (Fig. 3-26 E, H).

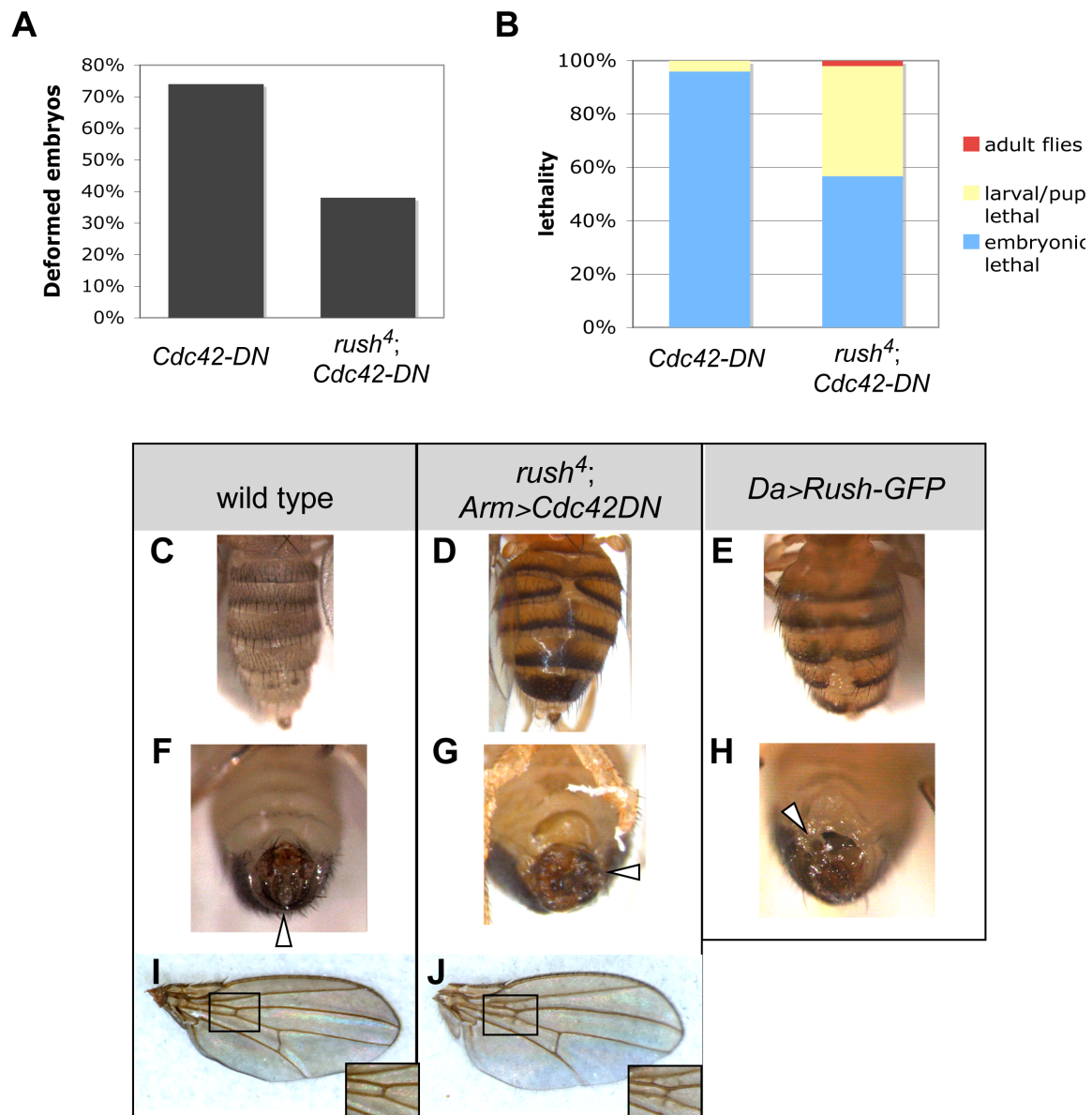


Figure 3-26. Loss of *rush* rescues *arm>Cdc42DN* phenotype. **A** – Loss of *rush* reduces number of deformed *arm>Cdc42DN* embryos. **B** – Loss of *rush* decreases *arm>Cdc42DN* induced lethality. Survival of 200 embryos of each genotype is depicted. Phenotypes of *rush⁴; arm>Cdc42DN* adult flies resemble Rush-GFP overexpression phenotype. Similar phenotypes include cuticle clefts in abdominal segments (D, E) and defects in rotation of terminal segments of male genitalia (G,H). Wild type male genitals rotate during pupal stage to become aligned along the dorsal-ventral axis, indicated by the white arrowhead (F). *rush⁴; arm>Cdc42DN* and *da>Rush-GFP* males in some cases do not undergo complete genital rotation. Wings of *arm>Cdc42DN* flies (J) often have additional crossveins, as shown in the inset (J) in comparison to wild type wings (I).

Taken together, Rush and Cdc42 have opposing effects on Crb endocytosis. Increase of Rush expression led to accumulation of Crb in endocytic vesicles. A similar effect is exhibited upon overexpression of Cdc42DN. Loss of *rush* was able rescue the Cdc42DN overexpression phenotype, suggesting that Rush acts downstream of Cdc42 in regulation of Crb endocytosis. Overexpression of Rush-GFP in the *arm>Cdc42DN* background did not lead to increased defects in embryonic development (data not shown), suggesting that both proteins act in the same pathway.

3.7. Rush interacts with Rab GDI and *Drosophila* homolog of GDF

Multiple effects of Rush on the endocytic pathway were observed, therefore posing the question about the molecular mechanism behind the effect of Rush on late endosome formation, morphology of early endosomes and Cdc42 activity. Genome-wide yeast two-hybrid screens with mammalian and yeast proteins have identified possible interaction partners of Rush homologs in these organisms. Among the putative interaction partners is GDF, a protein that is involved in vesicular trafficking (Ito et al., 2001; Rual et al., 2005). GDF promotes the release of inactive Rabs from GDI and their integration in the membrane, where Rabs can be activated again (Sivars et al., 2003). The interaction between GDF and GDI factors has been described in mammalian cells (Hutt et al., 2000). In *Drosophila*, only one homolog of GDF factors exist, namely CG1418. To test whether Rush interacts with CG1418, I performed pulldown experiments with purified recombinant proteins. *Drosophila* Rab GDI was used as a positive control. GST-Rush bound to both MBP-CG1418 and MBP-GDI, but not MBP alone (Fig. 3-27 A). As a direct interaction between Rush and GDI has not been described, I repeated the experiment by pulling down GST-GDI with MBP-Rush and MBP-CG1418. GST-GDI could be precipitated with both proteins, while interaction with MBP-Rush was stronger than with MBP-CG1418 (Fig. 3-27 B). Therefore pulldown experiments with purified proteins indicate that an interaction between Rush and CG1418 can take place. The pulldown shows that *Drosophila* GDI and GDF can interact with each other, as described in mammalian cells (Hutt et al., 2001). Interestingly, Rush also directly interacted with GDI, suggesting that Rush might participate in regulation of the Rab activation cycle.

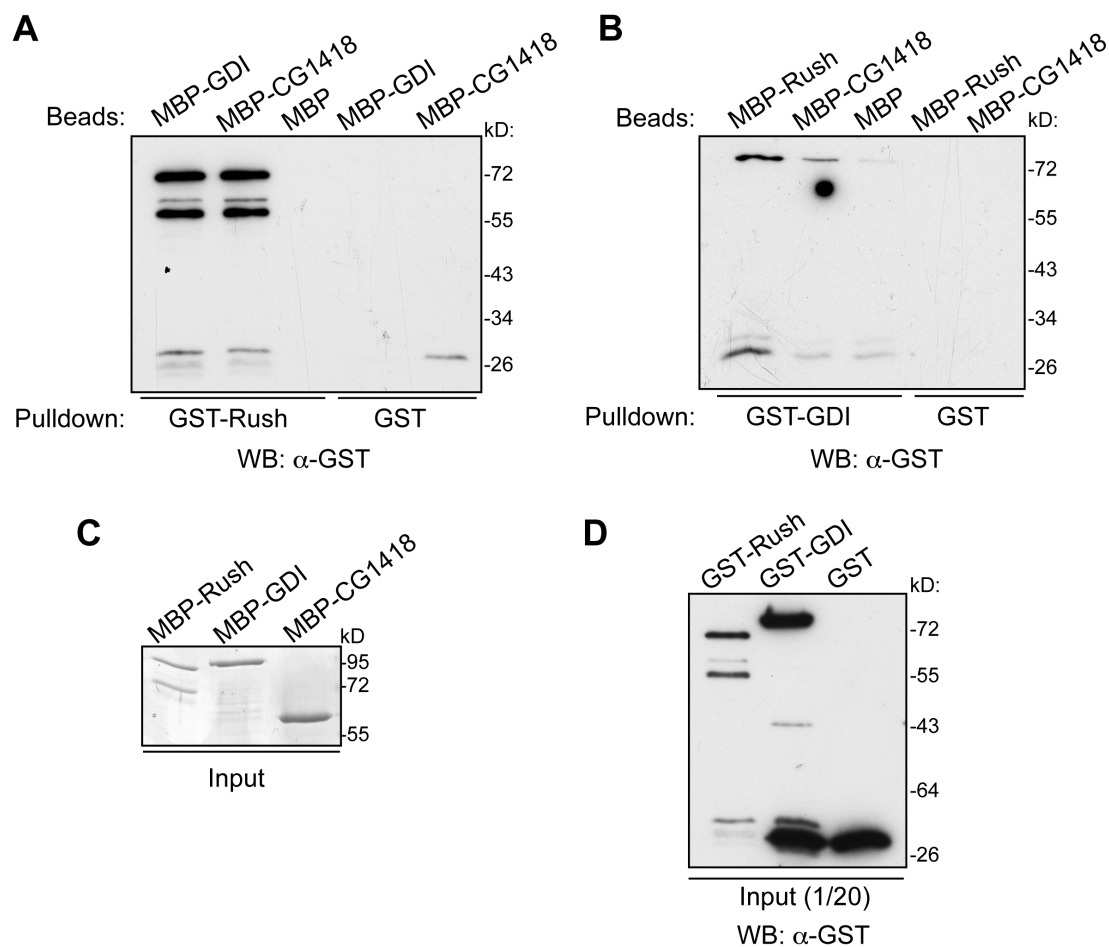


Figure 3-27. Rush directly interacts with CG1418 and GDI. MBP-fusion proteins were bound to amylose beads and incubated with GST-tagged proteins or GST alone. Proteins that were precipitated together with beads were analyzed with a Western blot. **A** – GST-Rush precipitates with MBP-GDI and MBP-CG1418, but not MBP alone, as shown by blotting with anti-GST antibody. GST alone was used as a negative control. **B** – GST-GDI precipitates with MBP-Rush and MBP-CG1418, but not MBP alone. GST alone was used as a negative control. Blotting was done with anti-GST antibody. **C** – Input for MBP-fusion proteins, used for pulldowns, shown by Coomassie staining. **D** – Input for GST-fusion proteins.

Since pulldown experiments indicated that Rush can interact with CG1418 and GDI, I expressed all three proteins in *Drosophila* S2 cells to observe their localization. Endogenous Rush localizes to the cytoplasm and plasma membrane of S2 cells (Fig. 3-28 A). HA-CG1418 is localized to large intracellular compartments, while GFP-GDI is cytosolic. There is no significant colocalization between HA-CG1418 and endogenous Rush, while GFP-GDI partially colocalizes with Rush (Fig. 3-28 A). Upon overexpression of Rush-HA, the protein accumulates asymmetrically at the plasma membrane (Fig. 3-28 B, C). Interestingly, GFP-GDI becomes relocalized to the accumulations of Rush,

suggesting that Rush and GDI can interact with each other in S2 cells (Fig. 3-28 B, C). HA-Rush does not colocalize with GFP-CG1418 and does not cause relocalization of GFP-CG1418 (Fig. 3-28 D).

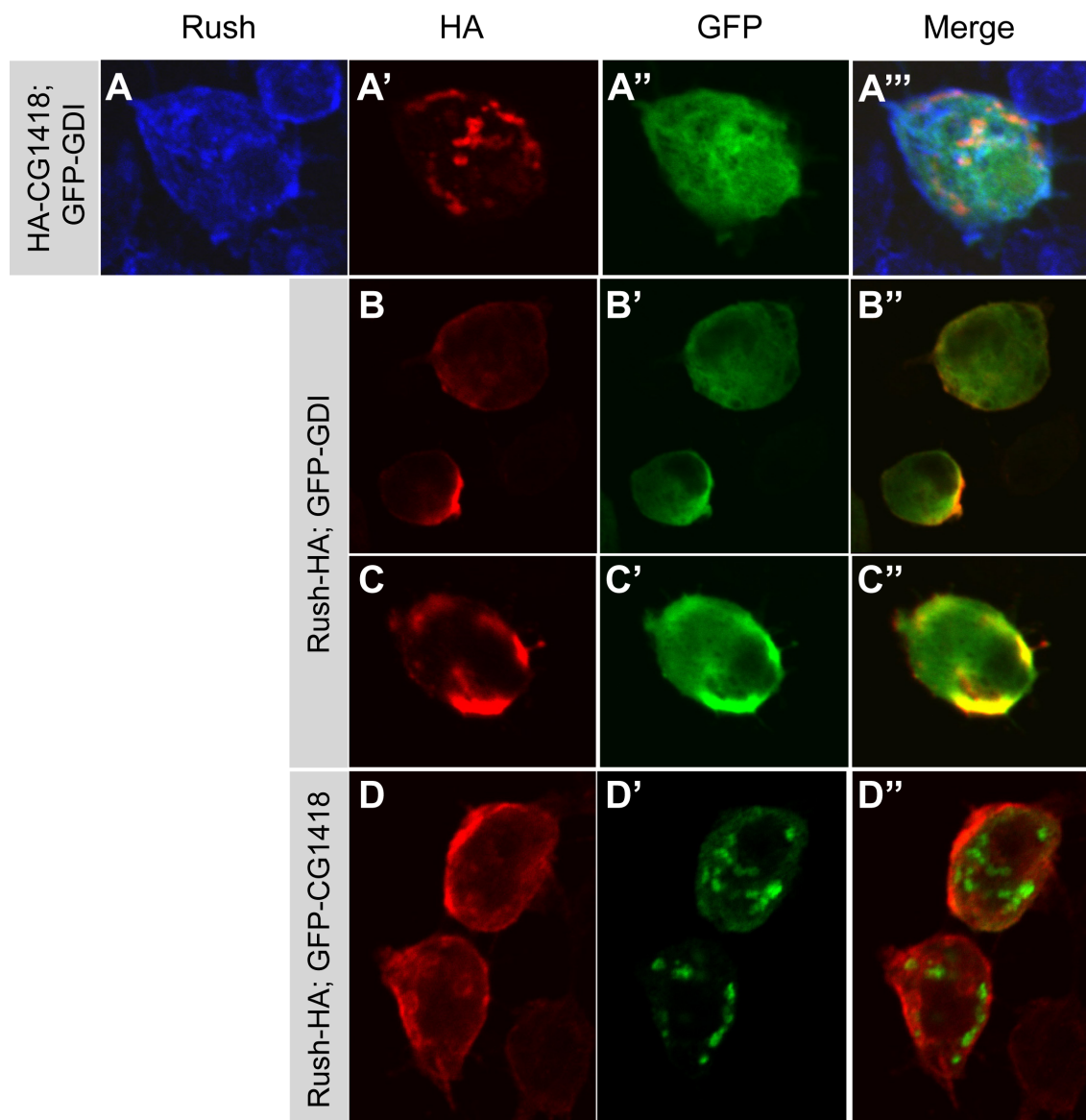


Figure 3-28. Localization of GDI and CG1418 in S2 cells. HA- or GFP-tagged Rush, GDI and CG1418 were expressed in S2 cells and their localization was observed. **A** – HA-CG1418 localizes in large intracellular organelles, while GFP-GDI is cytoplasmic. Endogenous Rush localizes in the cytoplasm and at the plasma membrane. Endogenous Rush partially colocalizes with GFP-GDI. **B, C** – When overexpressed, Rush-HA accumulates at the plasma membrane. GFP-GDI is recruited to the sites of Rush-HA accumulation. **D** – GFP-CG1418 does not colocalize with Rush-HA.

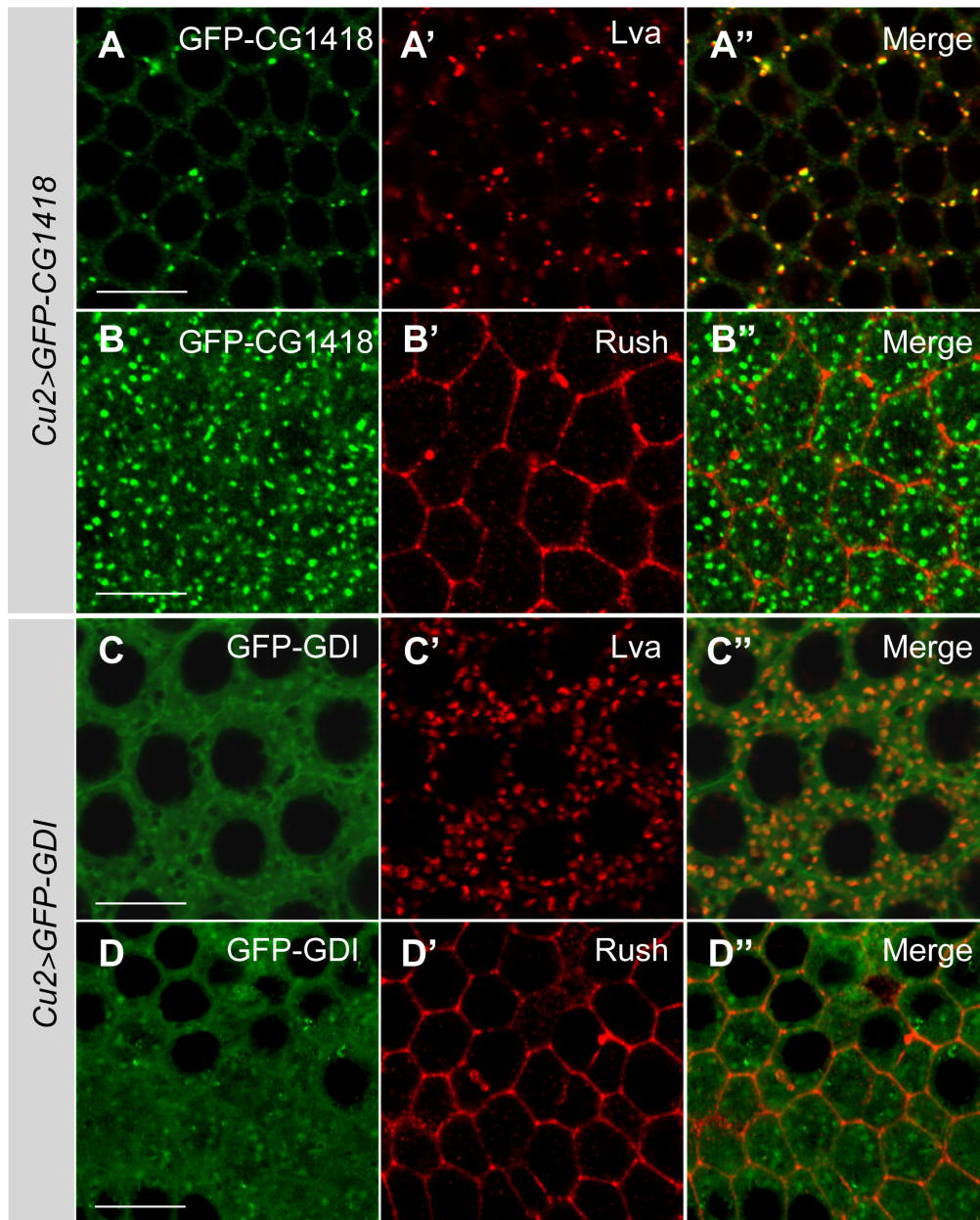


Figure 3-29. Localization of GFP-GDI and GFP-CG1418 in the follicle epithelium. **A** - GFP-CG1418 colocalizes with Golgi marker Lva. **B** – GFP-CG1418 does not colocalize with Rush. **C** – GFP-GDI localizes to the cytoplasm. Slightly increased GDI staining was observed at the plasma membrane and in Lva-positive compartments. **D** – Localization of Rush in *Cu2>GFP-GDI* follicle epithelium. All panels represent tangential sections of stage 10 egg chamber follicle epithelium. Scale bars = 10 μ m.

For further analysis of Rush interaction with GDI and CG1418 I generated transgenic flies that carry UAS-GFP-GDI and UAS-GFP-CG1418. I expressed the transgenes under control of *Cu2*-Gal4 in follicle epithelia to observe their localization. GFP-CG1418 localized to large cytoplasmic puncta, which colocalized with Golgi marker Lava Lamp (Lva) (Fig. 3-29 A). Mammalian GDF PRA1 also localizes to Golgi complex in addition to its localization at endosomes (Abdul-Ghani et al., 2001; Hutt et al., 2000). Rush did not

colocalize with GFP-CG1418 in follicle epithelium (Fig. 3-29 B), therefore, although biochemically possible, the interaction between Rush and CG1418 most probably does not take place in cells. GFP-GDI, similarly as in S2 cells, was localized to the cytosol (Fig. 3-29 C, D). More intensive GFP-GDI signal was observed at the plasma membrane and in cytoplasmic accumulations, which co-stained with anti-Lva antibody (Fig. 3-29 C).

A fraction of mammalian GDI is associated with membranes (Ullrich et al., 1993). To test whether *Drosophila* GDI associates with endosomes, I performed sucrose gradient fractionation of embryo lysates. GDI was detected in the early endosome fraction together with Rab5 and Rab7 (Fig. 3-30). Rush also cofractionates with Rab5 and Rab7 (Fig. 3-6). Thus GDI localizes to similar membrane compartments as Rush and an interaction between the two proteins could take place on endosomal membranes.

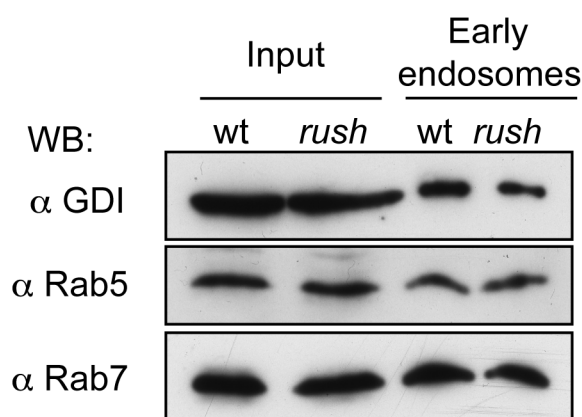


Figure 3-30. GDI associates with endosomes. Wild type and rush embryo extracts were fractionated on a sucrose gradient. GDI is found in the early endosome fraction together with Rab5 and Rab7 in wild type and *rush*⁴ embryo lysates.

Thus, Rush is able to directly interact with GDI and CG1418, the *Drosophila* homolog of GDF. Rush colocalized with GDI in S2 cells and could relocate GDI upon overexpression. GDI localizes to a similar endosome fraction as Rush and could interact with Rush on endosomal membranes.

4. Discussion

Over the years endocytosis has been found to participate in a wide range of cellular functions, including regulation of cell polarity. Interestingly, the polarity proteins themselves can influence endocytosis (Balklava et al., 2007; Harris and Tepass, 2008). The regulation of endocytosis in regard to uptake of polarity proteins is still largely unknown. In this work I describe a novel endosome associated protein Rush hour (Rush). Rush influences formation of late endosomes and affects endocytosis of the apical protein Crb. *rush* genetically interacts with *Cdc42*, implicating a role of Rush in Cdc42-regulated endocytosis. Rush directly interacts with Rab GDI in biochemical assays and might thus affect the Rab activation cycle.

4.1. Localization of Rush

4.1.1. Subcellular localization of Rush

Rush exhibited a dual localization in epithelial cells and is found both at the lateral plasma membrane and on endosomes. Localization of Rush to endosomes was confirmed by both immunofluorescence and cell fractionation experiments. Immunofluorescence experiments revealed colocalization of Rush with Hrs and Rab7. Rab7 is a marker of late endosomes (Chavrier et al., 1990), while Hrs localizes to the early endosomes via its FYVE domain (Raiborg et al., 2001) and facilitates the transition between early and late endosomes (Lloyd et al., 2002; Sun et al., 2003). Interestingly, a recent report indicates that a fraction of Hrs remains associated with late endosomes (Mari et al., 2008). Rush colocalized only partially with Rab5, possibly reflecting the Hrs-positive fraction. In cell fractionation experiments Rush co-fractionated with both Rab5 and Rab7, but not the fraction that contained Rab7 alone. These results suggest that Rush associates with late endosomes and/or early-late endosome intermediates. The human ortholog of Rush, Phafin2 (70% sequence identity to Rush) colocalizes with EEA1, a FYVE domain-containing early endosome protein, in the HepG2 human liver cancer cell line (Lin et al. 2010). However, only a fraction of Phafin2 puncta colocalize with EEA1, suggesting that Phafin2 might be associated also with later endocytic compartments. In contrast, other publications describe cytoplasmic localization of Phafin2 and Phafin1, another homolog of Rush (57% sequence identity to Rush) GFP fusion proteins in L929 mouse fibroblast cell line (Li et al., 2008; Chen et al., 2005). However, colocalization of Phafins with endosomal markers was not

analyzed in these publications. The difference between the observations may also arise from the use of different experimental cell systems or the effects of overexpression.

Rush localized to the plasma membrane in a polarized manner and was found exclusively at the lateral plasma membrane. Rush colocalized with E-cadherin at the adherens junctions, however, the role of the polarized plasma membrane localization of Rush is not clear. Rush is not required for localization of other polarity proteins, since overexpression and loss of Rush did not lead to defects in cell polarity. The polarized localization of Rush might be necessary for its function in endocytosis, although Rush mainly influenced formation of late and not early endosomes as discussed in further chapters. Rush participated in regulation of Crb endocytosis together with Cdc42. Rush could affect endocytosis of plasma membrane proteins that are localized in a polarized fashion. In mammalian cells the Rich1/Amot protein complex localizes to tight junctions and selectively activates Cdc42 to promote endocytosis of polarity proteins (Wells et al., 2006). Homologs of Amot are not present in *Drosophila*, while a homolog of Rich1, a presumed GAP of Cdc42, is encoded by RhoGAP92B. Genetic interaction studies could clarify whether the fly homolog of Rich1 participates in Cdc42-regulated endocytosis and if Rush and Rich1 might act together at the plasma membrane.

4.1.2. Role of lipid binding domains in Rush localization

Rush contains two lipid binding domains – a PH and a FYVE domain. Results of lipid overlay assays revealed that Rush can bind to a number of phosphatidylinositides. Rush bound most strongly to PI(3)P. Interaction of Rush with PI(3)P was mediated mainly by its FYVE domain. The PH domain of Rush was able to bind to PI(3)P, PI(4)P and PI(3,4)P₂. Surprisingly, full length Rush interacted not only with PIPs that were specific for its separate domains, but also to PI(4,5)P₂ and PI(3,4,5)P₃. It could be possible that both lipid domains interact with each other on a functional level and broaden lipid binding capabilities of Rush. In addition, the lipid domains of Rush could act as so-called coincidence detectors and act together to increase the affinity of Rush towards the membrane (Carlton and Cullen, 2005; Lemmon, 2008).

Experiments with lipid binding defective Rush constructs indicated that the FYVE domain plays the main role in the endosome localization of Rush. Rush^{K48E}, which harbors a lipid binding defective PH domain, was able to bind only to PI(3)P in lipid overlay assays. Rush^{K48E} could still localize to endosomes and, surprisingly, also to the plasma membrane.

PI(3)P, the target lipid of the FYVE domain, is almost exclusively found in early endosomes and multivesicular bodies (Gillooly et al., 2001; van Meer et al., 2008). The levels of PI(3)P are low at the plasma membrane, where most abundant PIPs are PI(4,5)P₂ and PI(3,4,5)P₃ (Di Paolo and De Camilli, 2006; van Meer et al., 2008). The localization of Rush^{K48E} to the plasma membrane could be mediated by an interaction with another membrane-associated protein or by dimerization with wild type Rush. Dimerization of FYVE domains has been described to take place for several endosomal proteins like EEA1 and Hrs (Hayakawa et al., 2004) and increases affinity of the domain to PI(3)P, but in this case it could lead to plasma membrane recruitment of Rush^{K48E}. The localization of the Rush homolog Phafin2 to endosomes is also mediated by its FYVE domain, and deletion of the N-terminus together with the PH domain did not lead to mislocalization of the protein (Lin et al., 2010).

The Rush^{R176G} mutant with a nonfunctional FYVE domain localized solely to the plasma membrane. Therefore the PH domain or the activity of both lipid binding domains together, as indicated by Rush^{K48E} localization, is needed for the plasma membrane association of Rush. Localization of the PH domain to the plasma membrane may be mediated by its interaction with PI(3,4)P₂, which is produced in the plasma membrane by dephosphorylation of PI(3,4,5)P₃ (Di Paolo and De Camilli, 2006; Ivetac et al., 2005). Rush^{R176G} exhibited only a background interaction with PIPs in lipid overlay assays. The PIP binding ability of the PH domain might be diminished due to the mutation in the FYVE domain, possibly because of surface charge changes or conformational changes caused by the R176G mutation. The presence of at least one functional lipid binding domain is necessary for the membrane localization of Rush, since Rush^{K48ER176G} was cytoplasmic. Thus the two lipid binding domains are responsible for the dual localization of Rush in epithelial cells, with the PH domain localizing Rush to the plasma membrane and the FYVE domain regulating the localization to endosomes.

4.2. Function of Rush in endocytosis

4.2.1. Rush regulates late endosome formation

Results presented in this work show that Rush has a positive effect on late endosome size. Overexpression of Rush led to formation of enlarged late endosomes, while the late endosome size was decreased in *rush* mutants. Formation of early endosomes, monitored

by expression of Rab5CA, was not affected in *rush* mutants, suggesting that Rush acts downstream of Rab5. Also in human cells dominant negative Rab5 disrupted formation of Phafin2-induced large endosomes, positioning Rab5 activity upstream of Phafin2 (Lin et al., 2010). The effect of Rush on late endosomes can be caused by increased transition from early to late endosome, or by downregulated late endosome to lysosome traffic. Rush overexpressing cells exhibited a weaker staining for the pH sensitive LysoTracker dye, which marks acidic intracellular compartments, such as lysosomes. Mutants for *Drosophila* V-ATPase, a proton pump necessary for acidification of the lysosomal lumen, also develop enlarged late endosomes and show decreased LysoTracker staining (Yan et al., 2009). Therefore the increase in late endosome size in cells that overexpress Rush might be caused by defects in transport from late endosomes to lysosomes. A staining against an alternative lysosome marker, e.g. lysobiphosphatidic acid that accumulates in mature late endosomes and lysosomes (Kim et al., 2010), will be used to verify this result. In the future I also plan to investigate lysosome formation in *rush* mutant epithelia by LysoTracker staining. If Rush negatively regulates trafficking to lysosomes, the transport to lysosomes would be increased in *rush* mutants, thus also explaining the decrease in late endosome size.

Increased late endosome size could also be caused by defects in endocytic recycling, thus directing all endocytosed material for degradation. Recycling of endocytosed proteins like Crumbs or E-cadherin plays an important role in the regulation of cell polarity (Roeth et al., 2009). When Rush is overexpressed, the apical polarity protein Crumbs accumulates in Rush positive enlarged endosomes. However, if Rush overexpression would cause disruption of the recycling endosome pathway, one would expect a gradual loss of membrane proteins like Crumbs or E-cadherin, in the end resulting in loss of cell polarity (Desclozeaux et al., 2008; Roeth et al., 2009). On the contrary, the polarity of follicle epithelial cells was not disrupted either by overexpression or loss of Rush. In addition, the size of Rab11-marked recycling endosomes was not affected in *rush* mutant cells. Thus the Rush-mediated effects on late endosome morphology are most probably not caused by defects in recycling of endocytosed proteins.

Phafin2, the human homolog of Rush, has been shown to increase the binding of Rab5 with its effectors, monitored by a FRET (fluorescence resonance energy transfer) assay with the Rab5 binding domain of Rabaptin5 (Lin et al., 2010). The data presented here rather position Rush downstream of Rab5 on the endocytic pathway, since overexpression of Rush resulted in increased late, but not early, endosome size. In addition, Rush and

Rab5 did not substantially colocalize in the follicle epithelium, although Rush colocalized with Hrs, a protein that associates with early endosomes but also to a lesser degree to late endosomes (Komada et al., 1997; Mari et al., 2008).

4.2.2. Rush changes the morphology of Rab5CA vesicles

Although a significant colocalization between wild type Rab5 and Rush was not observed, expression of constitutively GTP-bound Rab5CA led to association of Rush with early endosomes. Also Rab7, the marker of late endosomes, was found in Rab5CA vesicles. In line with this observation, several publications have described association of late endosome and even lysosome proteins with enlarged Rab5CA vesicles (Rink et al., 2005; Rosenfeld et al., 2001; Wegner et al., 2010). In cell culture experiments it has been shown that activated Rab5 recruits Rab7 to endosomes via the class C VPS/HOPS complex (Rink et al. 2005). In the case of Rab5CA, Rab5 is constantly bound to GTP and cannot be inactivated and removed from the endosome after Rab7 recruitment, thus resulting in formation of Rab5/Rab7 double labeled endosomes (Rink et al., 2005). Similarly, I observed double Rab5 and Rab7 staining of enlarged Rab5CA endosomes in *Drosophila* follicle cells. This result supports the Rab conversion mode of late endosome formation, according to which the transition between early and late endosomes takes place by exchange of Rabs (Spang, 2009). The recycling endosome marker Rab11 did not associate with the Rab5CA and/or Rush-induced large endosomes, in line with the observation that expression of Rab5CA does not affect endocytic recycling (Ceresa et al., 2001; Rosenfeld et al., 2001).

Surprisingly, a simultaneous overexpression of Rush and Rab5CA induced fractionation of Rab5CA vesicles. Interestingly, downregulation of Vps39, a component of the class C VPS/ HOPS complex, has a similar effect on the morphology of Rab5 vesicles (Rink et al., 2005). Vps39 acts as a GEF of the yeast ortholog of Rab7 (Wurmser et al., 2000). The phenotype caused by loss of Vps39 is proposed to arise due to delayed recruitment and activation of Rab7 to the endosomes (Rink et al., 2005). So far it is not clear whether the Rush-induced fractionation of early endosomes is caused by regulation of Rab7 activation. The *Drosophila* homolog of Vps39 has not been characterized so far. However, mutations in other class C VPS/HOPS complex genes – *vps16A*, *deep orange* (*vps18*) and *carnation* (*vps33*) cause defects in lysosome formation (Akbar et al., 2009; Pulipparacharuvil et al., 2005; Sriram et al., 2003). As overexpression of Rush caused weaker lysosome staining in

epithelial cells, one can speculate that Rush might counteract the class C VPS/HOPS complex in Rab7 activation and therefore delay the transition between late endosomes and lysosomes. The interaction between Rush and GDI might affect the activation of Rab7 on late endosomes by removing the inactive Rab7-GDP from the membrane and preventing reactivation of Rab7 by its GEF.

The phenotype of fractionated Rush/Rab5CA-containing early endosomes resembles a cluster of smaller vesicles. Rab5CA causes formation of large early endosomes by promoting homotypic fusion of early endosomes (Gorvel et al., 1991). The clustering of early endosomes might be caused by an inhibition of the early endosome fusion by Rush. The early endosomal protein Hrs has been found to promote the transition to late endosomes by inhibiting the homotypic fusion of early endosomes (Sun et al., 2003; Visser Smit et al., 2009). Inhibition of the early endosome fusion leads to clustering of early endosomes that resembles the effect of Rush on Rab5CA-induced early endosomes (Visser Smit et al., 2009). Rush colocalized with the Hrs-positive endosome fraction and could function together with Hrs at this step of endocytosis. However, at the moment it is not clear, how Rush could affect early endosome homotypic fusion.

Thus the clustering of Rab5CA vesicles, caused by Rush overexpression, can be a result of either a delayed activation of Rab7, or an inhibition of early endosome homotypic fusion. Future experiments in *rush* mutant and Rush-overexpressing flies harboring mutations in Hrs and the class C VPS/HOPS complex genes will be needed to clarify the cause of Rush-induced changes of Rab5CA-induced large early endosome morphology.

4.3. Possible role of Rush in signaling pathways

Ovaries of flies that are mutant for *rush* showed low penetrance egg chamber fusion defects and an increased length of stalks that separate egg chambers. The fusion between egg chambers seems to be caused by defects in polar cell differentiation. Polar and stalk cell formation is induced by JAK/STAT and Notch signaling pathways in early egg chamber development stages (McGregor et al., 2002; Grammont and Irvine, 2001). The specification of polar cells is induced by Delta signaling from the germline that activates Notch in the follicle epithelium (Grammont and Irvine, 2001; Lopez-Schier and St. Johnston, 2001). Polar cells in turn express Unpaired, a ligand which activates JAK/STAT signaling in stalk cell precursors and specifies their fate (McGregor et al., 2002). Overactivation of the JAK/STAT pathway due to overexpression of Unpaired results in a

decreased polar cell number, increased stalk length and egg chamber fusions (McGregor et al., 2002). Defects in Notch signaling cause egg chamber fusion, lack of polar cells and increased stalk length (Grammont and Irvine, 2001). A similar phenotype was observed in *rush* mutant egg chambers. Both JAK/STAT and Notch signaling pathways require endocytosis for their activation (Devergne et al., 2007; Le Borgne, 2006). Thus Rush might affect polar cell and stalk cell differentiation by modifying JAK/STAT and/or Notch pathways. Receptors of both pathways become endocytosed upon binding with a ligand and activated in late endosomes (Devergne et al., 2007; Vaccari et al., 2008). Deletion of *rush* decreased the size of late endosomes, possibly by affecting the transport to or from the late endosomal compartment. It has been shown that disruption of endocytic trafficking of Dome, the receptor of JAK/STAT pathway, to or from late endosomes downregulated the JAK/STAT signaling pathway (Devergne et al., 2007). Similarly, Notch signaling requires the transport to early endosomes and multivesicular bodies for the activation of the pathway (Vaccari et al., 2008). Thus the egg chamber fusion defects observed in *rush* mutants might be caused by perturbations in JAK/STAT and/or Notch signaling pathways, most probably due to changes in trafficking through late endosomes.

Overexpression of Rush in the follicle epithelium in some cases led to apoptosis in the germline. This unexpected non-cell-autonomous effect might be caused by changes in signaling between the germline and the follicle epithelium. Some evidence that signals from the follicle epithelium can regulate germline survival can be found in the literature. Removal of the TGF β receptor Saxophone (Sax) in the germline leads to germline cell apoptosis, suggesting that a TGF β signal from the follicle epithelium might be necessary for oogenesis (Twombly et al., 1996). Overexpression of the c-Jun N-terminal kinase (JNK) pathway activator D-GADD45 in follicle cells also induces apoptosis of the germline (Peretz et al., 2007). At the moment it is not clear, how overexpression of Rush in follicle epithelium induces germline apoptosis. For example, increased endocytosis in Rush overexpressing follicle cells could titrate out a ligand that is required for germline survival, or, alternatively, inhibit activation of a yet unknown signaling pathway in follicle cells that is needed for the communication with germline cells.

4.4. Genetic interaction between *rush* and *Cdc42*

Cdc42 has been described to play an important role in endocytosis from yeast to mammals. In recent years the evidence for a role of Cdc42 together with the Par/aPKC complex in

trafficking of polarity proteins has accumulated (Balklava et al., 2007; Duncan and Peifer, 2008). In *Drosophila* epithelial cells, Cdc42 acts on several steps of endocytosis, including protein uptake into early endosomes and trafficking to late endosomes (Harris and Tepass, 2008; Georgiou et al., 2008; Leibfried et al., 2008). The effects of Cdc42DN expression in the embryonic ectoderm, that are described in this thesis, generally are in line with the data by Harris and Tepass (2008). Similarly as published by Harris and Tepass (2008), expression of Cdc42DN caused loss of Crb from the plasma membrane and accumulation of Crb in intracellular vesicles. In addition, an increased loss of E-cadherin from the plasma membrane at the ventral ectoderm was observed. Interestingly, E-cadherin did not accumulate in vesicles together with Crb, suggesting different trafficking routes for the two proteins. In *C. elegans* Cdc42 together with other members of the Par/aPKC complex differentially regulates trafficking of molecules by promoting uptake via the clathrin-dependent pathway and increasing the recycling of molecules endocytosed via clathrin independent pathways (Balklava et al., 2007). These effects could account for the different behavior of Crb and E-cadherin in Cdc42DN cells. However, the clathrin-dependent and independent endocytic pathways in *Drosophila* have not been investigated in detail.

Rush and Cdc42DN overexpression results in similar phenotypes in epithelial cells – an increase of late endosome size and increased Crb accumulation in late endosomes. Thus Rush and Cdc42 have opposing effects in regulation of endocytosis. It is not clear, whether Rush is directly regulated by Cdc42, or is a part of another pathway. Loss of *rush* could rescue the Cdc42DN overexpression phenotype, suggesting that Rush acts downstream of Cdc42. Studies in a human breast cancer cell line indicate a role of Cdc42 in targeting of E-cadherin to lysosomes (Shen et al., 2008). One possibility is that Cdc42 promotes transition between late endosomes and lysosomes, and inactivates or counteracts Rush in this process. In such case Cdc42DN expression would inhibit, e.g. via Rush, endocytic transport to lysosomes and would cause accumulation of endocytosed molecules like Crb in late endosomes. Upon deletion of *rush* the degradation of endocytosed Crb would proceed normally. However, it is not clear how the deletion of *rush* leads to rescue of cell polarity loss, caused by Cdc42DN expression in embryos. Another possible explanation is that in Cdc42DN-expressing epithelial cells endocytic recycling is inhibited by enhanced transition from early to late endosomes, thus disrupting the sorting into recycling endosomes. For example, overexpression of Hrs increases retention of transferrin receptors in endosomes (Raiborg et al., 2002). If Rush promotes the transition from early to late endosomes, as suggested by the Rush overexpression phenotype, loss of Rush could slow

down the formation of late endosomes and allow endocytic recycling to take place.

In this work I analyzed the genetic interaction between *rush* and *Cdc42*. However, other members of the Par/aPKC complex, like Baz, Par6 and aPKC, have been shown to be involved in Cdc42-regulated endocytosis (Harris and Tepass, 2008; Georgiou et al., 2008; Leibfried et al., 2008). Further experiments will be needed to show whether *rush* genetically interacts with other Par/aPKC complex members in regulation of endocytosis. Expression of constitutively active aPKC rescued the Cdc42DN overexpression phenotype – the loss of Crb from the plasma membrane and the accumulation of Crb in endosomes (Harris and Tepass, 2008). Expression of dominant negative Rab5 rescued the loss of Crb from the plasma membrane, but not the defect in Crb endosomal trafficking, suggesting that the accumulation of Crb in endosomes is independent of Rab5 function. Rush might be the effector of the Par/aPKC complex at later stages of endocytosis. To test this possibility, I plan to analyze the effect of aPKC and Cdc42 constitutive activation on late endosome size in Rush overexpressing and *rush* mutant flies.

4.5. Rush interaction with Rab GDI and GDF

Yeast two-hybrid screens with yeast and mammalian proteins suggested an interaction between Rush orthologs and Rab GDI (Ito et al., 2001; Rual et al., 2005). GDI interacts with GDI and promotes insertion of Rab into the membrane and the release of Rab from GDI (Dirac-Svejstrup et al., 1997; Hutt et al., 2000; Sivars et al., 2003). Pulldown experiments with purified proteins supported the possibility of the interaction between Rush and CG1418, the *Drosophila* ortholog of GDI. Interestingly, Rush could also bind GDI and recruits GDI to the cortex of S2 cells. However, the localization of Rush and CG1418 to different subcellular compartments indicates that Rush and CG1418 most probably do not interact *in vivo*. As both GDI and Rush were associated with a Rab5 and Rab7 positive endosomal fraction, an interaction between GDI and Rush on the endosomal membrane is possible.

The function of GDI in *Drosophila* has not been well characterized. The work by Ricard et al. (2001) shows that *Drosophila* GDI is able to extract Rab5 from membranes, similarly to the mammalian homolog (Ullrich et al., 1993). Rush could facilitate recruitment of GDI to late endosomes and thus regulate the activity of Rabs. GDI has been shown to inhibit the fusion of late endosomes with lysosomes (Mullock et al., 1998). Therefore the interaction between Rush and GDI on late endosomes might cause the decrease in the transition from

late endosomes to lysosomes upon overexpression of Rush. Rab7 activity is needed for delivery of endocytosed material from late endosomes to lysosomes (Bucci et al., 2000). Increased recruitment of GDI to late endosomes would lead to removal of inactive Rab7 from the endosome membrane and prevent the reactivation of Rab7 by GEF-catalyzed nucleotide exchange. Further experiments will be necessary to characterize the interaction between Rush and GDI and its possible implications in Rush overexpression and deletion phenotypes.

4.6. Model of Rush function

The results presented in this thesis suggest multiple roles of Rush in endocytosis in epithelial cells. Rush localizes to late endosomes, and positively influences late endosome size. On the contrary, loss of Rush leads to a decreased late endosome size. Rush overexpression leads to a weaker staining for the lysosomal marker LysoTracker, therefore Rush might increase the size of late endosomes by inhibiting the transition between late endosomes and lysosomes. Rush interacts directly with GDI and might delay transition to lysosomes by a GDI-mediated inhibition of Rab7 activity. Alternatively, Rush might promote the transition from early to late endosomes. Rush overexpression together with Rab5CA leads to fractionation of the early endosomes. The effects of Rush on early endosome shape suggest a possible role of Rush in inhibition of early endosome fusion.

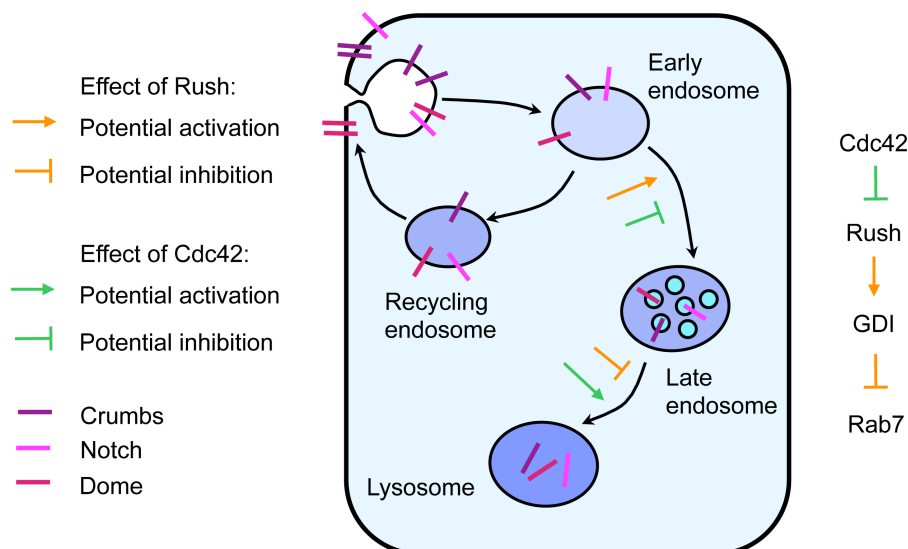


Figure 4.1. Model of Rush function in endocytosis. Activation or inhibition of trafficking steps is indicated with orange (Rush) or green (Cdc42) arrows. Colored bars indicate endocytosed proteins.

Rush plays a role in the endocytosis of Crb, and causes accumulation of Crb in late endosomes upon Rush overexpression. Rush might be also involved in endocytic regulation of Notch and JAK/STAT pathway signaling, as deduced from the *rush* mutant phenotype. The Rush overexpression phenotype is similar to the effect of Cdc42DN overexpression, suggesting that Rush counteracts Cdc42 in regulation of Crumbs endocytosis. This hypothesis is supported by the rescue of Cdc42DN overexpression flies by deletion of *rush*. Judging from this result, Rush most probably acts downstream of Cdc42, and might be inhibited by active Cdc42.

In the sum, Rush promotes formation of late endosomes, either by increasing the transition from early to late endosomes, or by inhibition of downstream transport to lysosomes (Fig. 4-1). Rush counteracts Cdc42 in this process, possibly via its binding to GDI. Further experiments will be needed to clarify the molecular mechanism of Rush function in regulation of endocytosis.

5. Summary and conclusions

Endocytosis and endosome trafficking regulates many cellular processes, including regulation of plasma membrane composition, cell polarity and intercellular signaling. Overactivation or inhibition of different steps of endocytosis can lead to defects in diverse cell functions. Although many factors that participate in endocytosis have already been identified, still many aspects of regulation of endocytosis are not known. In recent years Cdc42 together with other members of the Par/aPKC complex have been described to function in endocytosis. The Par/aPKC complex proteins are well known as cell polarity regulators. However, the molecular mechanism of the activity of Cdc42 and other Par/aPKC complex members in regulation of endocytosis is largely unknown.

In this work I describe the characterization of a novel endocytosis regulating protein Rush hour (Rush). Rush is a highly conserved protein and contains two lipid binding domains – a PH and a FYVE domain. Rush is ubiquitously expressed and localizes to the lateral plasma membrane of epithelial cells and to late endosomes. Generation of Rush mutants with lipid binding defective PH and FYVE domains revealed that a functional PH domain is sufficient to localize Rush to the plasma membrane, while the FYVE domain mediates endosomal association of Rush. Overexpression of Rush led to formation of enlarged late endosomes. Flies that are mutant for *rush* are homozygous viable, but have a decreased late endosome size, which is consistent with the role of Rush in regulation of late endosome formation. Rush mutants show a number of low penetrance phenotypes in oogenesis, including egg chamber fusions and an increased number of stalk cells. Similar phenotypes are observed in mutants of Notch and JAK/STAT signaling pathway genes. Both pathways require endosomal trafficking for their activation. Therefore the oogenesis phenotypes in *rush* flies are most probably caused by defects in signaling pathways due to changes in late endosome formation.

Rush seems to affect endocytosis at several levels. Overexpression of Rush led to the fractionation of Rab5CA-induced large early endosomes, suggesting that Rush acts in the transition between early and late endosomes. Rush might inhibit Rab5-induced homotypic fusion of early endosomes, thus promoting the transition to late endosomes. In addition, the staining of LysoTracker, a lysosome specific dye, was decreased upon overexpression of Rush, suggesting that Rush negatively affects lysosome formation.

Remarkably, Rush enhanced endocytosis of Crumbs, a determinant of apical characteristics of the plasma membrane, and caused accumulation of Crumbs in late

endosomes. A similar phenotype has been observed in Cdc42DN-expressing tissues, pointing to a common function for both proteins. Loss of *rush* rescued Cdc42DN overexpression phenotype, suggesting that Rush acts downstream of Cdc42 in regulation of late endosome formation. I found that Rush interacted directly with GDI and recruited GDI to the membrane in S2 cells. Thus Rush might regulate endosome formation by directing GDI to the endosomal membrane.

Taken together, the results presented here describe Rush as a novel regulator of late endosome formation. Rush acts downstream of Cdc42 in trafficking to late endosome, and regulates together with Cdc42 endocytosis of the polarity marker Crumbs. Rush binds to GDI directly and might thus regulate endocytosis by affecting the Rab activation cycle.

6. Bibliography

- Abdul-Ghani M., Gougeon P.Y., Prosser D.C., Da-Silva L.F., Ngsee J.K. 2001. PRA isoforms are targeted to distinct membrane compartments. *J. Biol. Chem.* 276: 6225-6233.
- Akbar M.A., Ray S., Krämer H. 2009. The SM protein Car/Vps33A regulates SNARE-mediated trafficking to lysosomes and lysosome-related organelles. *Mol. Biol. Cell* 20: 1705-1714.
- Ashburner M. 1989. *Drosophila: a laboratory handbook*. Cold Spring Harbor Press, Plainview, NY.
- Babst M., Katzmann D.J., Estepa-Sabal E.J., Merloo T., Emr S.D. 2002a. ESCRT-III: an endosome-associated heterooligomeric protein complex required for MVB sorting. *Dev. Cell* 3: 271–282.
- Babst M., Katzmann D.J., Snyder W.B., Wendland B., Emr S.D. 2002b. Endosome-associated complex, ESCRT-II, recruits transport machinery for protein sorting at the multivesicular bodies. *Dev. Cell* 3: 283–289.
- Bache K.G., Brech A., Mehlum A., Stenmark H. 2003. Hrs regulates multivesicular body formation via ESCRT recruitment to endosomes. *J. Cell Biol.* 162: 435-442.
- Bachmann A. and Knust E. 2008. The use of P-element transposons to generate transgenic flies. From: *Methods in Molecular biology: Drosophila: Methods and Protocols*. Ed. Dahmann C. Humana Press, Totowa, NJ, pp 71-77.
- Bachmann A., Schneider M., Theilenberg E., Grawe F., Knust E. 2001. *Drosophila* Stardust is a partner of Crumbs in the control of epithelial cell polarity. *Nature* 414: 638-643.
- Balklava Z., Pant S., Fares H., Grant B.D. 2007. Genome-wide analysis identifies a general requirement for polarity proteins in endocytic traffic. *Nat. Cell Biol.* 9: 1066-1073.
- Baron M., O’Leary V., Evans D.A.P., Hicks M. 2000. Multiple roles of the Dcdc42 GTPase during wing development in *Drosophila melanogaster*. *Mol. Gen. Genet.* 264: 98-104.
- Betschinger J., Mechtler K., Knoblich J.A. 2003. The Par complex directs asymmetric cell division by phosphorylating the cytoskeletal protein Lgl. *Nature* 422: 326–330.
- Bilder D., Li M., Perrimon N. 2000. Cooperative regulation of cell polarity and growth by *Drosophila* tumor suppressors. *Science* 289: 113-116.
- Bilder D. and Perrimon N. 2000. Localization of apical epithelial determinants by the

- basolateral PDZ protein Scribble. *Nature* 403: 676-680.
- Bilder, D., Schober, M., Perrimon, N. 2003. Integrated activity of PDZ protein complexes regulates epithelial polarity. *Nat. Cell Biol.* 5: 53-57.
- Bökel C., Schwabedissen A., Entchev E., Renaud O., Gonzalez-Gaitan M. 2006. Sara endosomes and the maintenance of Dpp signaling levels across mitosis. *Science* 314: 1135-1139.
- Bond J.S. and Butler P.E. 1987. Intracellular proteases. *Annu. Rev. Biochem.* 56:333-364.
- Brand A.H. and Perrimon N. 1993. Targeted gene expression as a means of altering cell fates and generating dominant phenotypes. *Development* 118: 401-415.
- Bucci C., Parton R.G., Mather I.H., Stunnenberg H., Simons K., Hoflack B., Zerial M. 1992. The small GTPase rab5 functions as a regulatory factor in the early endocytotic pathway. *Cell* 70: 715-728.
- Bucci C., Thomsen P., Nicoziani P., McCarthy J., van Deurs B. 2000. Rab7: a key to lysosome biogenesis. *Mol. Biol. Cell* 11: 467-480.
- Burd C.G. and Emr S.D. 1998. Phosphatidylinositol (3)-phosphate signaling mediated by specific binding to RING FYVE domains. *Mol. Cell* 2: 157-162.
- Buszczak M. and Cooley L. 2000. Eggs to die for: cell death during *Drosophila* oogenesis. *Cell Death Differ.* 7: 1071-1074.
- Candiano G., Bruschi M., Musante L., Santucci L., Ghiggeri G.M., Carnemolla B., Orecchia P., Zardi L., Righetti P.G. 2004. Blue silver: a very sensitive colloidal Coomassie G-250 staining for proteome analysis. *Electrophoresis* 25: 1327-1333.
- Carlton J.G. and Cullen P.J. 2005. Coincidence detection in phosphoinositide signaling. *Trends Cell Biol.* 15: 540-547.
- Ceresa B.P., Lotscher M., Schmid S.L. 2001. Receptor and membrane recycling can occur with unaltered efficiency despite dramatic Rab5(q79I)-induced changes in endosome geometry. *J. Biol. Chem.* 276: 9649-9654.
- Chavrier P., Parton R.G., Hauri H.P., Simons K., Zerial M. 1990. Localization of low molecular weight GTP binding proteins to exocytic and endocytic compartments. *Cell* 62: 317-329.
- Chen X., Cheung S.T., So S., Fan S.T., Barry C., Higgins J., Lai K.M., Ji J., Dudoit S., Ng I.O., Van De Rijn M., Botstein D., Brown P.O. 2002. Gene expression patterns in human liver cancers. *Mol. Biol. Cell* 13: 1929-1939.
- Chen W., Feng Y., Chen D., Wandinger-Ness A. 1998. Rab11 is required for trans-Golgi network-to-plasma membrane transport and a preferential target for GDP

- dissociation inhibitor. *Mol. Biol. Cell* 9: 3241-3257.
- Chen W., Li N., Chen T., Han Y., Li C., Wang Y., He W., Zhang L., Wan T., Cao X. 2005. The lysosome-associated apoptosis-inducing protein containing the pleckstrin homology (PH) and FYVE domains (LAPF), representative of a novel family of PH and FYVE domain-containing proteins, induces caspase-independent apoptosis via the lysosomal-mitochondrial pathway. *J Biol Chem.* 280: 40985-40995.
- Christoforidis S., Miaczynska M., Ashman K., Wilm M., Zhao L., Yip S.C., Waterfield M.D., Backer J.M. and Zerial M. 1999. Phosphatidylinositol-3-OH kinases are Rab5 effectors. *Nat. Cell Biol.* 1: 249–252.
- Cox R.T., Kikpatrick C., Peifer M. 1996. Armadillo is required for adherens junction assembly, cell polarity, and morphogenesis during *Drosophila* embryogenesis. *J. Cell Biol.* 134: 133-148.
- Currie R.A., Walker K.S., Gray A., Deak M., Casamayor A., Downes C.P., Cohen P., Alessi D.R., Lucocq J. 1999. Role of phosphatidylinositol 3,4,5-triphosphate in regulating the activity and localization of 3-phosphoinositide-dependent protein kinase-1. *Biochem. J.* 337: 575-583.
- Del Conte-Zerial P., Brusch L., Rink J.C., Collinet C., Kalaidzidis Y., Zerial M., Deutsch A. 2008. Membrane identity and GTPase cascades regulated by toggle and cut-out switches. *Mol. Syst. Biol.* 4: 206.
- Delva E. and Kowalczyk A.P. 2009. Regulation of cadherin trafficking. *Traffic* 10: 259-267.
- Desclozeaux M., Venturato J., Wylie F.G., Kay J.G., Joseph S.R., Le H.T., Stow J.L. 2008. Active Rab11 and functional recycling endosome are required for E-cadherin trafficking and lumen formation during epithelial morphogenesis. *Am. J. Physiol. Cell Physiol.* 295: C545-C556.
- Devergne O., Ghiglione C., Noselli S. 2007. The endocytic control of JAK/STAT signalling in *Drosophila*. *J. Cell Sci.* 120: 3457-3464.
- DiMario P.J. and Mahowald A.P. 1987. Female sterile (1) yolkless: a recessive female sterile mutation in *Drosophila melanogaster* with depressed numbers of coated pits and coated vesicles within the developing oocytes. *J. Cell Biol.* 105: 199-206.
- Di Paolo G. and De Camilli P. 2006. Phosphoinositides in cell regulation and membrane dynamics. *Nature* 443: 651-657.
- Dirac-Svejstrup, A.B., Sumizawa T., Pfeffer S.R. 1997. Identification of a GDI displacement factor that releases endosomal GTPases from Rab-GDI. *EMBO J.* 16:

- 465-472.
- Doherty G.J. and McMahon H.T. 2009. Mechanisms of endocytosis. *Annu. Rev. Biochem.* 78: 857-902.
- Drubin, D.G. and Nelson, W.J. 1996. Origins of cell polarity. *Cell* 84: 335-344.
- Egger-Adam, D. 2005. Identifikation neuer Interaktionspartner des Bazooka Proteins in *Drosophila melanogaster*. Inaugural-Dissertation, Heinrich-Heine-Universität Düsseldorf.
- Entchev E.V., Schwabedissen A., Gonzalez-Gaitan M. 2000. Gradient formation of the TGF- β homolog Dpp. *Cell* 103: 981-991.
- Emery G. and Knoblich J.A. 2006. Endosome dynamics during development. *Curr. Opin. Cell Biol.* 18: 407-415.
- Fischer J.A., Eun S.H., Doolan B.T. 2006. Endocytosis, endosome trafficking, and the regulation of *Drosophila* development. *Annu. Rev. Cell Dev. Biol.* 22: 181-2006.
- Friche R., Gohl C., Dharmalingam E., Grevelhörster A., Zahedi B., Harden N., Kessels M., Qualmann B., Bogdan S. 2009. *Drosophila* Cip4/Toca-1 integrates membrane trafficking and actin dynamics through WASP and SCAR/WAVE. *Curr. Biol.* 19: 1429-1437.
- Gassama-Diagne, A., Yu, W., ter Beest, M., Martin-Belmonte, F., Kierbel, A., Engel, J., Mostov, K. 2006. Phosphatidylinositol-3,4,5-triphosphate regulates the formation of the basolateral plasma membrane in epithelial cells. *Nat. Cell Biol.* 8: 963-970.
- Gaullier J.M., Simonsen A., D'Arrigo A., Bremnes B., Stenmark H. 1998. FYVE fingers bind PtdIns(3)P. *Nature* 394: 432-433.
- Gaullier J.M., Ronning E., Gillooly D., Stenmark H. 2000. Interaction of the EEA1 FYVE finger with phosphatidylinositol 3-phosphate and early endosomes. Role of conserved residues. *J. Biol. Chem.* 275: 24595-24600.
- Genova J.L., Jong S., Camp J.T., Fehon R. G. 2000. Functional analysis of *Cdc42* in actin filament assembly, epithelial morphogenesis, and cell signaling during *Drosophila* development. *Dev. Biol.* 221: 181-194.
- Georgiou M., Marinari E., Burden J., Baum B. 2008. Cdc42, Par6, and aPKC regulate Arp2/3-mediated endocytosis to control local adherens junction stability. *Curr. Biol.* 18: 1631-1638.
- Gilbert M.M., Robinson B.S., Moberg K.H. 2009. Functional interactions between the erupted/tsg101 growth suppressor gene and the DaPKC and rbf1 genes in *Drosophila* imaginal disc tumors. *PloS One* 4: e7039.

- Gillooly D.J., Morrow I.C., Lindsay M., Gould R., Bryant N.J., Gaulier J.M., Parton R.G., Stenmark H. 2000. Localization of phosphatidylinositol 3-phosphate in yeast and mammalian cells. *EMBO J.* 19: 4577-4588.
- Gillooly D.J., Simonsen A., Stenmark H. 2001. Cellular functions of phosphatidylinositol 3-phosphate and FYVE domain proteins. *Biochem J.* 355: 249-258.
- Goldstein B. and Macara I.G. 2008. The PAR proteins: fundamental players in animal cell polarization. *Dev. Cell* 13: 609-622.
- Gorvel J.P., Chavrier P., Zerial M., Gruenberg J. 1991. Rab5 controls early endosome fusion in vitro. *Cell* 64: 915-925.
- Grammont M. and Irvine K.D. 2001. *fringe* and *Notch* specify polar cell fate during *Drosophila* oogenesis. *Development* 128: 2243-2253.
- Grosshans B.L., Ortiz D., Novick P. 2006. Rabs and their effectors: achieving specificity in membrane traffic. *PNAS* 103: 11821-11827.
- Gruenberg J. 2001. The endocytic pathway: a mosaic of domains. *Nat. Rev. Mol. Cell Biol.* 2: 721-730.
- Harris T.J.C. and Pfeifer M. 2004. Adherens junction-dependent and -independent steps in the establishment of epithelial cell polarity in *Drosophila*. *J. Cell Biol.* 167: 135-147.
- Harris T.J.C. and Pfeifer M. 2005. The positioning and segregation of apical cues during epithelial polarity establishment in *Drosophila*. *J. Cell Biol.* 170: 813-823.
- Harris K.P. and Tepass U. 2008. Cdc42 and Par proteins stabilize dynamic adherens junctions in the *Drosophila* neuroectoderm through reorganization of apical endocytosis. *J. Cell Biol.* 183: 1129-1143.
- Hayakawa A., Hayes S.J., Lawe D.C., Sudharshan E., Tuft R., Fogarty K., Lambright D., Corvera S. 2004. Structural basis for endosomal targeting by FYVE domains. *J. Biol. Chem.* 279: 5958-5966.
- Hong Y., Stronach B., Perrimon N., Jan L.Y., Jan Y.N. 2001. *Drosophila* Stardust interacts with Crumbs to control polarity of epithelia but not neuroblasts. *Nature* 414: 634-638.
- Hou Y.C., Chittaranjan S., Barbosa S.G., McCall K., Gorski S.M. 2008. Effector caspase Dcp-1 and IAP protein Bruce regulate starvation-induced autophagy during *Drosophila melanogaster* oogenesis. *J. Cell Biol.* 182: 1127-1139.
- Humbert P.O., Dow L.E., Russell S.M. 2006. The Scribble and Par complexes in polarity and migration: friends or foes? *Trends Cell Biol.* 16: 622-630.
- Hutt D.M., Da-Silva L.F., Chang L.H., Prosser D.C., Ngsee J.K. 2000. PRA1 inhibits the

- extraction of membrane-bound Rab GTPase by GDI1. *J. Biol. Chem.* 275: 18511-18519.
- Hutterer A., Betschinger J., Petronczki M., Knoblich J.A. 2004. Sequential roles of Cdc42, Par-6, aPKC, and Lgl in the establishment of epithelial polarity during *Drosophila* embryogenesis. *Dev. Cell* 6: 845-854.
- Ito T., Chiba T., Ozawa R., Yoshida M., Hattori M., Sakaki Y. 2001. A comprehensive two-hybrid analysis to explore the yeast protein interactome. *PNAS* 98: 4569-4574.
- Ivetac I., Munday A.D., Kisseleva M.V., Zhang X.M., Luff S., Tiganis T., Whisstock J.C., Rowe T., Majerus P.W., Mitchell C.A. 2005. The type Ia inositol polyphosphate 4-phosphatase generates and terminates phosphoinositide 3-kinase signals on endosomes and the plasma membrane. *Mol. Biol. Cell* 16: 2218-2233.
- Izumi G., Sakisaka T., Tanaka S., Morimoto K., Takai Y. 2004. Endocytosis of E-cadherin regulated by Rac and Cdc42 small G proteins through IQGAP1 and actin filaments. *J. Cell Biol.* 166: 237-248.
- Januschke J., Nicolas E., Compagnon J., Formstecher E., Goud B., Guichet A. 2007. Rab6 and the secretory pathway affect oocyte polarity in *Drosophila*. *Development* 134: 3419-3425.
- Johnson K. and Wodarz A. 2003. A genetic hierarchy controlling cell polarity. *Nat. Cell Biol.* 5: 12-14.
- Katzmann D.J., Babst M., Emr S.D. 2001. Ubiquitin-dependent sorting into the multivesicular body pathway requires the function of a conserved endosomal protein sorting complex, ESCRT-I. *Cell* 106: 145-155.
- Kavran J.M., Klein D.E., Lee A., Falasca M., Isakoff S.J., Skolnik E.Y., Lemmon M.A. 1998. Specificity and promiscuity in phosphoinositide binding by pleckstrin homology domains. *J. Biol. Chem.* 273: 30497-30508.
- Kim S., Gailite I., Moussian B., Luschnig S., Goette M., Fricke K., Honemann-Capito M., Grubmüller H., Wodarz A. 2009. Kinase-activity-independent functions of atypical protein kinase C in *Drosophila*. *J. Cell Sci.* 122: 3759-3771.
- Kim S., Wairkar Y.P., Daniels R.W., DiAntonio A. 2010. The novel endosomal membrane protein Ema interacts with the class C Vps-HOPS complex to promote endosomal maturation. *J. Cell Biol.* 188: 717-734.
- Knust E. 2000. Control of epithelial cell shape and polarity. *Curr. Opin. Gen. Dev.* 10: 471-475.
- Knust E. and Bossinger O. 2002. Composition and formation of intercellular junctions in

- epithelial cells. *Science* 298: 1955-1959.
- Komada M., Masaki R., Yamamoto A., Kitamura N. 1997. Hrs, a tyrosine kinase substrate with a conserved double zinc finger domain, is localized to the cytoplasmic surface of early endosomes. *J. Biol. Chem.* 272: 20538-20544.
- Kuchinke U., Grawe F., Knust E. 1998. Control of spindle orientation in *Drosophila* by the Par-3-related PDZ-domain protein Bazooka. *Curr. Biol.* 8: 1357-1365.
- Kutateladze T.G. 2006. Phosphatidylinositol 3-phosphate recognition and membrane docking by the FYVE domain. *Biochim. Biophys. Acta* 1761: 868-877.
- Lakadamyali M., Rust M.J., Zhuang X. 2006. Ligands for clathrin-mediated endocytosis are differentially sorted into distinct populations of early endosomes. *Cell* 124: 997-1009.
- Le T.L., Yap A.S., Stow J.L. 1999. Recycling of E-cadherin: a potential mechanism for regulating cadherin dynamics. *J. Cell Biol.* 146: 219-232.
- Le Borgne R. 2006. Regulation of Notch signalling by endocytosis and endosomal sorting. *Curr. Opin. Cell Biol.* 18: 213-222.
- Leibfried A. and Bellaiche Y. 2007. Functions of endosomal trafficking in *Drosophila* epithelial cells. *Curr. Opin. Cell Biol.* 19:446-452.
- Leibfried A., Fricke R., Morgan M.J., Bogdan S., Bellaiche Y. 2008. *Drosophila* Cip4 and WASp define a branch of the Cdc42-Par6-aPKC pathway regulating E-cadherin endocytosis. *Curr. Biol.* 18: 1639-1648.
- Lemmon M.A. 2008. Membrane recognition by phospholipid-binding domains. *Nat. Rev. Mol. Cell Biol.* 9: 99-111.
- Li N., Zheng Y., Chen W., Wang C., Liu X., He W., Xu H., Cao X. 2007. Adaptor protein LAPF recruits phosphorylated p53 to lysosomes and triggers lysosomal destabilization in apoptosis. *Cancer Res.* 67: 11176-11185.
- Li C., Liu Q., Li N., Chen W., Wang L., Wang Y., Yu Y., Cao X. 2008. EAPF/Phafin-2, a novel endoplasmic reticulum-associated protein, facilitates TNF-alpha-triggered cellular apoptosis through endoplasmic reticulum-mitochondrial apoptotic pathway. *J. Mol. Med.* 86:471-484.
- Lin W.J., Yang C.Y., Lin Y.C., Tsai M.C., Yang C.W., Tung C.Y., Ho P.Y., Kao F.J., Lin C.H. 2010. Phafin2 modulates the structure and function of endosomes by a Rab5-dependent mechanism. *Biochem. Biophys. Res. Commun.* 391: 1043-1048.
- Lloyd T.E., Atkinson R., Wu M.N., Zhou Y., Pennetta G., Bellen H.J. 2002. Hrs regulates endosome membrane invagination and tyrosine kinase receptor signaling in

- Drosophila*. Cell 108: 261-269.
- Lock J.G. and Stow J.L. 2005. Rab11 in recycling endosomes regulates the sorting and basolateral transport of E-Cadherin. Mol. Biol. Cell 16: 1744-1755.
- Lopez-Schier H. and St. Johnston D. 2001. Delta signaling from the germ line controls the proliferation and differentiation of the somatic follicle cells during *Drosophila* oogenesis. Genes Dev. 15: 1393-1405.
- Lu H. and Bilder D. 2005. Endocytic control of epithelial polarity and proliferation in *Drosophila*.
- Lu Z., Ghosh S., Wang Z., Hunter T. 2003. Downregulation of caveolin-1 function by EGF leads to the loss of E-cadherin, increased transcriptional activity of β -catenin, and enhanced tumor cell invasion. Cancer Cell 4: 499-515.
- Margolis B. and Borg J.P. 2005. Apicobasal polarity complexes. J. Cell Sci. 118: 5157-5159.
- Martin-Belmonte F., Gassama A., Datta A., Yu W., Rescher U., Gerke V., Mostov K. 2007. PTEN-mediated apical segregation of phosphoinositides controls epithelial morphogenesis through Cdc42. Cell 128: 383-397.
- Mari M., Bujny M.V., Zeuschner D., Geerts W.J., Petersen C.M., Cullen P.J., Klumperman J., Geuze H.J. 2008. SNX1 defines an early endosomal recycling exit for sortilin and mannose 6-phosphate receptors. Traffic 9: 380-393.
- McCall K. 2004. Eggs over easy: cell death in the *Drosophila* ovary. Dev. Biol. 274: 3-14.
- McGregor J.R., Xi R., Harrison D.A. 2002. JAK signaling is somatically required for follicle cell differentiation in *Drosophila*. Development 129: 705-717.
- McLauchlan H., Newell J., Morrice N., Osborne A., West M., Smythe E. 1998. A novel role for Rab5-GDI in ligand sequestration into clathrin-coated pits. Curr. Biol. 8 :34-45.
- Mellman I. 1996. Endocytosis and molecular sorting. Annu. Rev. Cell Dev. Biol. 12: 575-625.
- Melnick M.B., Noll E., Perrimon N. 1993. The *Drosophila stubarista* phenotype is associated with a dosage effect of the putative ribosome-associated protein D-p40 on spineless. Genetics 135: 553-564.
- Moberg K.H., Schelble S., Burdick S.K., Hariharan I.K. 2005. Mutations in *erupted*, the *Drosophila* ortholog of mammalian tumor susceptibility gene 101, elicit non-cell-autonomous overgrowth. Dev. Cell 9: 699-710.
- Morrison H.A., Dionne H., Rusten T.E., Brech A., Fisher W.W., Pfeiffer B.D., Celniker

- S.E., Stenmark H., Bilder D. 2008. Regulation of early endosomal entry by the *Drosophila* tumor suppressors Rabenosyn and Vps45. *Mol. Biol. Cell* 19: 4167-4176.
- Mu F.T., Callaghan J.M., Steele-Mortimer O., Stenmark H., Parton R.G., Campbell P.L., McCluskey J., Yeo J.P., Tock E.P.C., Toh B.H. 1995. EEA1, an early endosome-associated protein. EEA1 is a conserved α -helical peripheral membrane protein flanked by cysteine „fingers“ and contains a calmodulin-binding IQ motif. *J. Biol. Chem.* 270: 13503-13511.
- Mullock B.M., Bright N.A., Fearon C.W., Gray S.R., Luzio J.P. 1998. Fusion of lysosomes with late endosomes produces a hybrid organelle of intermediate intensity and is NSF dependent. *J. Cell Biol.* 140: 591-601.
- Müller H.A.J. 2000. Genetic control of epithelial cell polarity: lessons from *Drosophila*. *Dev. Dyn.* 218: 52-67.
- Müller H.A.J. and Wieschaus E. 1996. *armadillo*, *bazooka* and *stardust* are critical for early stages in formation of the zonula adherens and maintenance of the polarized blastoderm epithelium in *Drosophila*. *J. Cell Biol.* 134: 149-163.
- Murray J.T., Panaretou C., Stenmark H., Miaczynska M., Backer J.M. 2002. Role of Rab5 in the recruitment of hVps34/p150 to the early endosome. *Traffic* 3: 416-427.
- Navarro C., Nola S., Audebert S., Santoni M.J., Arsanto J.P., Ginestier C., Marchetto S., Jacquemier J., Isnardon D., Le Bivic A., Birnbaum D., Borg J.P. 2005. Junctional recruitment of mammalian Scribble relies on E-cadherin engagement. *Oncogene* 24: 4330-4339.
- Palacios F., Tushir J.S., Fujita Y., D'Souza-Schorey C. 2005. Lysosomal targeting of E-cadherin: a unique mechanism for the down-regulation of cell-cell adhesion during epithelial to mesenchymal transitions. *Mol. Cell. Biol.* 25: 389-402.
- Peretz G., Bakhrat A., Abdu U. 2007. Expression of the *Drosophila melanogaster* GADD45 homolog (CG11086) affects egg asymmetric development that is mediated by the c-Jun N-terminal kinase pathway. *Genetics* 177: 1691-1702.
- Parks A.L. et al. 2004. Systematic generation of high-resolution deletion coverage of the *Drosophila melanogaster* genome. *Nat. Genet.* 36: 288-292
- Patki V., Lawe D.C., Corvera S., Virbasius J.V., Chawla A. 1998. A functional PtdIns(3)P-binding motif. *Nature* 394: 433-434.
- Petronczki M. and Knoblich J.A. 2001. DmPar-6 directs epithelial polarity and asymmetric cell division of neuroblasts in *Drosophila*. *Nat. Cell Biol.* 3: 43-49.
- Pfeffer S.R. 2001. Rab GTPases: specifying and deciphering organelle identity and

- function. Trends Cell Biol. 11: 487-491.
- Pfeffer S.R. and Aivazian D. 2004. Targeting Rab GTPases to distinct membrane compartments. Nat. Rev. Mol. Cell Biol. 5: 886-896.
- Pons V., Luyet P.P., Morel E., Abrami L., van der Goot F.G., Parton R.G., Gruenberg J. 2008. Hrs and SNX3 functions in sorting and membrane invagination within multivesicular bodies. PLoS Biol. 6: 1924-1956.
- Pulipparacharuvil S., Akbar M.A., Ray S., Sevrioukov E.A., Haberman A.S., Rohrer J., Krämer H. 2005. *Drosophila* Vps16A is required for trafficking to lysosomes and biogenesis of pigment granules. J. Cell Sci. 118: 3663-3673.
- Raiborg C., Bremnes B., Mehlum A., Gillooly D.J., D'Arrigo A., Stang E., Stenmark H. 2001. FYVE and coiled-coil domains determine the specific localisation of Hrs to early endosomes. J. Cell Sci. 114: 2255-2263.
- Raiborg C., Bache K.G., Gillooly D.J., Madshus I.H., Stang E., Stenmark H. 2002. Hrs sorts ubiquitinated proteins into clathrin-coated microdomains of early endosomes. Nat. Cell Biol. 4: 394-398.
- Ricard C.S., Jakubowski J.M., Verbsky J.W., Barbieri M.A., Lewis W.M., Fernandez G.E., Vogel M., Tsou C., Prasad V., Stahl P.D., Waksman G. Cheney C.M. *Drosophila* GDI mutants disrupt development but have normal Rab membrane extraction. Genesis 31: 17-29.
- Rosenfeld J.L., Moore R.H., Zimmer K.P., Alpizar-Foster E., Dai W., Zarka M.N., Knoll B.J. 2001. Lysosome proteins are redistributed during expression of a GTP-hydrolysis-defective rab5a. J. Cell Sci. 114: 4499-4508.
- Rink J., Ghigo E., Kalaidzidis Y., Zerial M. 2005. Rab conversion as a mechanism of progression from early to late endosomes. Cell 122: 735-749.
- Rual et al. 2005. Towards a proteome-scale map of the human protein-protein interaction network. Nature 437: 1173-1178.
- Rubino M., Miaczynska M., Lippe R., Zerial M. 2000. Selective membrane recruitment of EEA1 suggests a role in directional transport of clathrin-coated vesicles to early endosomes. J. Biol. Chem. 275: 3745-3748.
- Sambrook, J., Russel, D.W. 2001. Molecular cloning: a laboratory manual. 3rd ed. Cold Spring Harbor Laboratory Press, New York, USA.
- Schneider, I. 1972. Cell lines derived from late embryonic stages of *Drosophila melanogaster*. J. Embryol. Exp. Morphol. 27: 353-365.
- Schober M., Schaefer M., Knoblich J.A. 1999. Bazooka recruits Inscuteable to orient

- asymmetric cell divisions in *Drosophila* neuroblasts. *Nature* 402: 548-551.
- Sheff D.R., Daro E.A., Hull M., Mellman I. 1999. The receptor recycling pathway contains two distinct populations of early endosomes with different sorting functions. *J. Cell Biol.* 145: 123-139.
- Shen Y., Hirsch D.S., Sasiela C.A., Wu W.J. 2008. Cdc42 regulates E-cadherin ubiquitination and degradation through an epidermal growth factor receptor to Src-mediated pathway. *J. Biol. Chem.* 283: 5127-5137.
- Simpson J.C., Wellenreuther R., Poustka A., Pepperkok R., Wiemann S. 2000. Systematic subcellular localization of novel proteins identified by large scale cDNA sequencing. *EMBO Reports* 1: 287-292.
- Sisson J.C., Field C., Ventura R., Royou A., Sullivan W. 2000. Lava lamp, a novel peripheral Golgi protein, is required for *Drosophila melanogaster* cellularization. *J. Cell Biol.* 151: 905-918.
- Sivars U., Aivazian D., Pfeffer S.R. 2003. Yip3 catalyzes the dissociation of endosomal Rab-GDI complexes. *Nature* 425: 856-859.
- Spang A. 2009. On the fate of early endosomes. *Biol. Chem.* 390: 753-759.
- Sriram V., Krishnan K.S., Mayor S. 2003. *deep-orange* and *carnation* define distinct stages in late endosomal biogenesis in *Drosophila melanogaster*. *J. Cell Biol.* 161: 593-607.
- Stenmark H., Aasland R., Toh B.H., D'Arrigo A. 1996. Endosomal localization of the autoantigen EEA1 is mediated by a zinc-binding FYVE motif. *J. Biol. Chem.* 271: 24048-24054.
- Stenmark H. and Olkkonen V. M. 2001. The Rab GTPase family. *Genome Biol.* 2: reviews3007.1-3007.7
- Sun W., Yan Q., Vida T.A., Bean A.J. 2003. Hrs regulates early endosome fusion by inhibiting formation of an endosomal SNARE complex. *J. Cell Biol.* 162: 125-137.
- Suzuki A. and Ohno S. 2006. The PAR-aPKC system: lessons in polarity. *J. Cell Sci.* 119: 979-987.
- Tanentzapf G. and Tepass U. 2003. Interaction between the *crumbs*, *lethal giant larvae* and *bazooka* pathways in epithelial polarization. *Nat. Cell Biol.* 5: 46-52.
- Tanaka T. and Nakamura A. 2008. The endocytic pathway acts downstream of Oscar in *Drosophila* germ plasm assembly. *Development* 135: 1107-1117.
- Thompson B.J., Mathieu J., Sung H.H., Loeser E., Rorth P., Cohen S.M. 2005. Tumor suppressor properties of the ESCRT-II complex component Vps25 in *Drosophila*.

- Dev. Cell 9: 711-720.
- Torres V.A., Mielgo A., Barila D., Anderson D.H., Stupack D. 2008. Caspase 8 promotes peripheral localization and activation of Rab5. *J. Biol. Chem.* 283: 36280-36289.
- Trischler M., Stoorvogel W., Ullrich O. 1999. Biochemical analysis of distinct Rab5- and Rab11-positive endosomes along the transferrin pathway. *J. Cell Sci.* 122: 4773-4783.
- Twombly V., Blackman R.K., Jin H., Graff J.M., Padgett R.W. 1996. The TGF- β signaling pathway is essential for *Drosophila* oogenesis. *Development* 122: 1555-1565.
- Ullrich O., Stenmark H., Alexandrov K., Huber L.A., Kaibuchi K., Sasaki T., Takai Y., Zerial M. 1993. Rab GDP dissociation inhibitor as a general regulator for the membrane association of Rab proteins. *J. Biol. Chem.* 268: 18143-18150.
- Ullrich O., Reinsch S., Urbe S., Zerial M., Parton R.G. 1996. Rab11 regulates recycling through the pericentriolar recycling endosome. *J. Cell Biol.* 135: 913-924.
- Vaccari T. and Bilder D. 2005. The *Drosophila* tumor suppressor Vps25 prevents nonautonomous overproliferation by regulating notch trafficking. *Dev. Cell* 9: 687-698.
- Vaccari T., Lu H., Kanwar R., Fortini M.E., Bilder D. 2008. Endosomal entry regulates Notch receptor activation in *Drosophila melanogaster*. *J. Cell Biol.* 180: 755-762.
- Vanlandingham P.A. and Ceresa B.P. 2009. Rab7 regulates late endocytic trafficking downstream of multivesicular body biogenesis and cargo sequestration. *J. Biol. Chem.* 284: 12110-12124.
- Van Meer, G., Voelker D.R., Feigenson G.W. 2008. Membrane lipids: where they are and how they behave. *Nat. Rev. Mol. Cell Biol.* 9: 112-124.
- Varnai P., Lin X., Lee S.B., Tuymetova G., Bondeva T., Spät A., Rhee S.G., Hajnoczky G., Balla T. 2002. Inositol lipid binding and membrane localization of isolated pleckstrin homology (PH) domains. *J. Biol. Chem.* 277: 27412-27422.
- Visser Smit G.D., Place T.L., Cole S.L., Clausen K.L., Vemuganti S., Zhang G., Koland J.G., Lill N.L. 2009. Cbl controls EGFR fate by regulating early endosome fusion. *Sci. Signal.* 2: ra86.
- Vonderheit A. and Helenius A. 2005. Rab7 associates with early endosomes to mediate sorting and transport of Semliki forest virus to late endosomes. *PLoS Biol.* 3: 1225-1238.
- Weisz A., Basile W., Scafoglio C., Altucci L., Bresciani F., Facchiano A., Sismondi P., Cicatiello L., De Bortoli M. 2004. Molecular identification of ERalpha-positive

- breast cancer cells by the expression profile of an intrinsic set of estrogen regulated genes. *J. Cell. Physiol.* 200: 440-450.
- Wegner C.S., Malerød L., Pedersen N.M., Progida C., Bakke O., Stenmark H., Brech A. 2010. Ultrastructural characterization of giant endosomes induced by GTPase-deficient Rab5. *Histochem. Cell. Biol.* 133: 41-55.
- Wells C.D., Fawcett J.P., Traweger A., Yamanaka Y., Goudreault M., Elder K. et al. 2006. A Rich1/Amot complex regulates the Cdc42 GTPase and apical-polarity proteins in epithelial cells. *Cell* 125: 535-548.
- Willert, K., Brink, M., Wodarz, A., Varmus, H., Nusse, R. 1997. Casein kinase 2 associates with and phosphorylates Dishevelled. *EMBO J.* 16: 3089-3096.
- Wodarz A. 2008. Extraction and immunoblotting of proteins from embryos. From: *Methods in Molecular biology: Drosophila: Methods and Protocols*. Ed. Dahmann C. Humana Press, Totowa, NJ, pp 335-345.
- Wodarz A., Hinz U., Engelbert M., Knust E. 1995. Expression of *crumbs* confers apical character on plasma membrane domains of ectodermal epithelia of *Drosophila*. *Cell* 82: 67-76.
- Wodarz A., Ramrath A., Kuchinke U., Knust E. 1999. Bazooka provides an apical cue for Inscuteable localization in *Drosophila* neuroblasts. *Nature* 402: 544-547.
- Wodarz A., Ramrath A., Grimm A., Knust E. 2000. *Drosophila* atypical protein kinase C associates with Bazooka and controls polarity of epithelia and neuroblasts. *J. Cell Biol.* 150: 1361-1374.
- Wucherpennig T., Wilsch-Bräuninger M., Gonzalez-Gaitan M. 2003. Role of *Drosophila* Rab5 during endosomal trafficking at the synapse and evoked neurotransmitter release. *J. Cell Biol.* 161: 609-624.
- Wurmser A.E., Sato T.K., Emr S.D. 2000. New component of the vacuolar class C-Vps complex couples nucleotide exchange on the Ypt7 GTPase to SNARE-dependent docking and fusion. *J. Cell Biol.* 151: 551-562.
- Yagisawa H., Sakuma K., Paterson H.F., Cheung R., Allen V., Hirata H., Watanabe Y., Hirata M., Williams R.L., Katan M. 1998. Replacements of single basic amino acids in the pleckstrin homology domain of phospholipase C- δ 1 alter the ligand binding, phospholipase activity, and interaction with the plasma membrane. *J. Biol. Chem.* 273: 417-424.
- Yan Y., Deneff N., Schüpbach T. 2009. The vacuolar proton pump, V-ATPase, is required for Notch signaling and endosomal trafficking in *Drosophila*. *Dev. Cell* 17: 387-402.

- Yap A.S., Briehar W.M., Gumbiner B.M. 1997. Molecular and functional analysis of cadherin-based adherens junctions. *Dev. Biol.* 13: 119-146.
- Zerial M. and McBride H. 2001. Rab proteins as membrane organizers. *Nat. Rev. Mol. Cell Biol.* 2: 107-117.
- Zhang J., Schulze K.L., Hiesinger P.R., Suyama K., Wang S., Fish M., Acar M., Hoskins R.A., Bellen H.J., Scott M.P. 2007. Thirty-one flavors of *Drosophila* Rab proteins. *Genetics* 176: 1307-1322.

Abbreviations

Apart from SI units, common abbreviations of the English language and the amino acid single code the following abbreviations were used in this thesis:

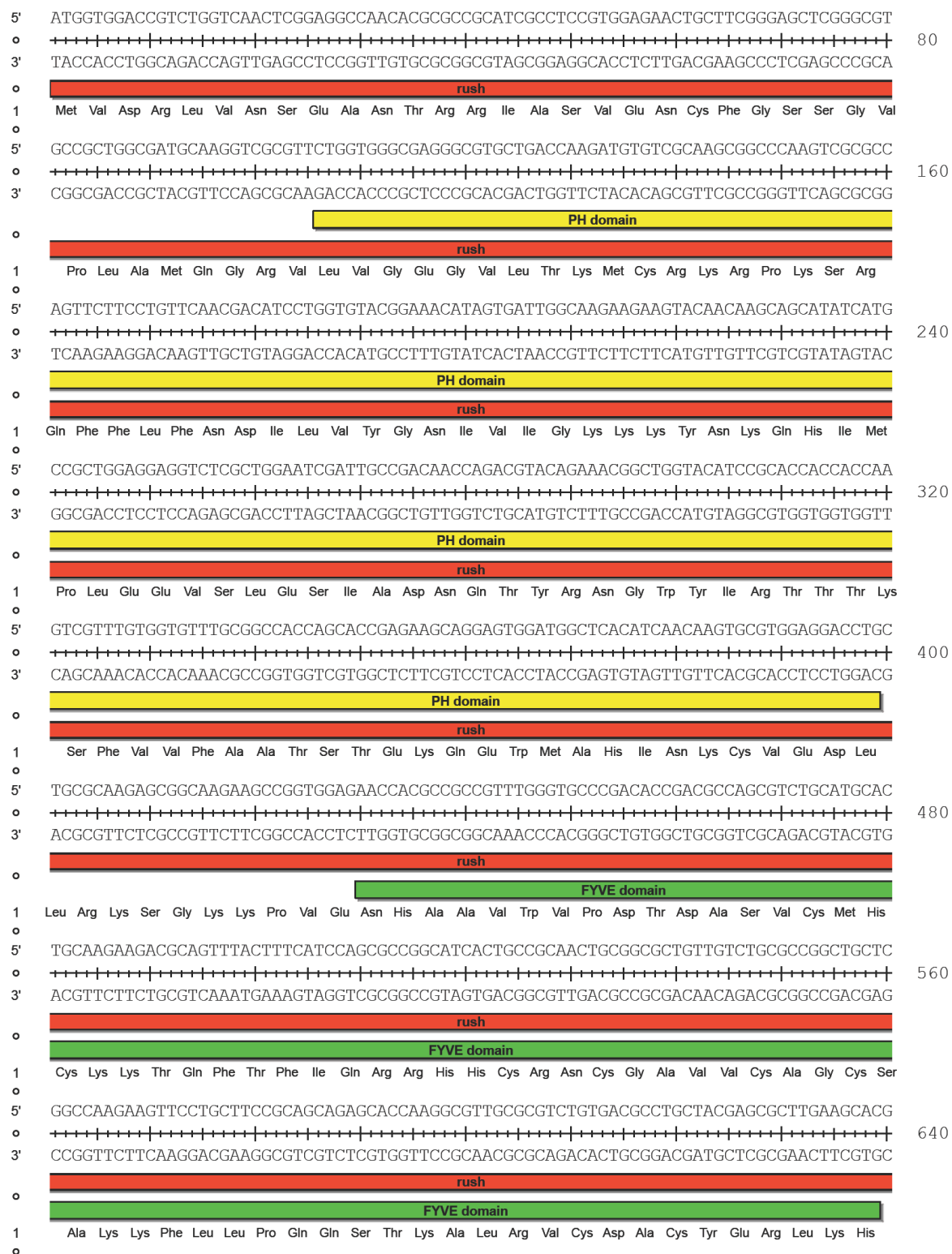
α	anti	Fig	figure
Act	Actin	FLP	Flipase
aPKC	atypical protein kinase C	FRT	Flipase recognition target
APS	ammonium persulfate		sequence
Arm	Armadillo	FYVE	Fab1p, YOTB, Vac1p, EEA1
Arp2/3	Actin related protein	Gal4	Gal4 transcription factor
Baz	Bazooka	GAP	GTPase activating protein
bp	base pairs	GDF	GDI displacement factor
CA	constitutively active	GDI	GDP dissociation inhibitor
Cdc42	Cell division control protein 42	GDP	guanine diphosphate
cDNA	complementary DNA	GEF	Guanine nucleotide exchange
Cip4	Cdc42 interacting protein 4		factor
Crb	Crumbs	GFP	Green fluorescent protein
da	daughterless	GST	Gluthatione-S-transferase
DABCO	diazabicyclo(2.2.2)octane	GTP	guanine triphosphate
DAPI	4',6-diamide-2'-phenylindole	HA	hemagglutinin
	dihydrochloride	HEPES	4-(2-hydroxyethyl)-1-
Dlg	Discs large		piperazine ethanesulfonic acid
DN	dominant negative	HOPS	Homotypic vacuole fusion and
DNA	deoxyribonucleic acid		protein sorting
dNTP	deoxynucleotide triphosphate	HRP	horseradish peroxidase
DTT	dithiothreitol	Hrs	Hepatocyte growth factor-
E-cad	E-cadherin		regulated tyrosine kinase
EDTA	ethylenediaminetetraacetic acid		substrate
EEA1	early endosomal antigen 1	IgG	Immunoglobulin G
Ept	Erupted	JAK	Janus kinase
ESCRT	endosomal complexes required	JNK	Jun-N-terminal kinase
	for transport	kb	kilobase
FasIII	Fasciclin III	kD	kilodalton

Abbreviations

LB	Luria Bertani broth	SDS	sodium dodecyl sulphate
Lgl	Lethal (2) giant larvae	Sdt	Stardust
LTR	LysoTracker	sec	second(s)
Lva	Lava lamp	sta	stubarista
MAGUK	membrane-associated guanylate kinase	STAT	Signal transducer and activator of transcription
MBP	Maltose binding protein	TEMED	N,N,N',N'- tetramethyldiamine
MVB	multivesicular body		
NHS	normal horse serum	TGF β	Transforming growth factor β
Orb	oo18 RNA-binding protein	TGN	<i>trans</i> -Golgi network
PAGE	polyacrylamide gel electrophoresis	Tris	Trishydroxymethylamino- methane
Par	Partitoning defective	U	unit (enzyme activity)
PATJ	Pals1-associated tight junction protein	UAS	upstream activating sequence
PBS	phosphate buffered saline	UTR	untranslated region
PCR	polymerase chain reaction	v/v	volume/volume
PDZ	PSD95, Discs large, Zona occludens-1	Vps	Vacuolar protein sorting
PH	pleckstrin homology	w	white
PIP	phosphatidyl inositol phosphate	w/v	weight/volume
PIPES	piperazine-1,4-bis-2- ethanesulfoic acid	wt	wild type
pnr	pannier	YFP	Yellow fluorescent protein
PNS	post nuclear supernatant		
PRA	Prenylated Rab acceptor protein		
rpm	rotations per minute		
Rush	Rush hour		
S2	Schneider 2		
SE	Standard error		
Scrib	Scribble		

Appendix

Appendix 1. The sequence of *rush* cDNA and the amino acid sequence of Rush. The PH domain is shown with a yellow box, the FYVE domain is marked with a green box.



Appendix

```

5'  TGCCAAGTTCCTTGGCTCTGGCGAGGACTCGGCAGCGGCTACCGGCGCTGCCCTCCGCAACAAGCTCAACACAACAGCC
o  +-----+-----+-----+-----+-----+-----+-----+-----+-----+-----+
3'  ACGGTTCAAGGGAACCGAGACCGCTCCTGAGCCGTCGCCGATGGCCGCGACGAGGCCGTTGTTTCGAGTTGTGTTCGG
o  +-----+-----+-----+-----+-----+-----+-----+-----+-----+-----+
o  rush
1  Val Pro Ser Ser Leu Gly Ser Gly Glu Asp Ser Ala Ala Ala Thr Gly Ala Ala Ser Gly Asn Lys Leu Asn Thr Thr Ala
o  +-----+-----+-----+-----+-----+-----+-----+-----+-----+-----+
5'  GCGGACAGCTCCAACGATGAGGACTCCGACGAGGAGACTGCCCTCCCCTGGTGCGAGTCGCACGATGAGCCGCGCTTCTA
o  +-----+-----+-----+-----+-----+-----+-----+-----+-----+-----+
3'  CCGCTGTTCGAGGTTGCTACTCCTGAGGCTGCTCCTCTGACGAGGGGACCACCGCTCAGCGTGCTACTCGGCGCGAAGAT
o  +-----+-----+-----+-----+-----+-----+-----+-----+-----+-----+
o  rush
1  Gly Asp Ser Ser Asn Asp Glu Asp Ser Asp Glu Glu Thr Ala Ser Pro Gly Gly Glu Ser His Asp Glu Pro Arg Phe Tyr
o  +-----+-----+-----+-----+-----+-----+-----+-----+-----+-----+
5'  CGGGGACAACAGCGTGCTATCCGCGCTCGAAGACTCCTCGACGATAACCTCGCCCTCCTCCGCCACCACTGGCAGCTTGG
o  +-----+-----+-----+-----+-----+-----+-----+-----+-----+-----+
3'  GCCCTGTGTGTCGACGATAGGCGGCAGCTTCTGAGGAGCTGCTATTGGAGCGGGAGGAGGCGGTGGTGACCGTCGAACC
o  +-----+-----+-----+-----+-----+-----+-----+-----+-----+-----+
o  rush
1  Gly Asp Asn Ser Val Leu Ser Ala Val Glu Asp Ser Ser Thr Ile Thr Ser Pro Ser Ser Ala Thr Thr Gly Ser Leu
o  +-----+-----+-----+-----+-----+-----+-----+-----+-----+-----+
5'  AGGCTCCCCAGGTGACACCGAGCGTCCAAAGCTCCCCGGCTGCCGTGCGACGACGGGCAGCCACTGTTGA
o  +-----+-----+-----+-----+-----+-----+-----+-----+-----+-----+
3'  TCCGAGGGGTCCACTGTGGCTCGCAGGTTTCGAGGGGCCACGGCAACGCTGCTGCCGTCGGTGACAACT
o  +-----+-----+-----+-----+-----+-----+-----+-----+-----+-----+
o  rush
1  Glu Ala Pro Gln Val Thr Pro Ser Val Gln Ser Ser Pro Ala Ala Val Ala Thr Thr Gly Ser His Cys
o  +-----+-----+-----+-----+-----+-----+-----+-----+-----+-----+

```

Appendix 2. The sequence of *GDI* cDNA and the amino acid sequence of GDI.

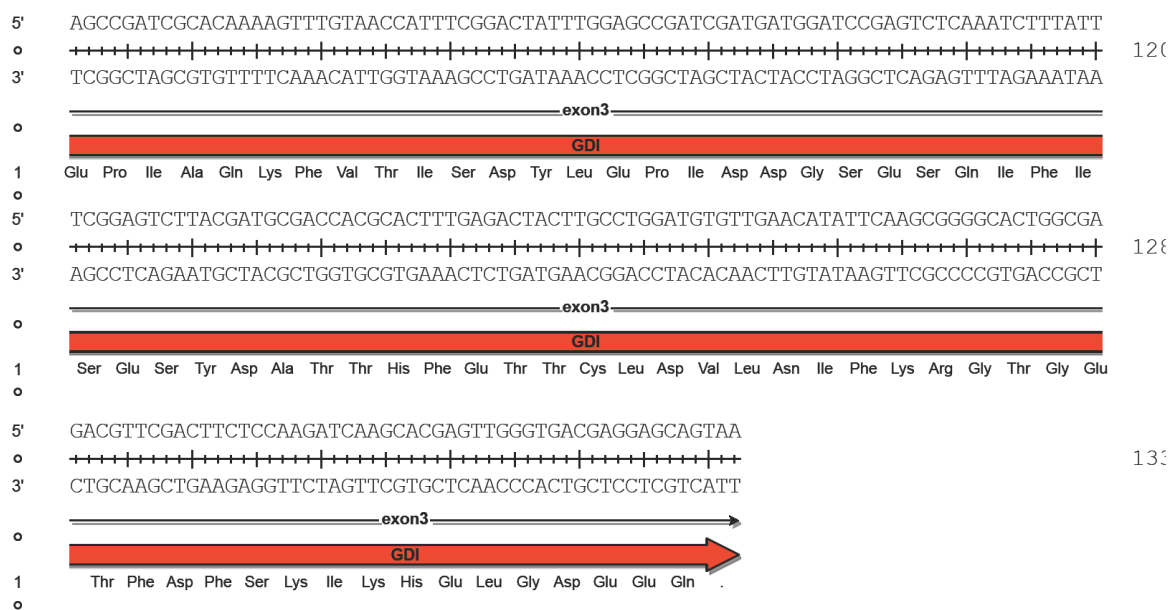
```

5'  ATGAATGAGGAATACGATGCGATTGTGCTAGGAACGGGCTCAAGGAGTGCATCCTCAGCGGGATGCTGTCCGTGTCCGG
o  +-----+-----+-----+-----+-----+-----+-----+-----+-----+-----+
3'  TACTTACTCCTTATGCTACGCTAACACGATCCTTGCCCGGAGTTCCCTCAGTAGGAGTCGCCCTACGACAGGCACAGGCC
o  +-----+-----+-----+-----+-----+-----+-----+-----+-----+-----+
o  exon1
o  GDI
1  Met Asn Glu Glu Tyr Asp Ala Ile Val Leu Gly Thr Gly Leu Lys Glu Cys Ile Leu Ser Gly Met Leu Ser Val Ser Gly
o  +-----+-----+-----+-----+-----+-----+-----+-----+-----+-----+
5'  CAAGAAGGTTTTGCATATTGATCGAAACAAGTACTACGGCGGCGAGTCCGCTCGATAACGCCGCTGGAGGAGCTCTTCC
o  +-----+-----+-----+-----+-----+-----+-----+-----+-----+-----+
3'  GTTCTTCCAAACGTATAACTAGCTTTGTTCATGATGCCGCCGCTCAGGCGGAGCTATTGCGGCGACCTCTCGAGAAGG
o  +-----+-----+-----+-----+-----+-----+-----+-----+-----+-----+
o  exon1
o  GDI
1  Lys Lys Val Leu His Ile Asp Arg Asn Lys Tyr Tyr Gly Gly Glu Ser Ala Ser Ile Thr Pro Leu Glu Glu Leu Phe
o  +-----+-----+-----+-----+-----+-----+-----+-----+-----+-----+
5'  AGCGCTACGGAAGTGGAGCCGCCGCGCAACGATTGGGCGTGGCCGCGACTGGAACGTGGACCTGATCCCCAAGTTCTCTG
o  +-----+-----+-----+-----+-----+-----+-----+-----+-----+-----+
3'  TCGCGATGCCGTGACCTCGGCGGCGCGCTTGCTAAACCCGACCGGCGCTGACCTTGACCTGGACTAGGGGTTCAAGGAC
o  +-----+-----+-----+-----+-----+-----+-----+-----+-----+-----+
o  exon1
o  GDI
1  Gln Arg Tyr Gly Leu Glu Pro Pro Gly Glu Arg Phe Gly Arg Asp Trp Asn Val Asp Leu Ile Pro Lys Phe Leu
o  +-----+-----+-----+-----+-----+-----+-----+-----+-----+-----+
5'  ATGGCCAATGGCCAGCTGGTCAAGCTGCTGATCCACACGGGCGTCACCCGCTATCTGGAGTTCAAGTCCATCGAGGCGAG
o  +-----+-----+-----+-----+-----+-----+-----+-----+-----+-----+
3'  TACCGGTTACCGGTCGACCAGTTCGACGACTAGGTGTGCCCGCAGTGGGCGATAGACCTCAAGTTCAGGTAGCTCCCGTC
o  +-----+-----+-----+-----+-----+-----+-----+-----+-----+-----+
o  exon1
o  GDI
1  Met Ala Asn Gly Gln Leu Val Lys Leu Leu Ile His Thr Gly Val Thr Arg Tyr Leu Glu Phe Lys Ser Ile Glu Gly Ser
o  +-----+-----+-----+-----+-----+-----+-----+-----+-----+-----+
5'  CTACGTTTACAAGGGCGGCAAGATAGCCAAGGTGCCGTTGGACAAAAGGAGGCCCTGGCATCCGATCTCATGGGTATGT
o  +-----+-----+-----+-----+-----+-----+-----+-----+-----+-----+
3'  GATGCAAATGTTCCCGCGTCTATCGGTTCACGGCCACCTGGTTTCTCCGGGACCGTAGGCTAGAGTACCCATACA
o  +-----+-----+-----+-----+-----+-----+-----+-----+-----+-----+
o  exon1
o  GDI
1  Tyr Val Tyr Lys Gly Gly Lys Ile Ala Lys Val Pro Val Asp Gln Lys Glu Ala Leu Ala Ser Asp Leu Met Gly Met
o  +-----+-----+-----+-----+-----+-----+-----+-----+-----+-----+

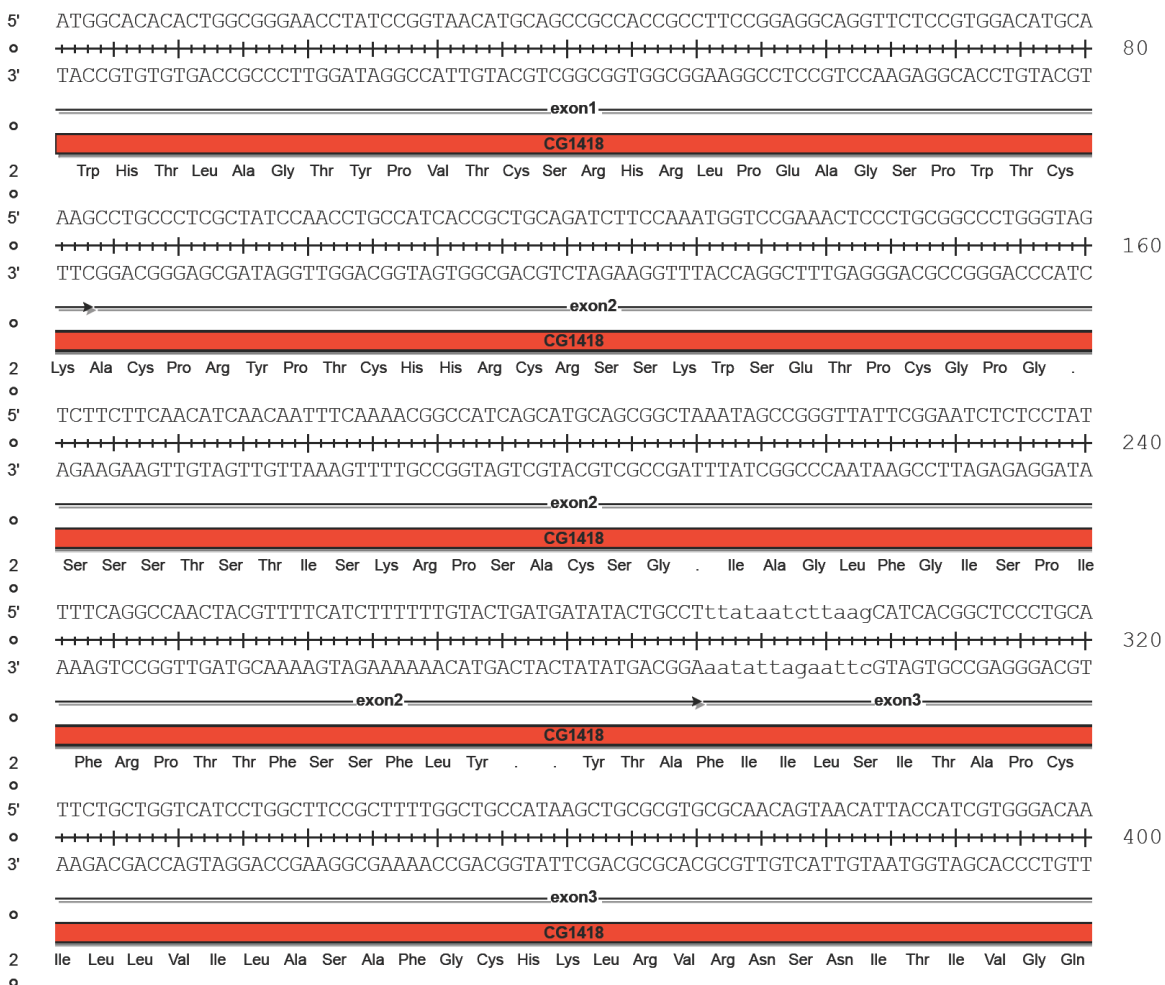
```

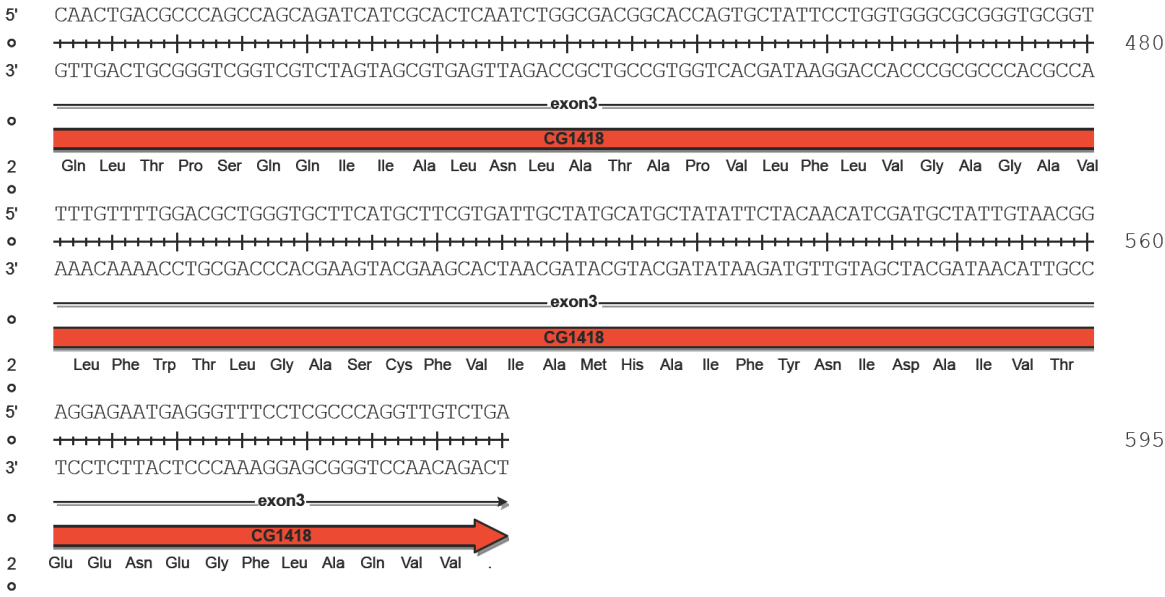

5'	TCGAGAAGCGTCGCTTCCGGAAC'TCCTCATCTACGTGCAGGATT'TCCGAGAAGATGACCCCAAGACCTGGAAGGACTTT	480
o	+	
3'	AGCTCTTCGCAGCGAAGGCCTTGAAGGAGTAGATGCACGTCTTAAAGGCTCTTCTACTGGGGTTCTGGACCTTCTCTGAAA	
o	exon2	
	GDI	
1	Phe Glu Lys Arg Arg Phe Arg Asn Phe Leu Ile Tyr Val Gln Asp Phe Arg Glu Asp Asp Pro Lys Thr Trp Lys Asp Phe	
o		
5'	GACCCACCAAGGCCAACATGCAGGGTCTGTACGACAAGTTCGGACTGGACAAGAACACGCAGGACTTCACCGGCCACGC	560
o	+	
3'	CTGGGGTGGTTCCGGTTGTACGTCCAGACATGCTGTTCAAGCCTGACCTGTTCTTGTGCGTCTGAAGTGGCCGGTGCG	
o	exon2	
	GDI	
1	Asp Pro Thr Lys Ala Asn Met Gln Gly Leu Tyr Asp Lys Phe Gly Leu Asp Lys Asn Thr Gln Asp Phe Thr Gly His Ala	
o		
5'	CCTGGCCCTTTTCCGCGACGATGAGTATCTGAACGAGCCGGCCGTGAACACCATCCGGCGGATTAAAGCTCTACTCCGATT	640
o	+	
3'	GGACCGGAAAAGCGCTGCTACTCATAGACTTGCTCGGCCGGCATTGTGGTAGGCCGCCTAATTCGAGATGAGGCTAA	
o	exon2	
	GDI	
1	Leu Ala Leu Phe Arg Asp Asp Glu Tyr Leu Asn Glu Pro Ala Val Asn Thr Ile Arg Arg Ile Lys Leu Tyr Ser Asp	
o		
5'	CGCTGGCGCGTTACGGCAAGTCGCCCTACCTTTATCCCATGTACGGCTGGGTGAGCTGCCCCAGGGATTTCGCACGTCTG	720
o	+	
3'	GCGACCGCGCAATGCCGTTACGCGGGATGAAATAGGGTACATGCCGGACCACTCGACGGGTCCCTAAGCGTGCAGAC	
o	exon2	
	GDI	
1	Ser Leu Ala Arg Tyr Gly Lys Ser Pro Tyr Leu Tyr Pro Met Tyr Gly Leu Gly Glu Leu Pro Gln Gly Phe Ala Arg Leu	
o		
5'	TCGGCCATCTACGGCGGCACCTACATGCTTGACAAGCCCATCGACGAGATTGTCTCGGCGAGGGCGGCAAGGTGGTGGG	800
o	+	
3'	AGCCGGTAGATGCCGCCGTGGATGTACGAACTGTTCGGGTAGCTGCTCTAACAGGAGCCGCTCCCGCGTTCCACCACCC	
o	exon2	
	GDI	
1	Ser Ala Ile Tyr Gly Gly Thr Tyr Met Leu Asp Lys Pro Ile Asp Glu Ile Val Leu Gly Glu Gly Gly Lys Val Val Gly	
o		
5'	AGTGCCTCCGGCGAAGAGGTGCGCAAGTGAAGCAGGTCTACTGCGATCCCAGCTACGTGCCGAGAAGGTGCGCAAGC	880
o	+	
3'	TCACGCGAGGCCGCTTCTCCAGCGGTTACGTTCTGTCAGATGACGCTAGGGTCGATGCACGGGCTCTTCCACGCGTTCG	
o	exon2	exon3
	GDI	
1	Val Arg Ser Gly Glu Glu Val Ala Lys Cys Lys Gln Val Tyr Cys Asp Pro Ser Tyr Val Pro Glu Lys Val Arg Lys	
o		
5'	GTGGCAAGGTGATTTCGCTGCATTTGCATTCTGGACCATCCGGTGGCCAGCACCAAGGATGGTCTCTCCACGCAGATTATC	960
o	+	
3'	CACCGTTCCACTAAGCGACGTAACGTAAGACCTGGTAGGCCACCGGTCGTGGTTCTTACCAGAGAGGTGCGTCTAATAG	
o	exon3	
	GDI	
1	Arg Gly Lys Val Ile Arg Cys Ile Cys Ile Leu Asp His Pro Val Ala Ser Thr Lys Asp Gly Leu Ser Thr Gln Ile Ile	
o		
5'	ATTCCACAAAAGCAGGTGCGCCGCAAGTCGGACATCTATGTGTGCTTGTGAGCTCCACTCATCAGGTGGCCGCCAAGGG	1040
o	+	
3'	TAAGGTGTTTTCGTCCAGCCGGCGTTCAGCCTGTAGATACACAGCAACACTCGAGGTGAGTAGTCCACCGCGGTTCCC	
o	exon3	
	GDI	
1	Ile Pro Gln Lys Gln Val Gly Arg Lys Ser Asp Ile Tyr Val Ser Leu Val Ser Ser Thr His Gln Val Ala Ala Lys Gly	
o		
5'	TTGGTTCGTGGGCATGGTCTCGACCACCGTTGAGACCGAGAACCCGGAGGTGGAGATCAAGCCTGGCTTGGACTTGCTGG	1120
o	+	
3'	AACCAAGCACCCGTACCAGAGCTGGTGGCAACTCTGGCTCTTGGGCCTCCACCTCTAGTTCGGACCGAACCTGAACGACC	
o	exon3	
	GDI	
1	Trp Phe Val Gly Met Val Ser Thr Thr Val Glu Thr Glu Asn Pro Glu Val Glu Ile Lys Pro Gly Leu Asp Leu Leu	
o		

Appendix



Appendix 3. The sequence of *CG1418* cDNA and the amino acid sequence of CG1418.





Curriculum vitae

Personal information

Name	Ieva Gailite
Date of birth	March 28, 1984
Nationality	Latvian

Education

2006 - 2010	PhD in Molecular Biology in Department of Stem Cell Biology, University of Göttingen, Germany Thesis: „The role of the novel endosomal protein Rush hour (CG14782) in endosomal trafficking in <i>Drosophila melanogaster</i> ”
2006 - 2007	MSc in Molecular Biology in Department of Stem Cell Biology, University of Göttingen, Germany Thesis: „Analysis of <i>CG14782</i> , the putative interaction partner of Bazooka in <i>Drosophila melanogaster</i> ”
2005 - 2006	MSc/PhD Program in Molecular Biology of International Max Planck Research School Georg August University of Göttingen, Göttingen, Germany
2002 - 2005	BSc in Biology in University of Latvia, Riga, Latvia. Thesis: “Viability in the state of anhydrobiosis of yeast <i>Saccharomyces cerevisiae</i> produced under aerobic and anaerobic conditions”

Teaching

2007 - 2010	Tutor of lectures „Model systems in molecular biology – <i>Drosophila</i> I and II“ within the International MSc/PhD program „Molecular Biology“
-------------	---

2007 - 2008 **Supervisor of labrotations**, students Mehdi Goudarzi and Hope Agbemenyah within International MSc/PhD programs „Molecular Biology“ and „Neurosciences“

Scholarships

2006 - 2008 Georg Christoph Lichtenberg Stipend from Ministry of Education of Lower Saxony

2005 – 2006 Stipend of the International Max Planck Research School for Molecular Biology

2004 Kristaps Morbergs Scholarship, University of Latvia

Extracurricular activities

2007 - 2009 Co-organizer of the International PhD Student Symposium „Horizons in Molecular Biology“, Göttingen, Germany

2002 - 2005 Member of the Students' Council of the Faculty of Biology, University of Latvia

Publications

2009 Kim S., **Gailite I.**, Moussian B., Luschnig S., Goette M., Fricke K., Honemann-Capito M., Grubmüller H., Wodarz A. 2009. Kinase-activity-independent functions of atypical protein kinase C in *Drosophila*. *J. Cell Sci.* 122: 3759-3771.